DISSERTATION

ANALYSIS OF EQUINE ZYGOTE DEVELOPMENT AFTER INTRACYTOPLASMIC

SPERM INJECTION

Submitted by

Elena Ruggeri

Department of Biomedical Sciences

In partial fulfillment of the requirements

For the Degree of Doctor of Philosophy

Colorado State University

Fort Collins, Colorado

Spring 2016

Doctoral Committee:

      Advisor: Elaine Carnevale
      Co-Advisor: Colin Clay

      David Albertini
      Jennifer DeLuca
      George Seidel

ABSTRACT

ANALYSIS OF EQUINE ZYGOTE DEVELOPMENT AFTER INTRACYTOPLASMIC

SPERM INJECTION

Intracytoplasmic sperm injection (ICSI) is an established and widely used method to achieve oocyte fertilization in equine reproductive assisted technologies. However, not all the oocytes fertilized by ICSI undergo cleavage and develop into viable embryos. Limited knowledge on equine zygote development after ICSI is available, and reasons why developmental failure occurs after ICSI have been only partially studied and need further investigation. Fertility decline and early embryo loss is associated with maternal aging in the mare, and it is concomitant with reduced oocyte quality. Relatively little is known about the effect of maternal aging and zygote developmental failure or success in the mare. Effects of in vitro maturation of the oocyte or zygote development in the mare still need to be clarified and further studied. The overall objective of this dissertation was to study equine zygote development after ICSI using confocal microscopy. Objectives were to: (1) compare cytoskeletal and nuclear changes during progression of equine zygote development after ICSI for in vivo versus in vitro matured oocytes; (2) compare changes in cytoskeletal and chromosomal configurations after ICSI between oocytes from young and old mares to define maternal-aging related alterations; (3) determine cytoskeletal and nuclear alterations associated with fertilization failure in ICSI-produced presumptive zygotes in young and old mares; (4) determine cell-aging and cell donor-aging effects on cytoskeleton and chromatin configurations. Specifically, in our studies we evaluated the tubulin and actin cytoskeleton, chromatin, and kinetochores/centromeres.

Immunostaining and confocal imaging of the equine zygotes was performed using a spinning disk confocal microscope.

After ICSI, five distinct events of development were observed with no major differences over time whether oocytes matured in vivo or in vitro. Oocytes matured in vivo appeared to reach the pronucleus stage earlier after ICSI compared to in vitro matured oocytes. Abnormal phenotypes associated with fertilization failure were more significant in oocytes matured in vitro than in vivo. When ICSI was performed in oocytes from young and old mares, similar stages of zygote development were observed, and the number of zygotes reaching the pronucleus stage was similar between the two age groups. Nucleolus like bodies, sites of ribosomal RNA involved in embryonic genome activation, were observed only in zygotes at the pronucleus stage from young mares; no nucleolus-like bodies were observed in pronuclei of zygotes from old mares. Pronuclei morphology, based on CREST staining, and DNA localization, also differed between pronuclei of young and old mares. Actin vesicles were observed significantly more often within zygotes from old mares compared to young mares during all stages of zygote developmental progression. When potential zygotes were analyzed after failure of cleavage after ICSI, actin vesicles were greater in area, perimeter and number in oocytes from old mares than those from young mares. Tubulin cytoskeletal multiasters were associated with cell aging and with increased interval after ICSI for young mares but not old mares.

In conclusion, zygotes produced from oocytes matured in vivo versus in vitro or collected from young and old mares went through similar stages of development, with pronuclei attainment appearing to be a crucial event in zygote development. Actin vesicles were a major cytoskeletal difference associated with oocyte origin and a potential factor involved in developmental failure of the oocyte. Confocal microscopy and image analysis were novel

methods used to describe the equine zygote development and allowed us to elucidate the

cytoskeletal and nuclear remodeling events that follow fertilization after ICSI in the mare.

ACKNOWLEDGEMENTS

I would like to thank my two advisors, Drs. Carnevale and Clay, for enabling me to conduct my research and pursue this challenging and satisfying adventure! Also thank you to Joanne Stokes and the ERL group for oocyte collections and ICSI procedures.

To Dr. Clay, you have been like a father for me in these last five years. To Dr. Seidel, thank you from the bottom of my heart for always having your door open to me, answering my questions and providing me with wise, knowledgeable advice and being such an inspiring mentor to me. To Dr. Jennifer (Jake) and Keith, thank you for hosting me in your incredible laboratory and making me feel like part of your brilliant, amazing crew! To Dr. Albertini, you have been such an inspiring scientist and a role model for me since the beginning. To Cesare and Giovanna, you have been a constant, incredible inspiration, empowering force, and wonderful mentors since I first met you both.

To my best friend Kristin/Kristina, you have been my family here. Molly, you have been such a groovy, wonderful friend! Michela and Viola, thank you for having been my life long best friends, no matter how far away we are.

Most importantly, to my Mom (Giovanna) and Dad (Cesare), my sister (Francesca/Luij), and my incredible grandma (Angiolina/Rinda). Your support, your love, and your strength is what made me who I am today. You were there for me, even from far away, every single day. I hope I make you all proud of me! You are everything for me. I love you so much.

To Fort Collins and the colorful Colorado, you have been a home for me and you always are going to be. See you soon! Arrivederci!!

TABLE OF CONTENTS

LIST OF TABLES

LIST OF FIGURES

LIST OF APPENDICES

CHAPTER I: REVIEW OF LITERATURE

Introduction

Equine oocyte meiotic maturation followed by fertilization and zygote development is a crucial sequence of nuclear and cytoskeletal modification events that determine whether normal embryonic growth and development occur. The oocyte goes through two major meiotic events prior to and after fertilization, leading to possible errors and delays in chromatin and cytoskeleton events for diverse reasons. The age of the oocyte donor can drastically affect quality of the oocyte during oocyte maturation in both animal and human models as well as the zygote's to develop into a viable embryo ability after fertilization. Whether or not in vivo versus in vitro maturation of the oocyte can affect success of fertilization needs further investigation. In animal models in vitro maturation may affect meiotic competence and the capability of the oocyte to develop into an embryo. Due to the lack of success of regular in vitro fertilization of the equine oocyte, intracytoplasmic sperm injection (ICSI) still remains the only successful and efficient assisted reproduction technology to evaluate fertilizability of equine oocytes in vitro, with cleavage rates between 60 and 70%. Along with the drop of quality of the oocyte and mare infertility due to advanced maternal age and the possible low quality and viability of sperm, additional questions regarding the effect of ICSI on early embryo development still need to be answered. In the equine clinical setting, all of the above-described conditions are part of the challenge to improve technologies and apply them in diverse scenarios to optimize retrieval of gametes from high quality animals and determine success of pregnancy. In women, assisted reproductive technologies are applied, as in the mare, to overcome infertility due to age or clinical conditions of the patients. ICSI is frequently applied successfully in human settings to

optimize the success of fertilization when female or male gametes quality is problematic. In both equine and human clinical cases, the necessity of studying early events of chromatin and cytoskeleton remodeling after sperm introduction in the oocyte is warranted. Early embryo development is a complex series of remodeling steps and combining of two sets of DNA are required to successfully approach meiosis II before the first mitotic event happens and the embryo is formed. Due to the decline of embryo development and increase of pregnancy loss rates in both women and mares of advanced maternal age and sub-fertile conditions, it is crucial to determine at what stage of zygote development cell events lead to embryo failure. Causes of early embryo arrest during zygote progression after ICSI need to be investigated and are decisive for success of the pregnancy.

In Vivo and In Vitro Equine Oocyte Maturation

Oocyte maturation is a crucial, although poorly understood process, necessary for successful fertilization and attainment of developmental competence of the embryo. Meiotic progression during maturation is a sequence of nuclear and cytoskeletal modifications that determine the fate of embryo growth, implantation and pregnancy success. Molecular and structural events culminate in arrest of the oocyte at metaphase II in preparation for sperm penetration and consequent activation at fertilization.

In monovular species, recruitment of primordial follicles for an extended period of follicular growth is followed by the selection of a dominant follicle that will subsequently ovulate and release the arrested oocyte, which will resume meiosis I. The nuclear arrest of the oocyte at this time inactivates the female gamete DNA, which decreases its vulnerability, ensuring reproductive success.

In the mare, final oocyte maturation occurs within the preovulatory dominant follicle 24 to 36 h preceding ovulation, due to the luteinizing hormone (LH) stimulus (Hinrichs *et al.* 1993). During the estrous cycle, a progressive rise of the concentration of LH results in rupturing the dominant follicle and expulsion of the oocyte (Evans & Irvine 1975, Bézard *et al.* 1989, Hinrichs *et al.* 1993). During the rise of LH, the oocyte, which was arrested in prophase of meiosis I at the germinal vesicle (GV) stage, undergoes germinal vesicle breakdown (GVBD) and subsequently proceeds to chromosome condensation and meiotic spindle formation, resulting in metaphase I. The metaphase I oocyte transitions from anaphase I to telophase I and will arrest at metaphase II, awaiting fertilization (Chen *et al.* 2010). The granulosa cells and cumulus cells, surrounding the oocyte undergoing meiotic maturation, simultaneously transition from compact and granular to expanded and mucoid during oocyte maturation (Carnevale & Maclellan 2006).

The transition from metaphase I to metaphase II is characterized by numerous molecular processes and an increase in activity of various kinases (Dell'Aquila *et al.* 2003). Maturation promoting factor (MPF) is a key factor involved in oocyte maturation and acquisition of competence. MPF appears shortly before germinal vesicle breakdown, peaks at metaphase I, decreases dramatically in the transition from metaphase I to metaphase II and re-establishes a peak at attainment of metaphase II (Trounson *et al.* 2001, Dell'Aquila *et al.* 2003, Mrazek & Fulka Jr 2003). In addition, the organelles and cytoskeleton are reorganized and redistributed during the asymmetric division of the oocyte as meiosis progresses and the collaborative relationship between the cumulus cells and the oocyte change during the meiotic transitions (Coticchio *et al.* 2015).

Equine oocytes can be collected from immature follicles undergoing maturation (Hinrichs *et al.* 1990, Carnevale & Ginther 1993, Cook *et al.* 1993). Oocyte retrieval from preovulatory

follicles results in a higher collection rate per follicle than from immature follicles and allows the oocyte to undergo a more natural maturation. In the mare, to collect preovulatory oocytes, maturation is triggered with human chorionic gonadotropin (hCG) and/or a gonadotropin-releasing hormone (GnRH) analog, such as deslorelin (Carnevale & Maclellan 2006, Carnevale & Sessions 2012). Oocytes collected at least 30 h after hCG administration will be predominantly at metaphase II and ready to be fertilized by the sperm, compared to oocytes collected prior to 30 h after administration of hCG, which need to be cultured in vitro for the completion of meiosis I (Bezard *et al.* 1997). To obtain oocytes for commercial ICSI or oocyte transfer in the mare, preovulatory follicles are usually targeted. Transvaginal, ultrasound-guided follicular aspiration is the primary method to collect oocytes, with collection rates varying between labs, but around 75% (Carnevale & Ginther 1993). When oocytes need to be obtained from smaller and/or non ovulatory follicles, for example, from ovaries of a mare post mortem, it is not feasible to collect in vivo-matured oocytes (Carnevale *et al.* 2004).

The collection of immature equine oocytes and in vitro maturation is used to overcome the limited number of mature oocytes that can be obtained from dominant preovulatory follicles. The technology of oocyte maturation in vitro has been established, partly due to use of ICSI for in vitro fertilization (Galli *et al.* 2013). When collected from the ovary of the live mare, immature oocytes are harder to retrieve due to the tight adherence of the oocyte to the follicle wall; therefore, the recovery rate is lower (Hawley *et al.* 1995). Rigorous flushing and scraping of the follicle wall during follicular aspiration is needed to recover immature oocytes at the germinal vesicle stage (Galli *et al.* 2013). After recovery, oocytes need to complete maturation in vitro to be capable of fertilization.

In vitro maturation primarily involves the addition of gonadotropins and serum to complex culture media (Carnevale & Sessions 2012). Evaluation of oocyte maturity, done by imaging of the extruded first polar body, is needed to determine whether or not the oocyte is ready to be fertilized (Dell'Aquila *et al.* 1996, Dell'Aquila *et al.* 2003). The first successful report of equine oocytes matured in vitro was in 1981, followed by the first embryo produced from an in vitro matured equine oocyte in 1989 (Fulka & Okolski 1981, Zhang *et al.* 1989). Whether or not in vitro maturation can adversely affect the oocyte's ability to complete meiotic maturation and be fertilized successfully still needs to be fully evaluated.

Recent studies have focused on the possible interference of in vitro maturation with establishment of post-translational histone H4 modifications, which are implicated in control of gene expression and determine chromatin remodeling that anticipates resumption of meiosis (De La Fuente *et al.* 2004, Kageyama *et al.* 2007, Franciosi *et al.* 2012). In vitro maturation conditions impact the pattern of H4 acetylation in a residue–specific manner compared to in vivo matured equine oocytes (Franciosi *et al.* 2012). The disruption of histone acetylation of in vitro matured oocytes could lead to defects in chromosomes segregation and alignment, necessary for completion of meiotic maturation, but further investigation is needed (van den Berg *et al.* 2011, Franciosi *et al.* 2012). Possible negative effects of in vitro maturation on epigenetic regulation have been reported in large animal-assisted reproduction where instability of genomic imprinting is represented by large offspring syndrome in ovine and bovine models (Young *et al.* 1998, Young *et al.* 2001). Previous studies confirmed successful in vitro maturation of equine oocytes used for ICSI and nuclear transfer, but also suggested the need for improving in vitro maturation conditions of equine oocytes to improve assisted reproduction technology success in the horse (Squires *et al.* 1996, Galli *et al.* 2013).

The structure of the equine oocyte after maturation in vitro has been described during nuclear maturation by labeling chromatin (Zhang *et al.* 1989, Palmer *et al.* 1990, Shabpareh *et al.* 1993). The first study that focused on using confocal microscopy to describe meiotic spindle organization during in vitro maturation of equine oocytes was in 1997 (Goudet *et al.* 1997). This study first described and defined the normal equine meiotic spindle as barrel-shaped with two distinct poles. It was also determined that the percentage of oocytes with a normal metaphase I spindle is low (63%) compared to the rate for normal metaphase II and telophase I spindles (74%) (Goudet *et al.* 1997). Abnormal spindles were characterized by disorganized microtubules of the two poles (Goudet *et al.* 1997). Spindles from in vitro matured oocytes were significantly wider and longer then spindles obtained from in vivo oocyte recovery (Goudet *et al.* 1997). In a following study, equine oocytes both matured in vivo and vitro were analyzed for chromatin and microtubule conformation at different stages of maturation. The reorganization of the cytoskeleton and chromatin involved in oocyte maturation was described using confocal imaging, but no differences between in vivo or in vitro matured oocytes were reported (Tremoleda *et al.* 2001). This study was the first detailed description of the cytoskeleton of the equine oocyte and its changes across maturation stages. Actin filaments were evenly distributed throughout the ooplasm during the germinal vesicle stage and then were concentrated subcortically during germinal vesicle breakdown (Tremoleda *et al.* 2001). When the spindle was formed, the actin filaments were concentrated around it and around the polar body. No obvious spindle abnormalities or chromosome mis-segregation was observed (Tremoleda *et al.* 2001). In the most recent paper on equine oocyte maturation using confocal microscopy, the focus was on in vivo maturation and its nuclear and cytoskeletal description. Actin filament content of the oocyte was considered as an indicator of cytoplasmic oocyte maturation (Siddiqui *et al.* 2009).

Normal and abnormal spindle and cytoskeletal configurations were reported in this study, and abnormal/detrimental microtubule organization was observed in arrested oocytes that did not complete meiotic maturation correctly (Siddiqui *et al.* 2009).

The analysis and understanding of nuclear and cytoskeletal configuration throughout meiotic maturation of the equine oocyte in vivo or in vitro can help to understand regulation of the cell cycle during meiosis and improve the ability to select highly competent oocytes for fertilization. Therefore, it is important to develop specific immunostaining and confocal imaging approaches for the maturation process of the equine oocyte to address developmental reproductive questions and determine the impact of assisted technologies on the quality of meiotic progression of the oocyte.

Fertilization of Equine Oocytes using Intracytoplasmic Sperm Injection (ICSI) and Zygote

Development

Intracytoplasmic sperm injection (ICSI) is the most common technique used to fertilize the equine oocyte; a selected sperm is injected directly in the cytoplasm of the oocyte. Conventional in vitro fertilization in the horse is inefficient and inconsistent due to the failure of equine sperm to efficiently penetrate the zona pellucida of the oocyte in vitro (Choi *et al.* 1994, Li *et al.* 1995). Only a few laboratories successfully applied in vitro fertilization (IVF) in horse oocytes (Palmer *et al.* 1990, Zhang *et al.* 1990). Only one laboratory reported the production of offspring from the use of IVF (Palmer *et al.* 1990, Zhang *et al.* 1990). Even in these studies, fertilization may actually have occurred in vivo because the eggs were returned to the oviducts shortly after "in vitro" fertilization so the site where sperm penetration occurred is uncertain. For these reasons, to successfully fertilize equine oocytes in vitro, ICSI is the only consistently repeatable technique (Carnevale & Sessions 2012). The first pregnancy derived from in vitro

maturation of equine oocytes and ICSI fertilization was in 1996 (Squires *et al.* 1996). Four

fertilized oocytes were produced using sperm injection, and one pregnancy was produced

(Squires *et al.* 1996). This first successful result was followed by a series of variable results that

had cleavage rates ranging from 20% to 65% (Squires *et al.* 2003a). The introduction of the

piezo drill (Primetech, Japan) in 2002 improved ICSI significantly. The Piezo drill is an

instrument that causes minute vibrations in the injection pipette facilitating the penetration of the

sperm through the zona pellucida and into the cytoplasm. The piezo drill has been used for ICSI

with fresh, cooled, and frozen semen, and the cleavage rates reported range from 69 to 89%

(Galli *et al.* 2002, Choi *et al.* 2004). The use of different sources of sperm, fresh or frozen,

showed no differences in pronucleus formation and cleavage rates (Galli *et al.* 2002).

The procedure of ICSI involves the selection of a highly viable oocyte, usually derived

from the preovulatory follicle, which should be associated with high rates of embryonic

development. The oocyte needs to be at metaphase II to be competent and to be successfully

fertilized; therefore, oocytes having a visible polar body are selected for manipulation. The

selection of the sperm for ICSI is performed using different methods and depends upon the

quality of the sperm and the protocol of different laboratories (Carnevale & Sessions 2012). A

morphologically normal, progressively motile sperm is selected for injection of the oocyte. Prior

to injection, and while semen preparation occurs, the oocyte is denuded from the cumulus cells

using hyaluronidase and gently pipetting (Carnevale & Sessions 2012). At injection, the sperm

is positioned at the tip of the injection pipette that will be inserted through the zona pellucida and

into the cytoplasm of the oocyte. The zona is drilled with the piezo device, and once the piezo

drill breaks the cytoplasmic membrane, the sperm is released, including the tail (Squires *et al.*

1996). After the oocyte is injected, culture of the presumptive zygote is needed to obtain

cleavage and produce viable blastocysts. To culture the injected presumptive zygotes, the most commonly used system is the medium DMEM/F12 with 10% Fetal Bovine Serum (FBS) (Hinrichs 2005, Altermatt *et al.* 2009, Galli *et al.* 2013). Between day 5 and 7 after ICSI, blastocoel formation is observed in those embryos developing normally (Carnevale & Sessions 2012). Comparison of cell counts between in vivo and in vitro cultured embryos at day 7 after fertilization showed a lower number of cells in in vitro-produced embryos (Tremoleda *et al.* 2003b, Galli *et al.* 2013). The delay in blastocyst development after ICSI is most likely caused by membrane damage, nuclei fragmentation and possible blastomere apoptosis (Tremoleda *et al.* 2003b, Pomar *et al.* 2005, Carnevale & Sessions 2012).

The most significant parameter to determine embryo development in the horse is the time to cleavage, which occurs between 12 and 24 h after ICSI (Carnevale & Sessions 2012). Embryos that cleave faster are more prone to result in a pregnancy than embryos that cleave at a slower pace, which is also true in other species (Lundin *et al.* 2001, Carnevale & Sessions 2012). Limited knowledge is available regarding the first 24 h of equine zygote development, and the changes in the oocyte that occur when the female and male genomes meet. Errors in the apposition of the two sets of chromosomes, asynchrony of the nuclear and cytoplasmic remodeling, and zygotic epigenetic modifications occur before the first mitotic cleavage, and can cause early embryo loss and pregnancy failure.

A complete description of the parental genome movements in horse zygotes after ICSI has been conducted using confocal microscopy (Tremoleda *et al.* 2003b). A series of cytoskeleton-mediated events is required for correct progression to the first mitotic division, and failure of this result in developmental arrest. This study characterized nuclear and cytoskeletal events after ICSI in the mare, particularly looking at morphological changes in the first 48 h after

sperm injection. The correct succession of events during zygote development and the abnormal

morphological stages of arrest when fertilization failed were determined. Oocyte activation

failure was the main cause of abnormal cytoskeletal morphology, and zygote arrest and

asynchrony between male and female gametes during fertilization can lead to early embryo

arrest. Beyond this study from 2003, there has not been substantial improvement in studying

chromatin and cytoskeletal factors involved in equine zygote development prior to the first

mitotic cleavage.
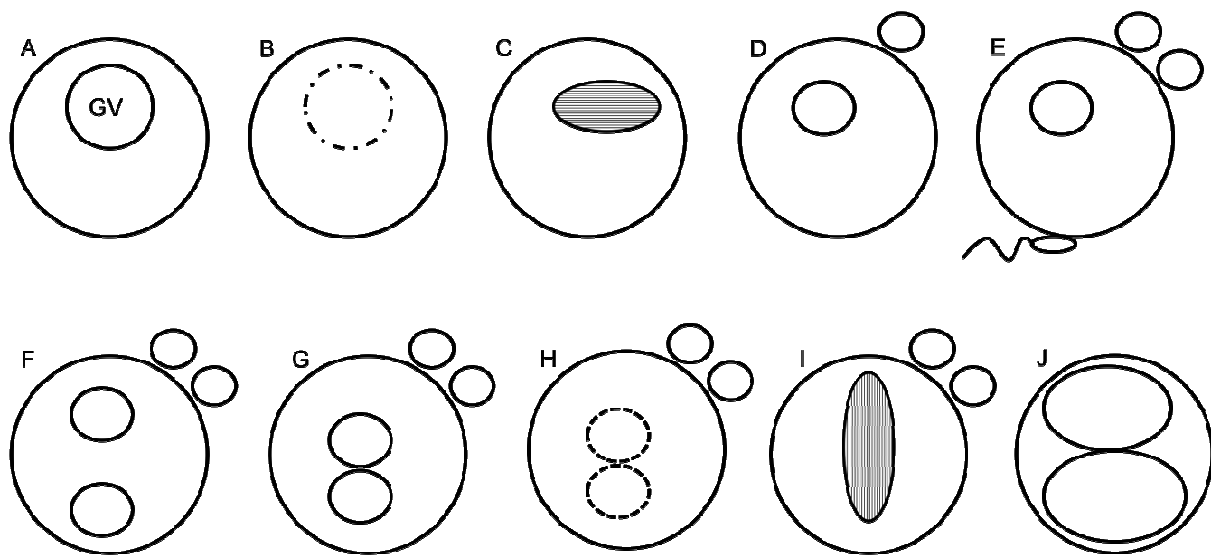
Fig 1.1
A summary cartoon of oocyte maturation, fertilization and zygote development. (A) oocyte at the LH surge when a germinal vesicle is present; (B) germinal vesicle breakdown as a result of the LH surge; (C) resumption of the first meiosis due to ovulation; (D) extrusion of the first polar body; (E) fertilization resulting in the expulsion of the second polar body; (F) formation of the male and female pronuclei in a distanced position; (G) male and female pronuclei in close apposition; (H) breakdown of the pronuclei membranes; (I) fusion of DNA from male and female pronuclei; (J) first cleavage event resulting in a 2 cell embryo.

Infertility and Maternal Aging

A decline in reproductive success is associated with maternal aging in various species

(Tilly 2001, Heffner 2004, Rambags *et al.* 2014, Boudoures & Moley 2015). The substantial use

of assisted reproductive technologies (ARTs) has been overpowering the limit of reduced fertility due to advancing age. Infertility due to advanced maternal age is one of the primary reasons ARTs have been improved and applied both in human and livestock species. In general, the age of the oocyte donor is a primary factor influencing developmental competence of the oocyte (Armstrong 2001). Abnormalities associated with donor age include meiotic incompetence of the oocyte, causing failure of fertilization, and errors in meiosis that allow fertilization but cause genetic abnormalities and cytoplasmic deficiencies at different developmental stages before or after fertilization (Armstrong 2001). Therefore, oocyte competence is crucial for the oocyte to undergo fertilization and develop into an embryo.

In women the age of the oocyte donor is a significant factor influencing oocyte meiotic competence (Boudoures & Moley 2015). Women's fertility declines with age, and aneuploidies have been shown to increase as women age (Battaglia *et al.* 1996, Chiang *et al.* 2012, Boudoures & Moley 2015). Within the human oocyte, reactive oxygen species (ROS) have been found to increase as women age, causing mitochondrial damage that affects oocyte maturation and fertilization success (Boudoures & Moley 2015). Reduction of oocyte mitochondrial competence in older women therefore adversely affects fertility and embryo development (Murakoshi *et al.* 2013).

In the mare, oocyte morphology changes with increased donor age, and a decline in fertility is associated with a high incidence of early embryo loss in old mares (Carnevale & Ginther 1992, Carnevale 2008). The primary factor that causes reduced fertility in old mares is oocyte developmental quality (Carnevale & Ginther 1995). Mare aging is associated with a higher susceptibility to mitochondrial damage, primarily during in vitro maturation (Rambags *et al.* 2014). Also, the lower mitochondrial DNA (mtDNA) number could be an effect of mare

11

aging (Hendriks *et al.* 2015)*,* and suboptimal coenzyme Q10 availability can cause age-associated deficits leading to infertility in women (Ben-Meir *et al.* 2015).

Analysis of chromatin and cytoskeletal changes in oocytes from young versus old donors before and after fertilization has been only minimally studied. Also, the effects of donor aging on microtubule and actin cytoskeleton remodeling, as well as chromatin patterns during meiosis and after the sperm is introduced have been poorly considered in both human and animal fields (Coticchio *et al.* 2014). This shows the necessity for further research on the impact of donor age on oocytes after fertilization and their potential to result in a successful pregnancy.

Oocyte aging and the decreased quality appear to be the main reason of infertility in both women and the mare, but the molecular causes of reproductive aging and decline in oocyte-cell quality still remain undefined. The aging female uterus doesn`t impact pregnancy success when oocytes are transferred into old or young females in both species (Navot *et al.* 1991, Carnevale *et al.* 2000b). Oocyte quality and donor age are independent variables from the quality of the uterine environment in younger or older individuals in women and mares (Navot *et al.* 1991, Carnevale *et al.* 2000b). These findings further validate that the aging oocyte, in particular the cytoskeleton and chromatin changes, is the main reason behind the fertility decline in aging individuals and is an area of research that needs to be investigated further.

CHAPTER II: USE OF CONFOCAL MICROSCOPY TO EVALUATE EQUINE

ZYGOTE DEVELOPMENT AFTER SPERM INJECTION OF OOCYTES MATURED IN

VIVO OR IN VITRO[1]

Summary

The progression of zygote development has not been well defined in the horse. We used confocal

microscopy to investigate zygote development at timed intervals after intracytoplasmic sperm

injection (ICSI) of equine oocytes that were either matured in vivo (IVO) or in vitro (IVM).

After fixation at 4, 6, 8, 12, or 16 h after ICSI, zygotes were incubated with α/β tubulin

antibodies and human anticentromere antibody (CREST/ACA) and washed in Alexa 488, 647,

561-Phalloidin and Hoechst 33258. Images were acquired using an Olympus IX81 spinning disk

confocal microscope. Chi-Square analysis and Fisher's exact test were used to analyze data. Five

different events of zygote development were observed, with only minor differences in

developmental phases over time for IVO and IVM. Oocytes after IVO appeared to form

pronuclei earlier (67% and 80% at 6 and 8 h, respectively) than oocytes after IVM (13% and

13% at 6 and 8 h, respectively); 80% of IVM zygotes formed pronuclei by 12 h. More (P=0.04)

[1] Authors include: Elena Ruggeri[A,], Keith F DeLuca[B], Cesare Galli[CD], Giovanna Lazzari[D], Jennifer G DeLuca[B], Joanne E Stokes[A] and Elaine M Carnevale[A]
[A] Department of Biomedical Sciences, Colorado State University, Equine Reproduction Laboratory, 1693 Campus Delivery, Fort Collins, Colorado, 80523-1693, USA.
[B] Department of Biochemistry and Molecular Biology, Colorado State University, 1870 Campus Delivery, Fort Collins, Colorado, 80523, USA.
[C] Department of Veterinary Medical Sciences, University of Bologna, Via Tolara di sopra, 50, 40064 Ozzano Emilia (Bologna) Italy.
[D] Avantea, Laboratory of Reproductive Technologies, Via Porcellasco 7f, 26100, Cremona, Italy.

zygotes from IVM (30%) than IVO (11%) had abnormal phenotypes, suggesting a failure of normal zygote development after ICSI. Some potential zygotes from IVO had normal phenotypes, although development appeared to be delayed or arrested. Confocal microscopy provided a feasible method to assess equine zygote development using limited samples.

Introduction

In the horse, intracytoplasmic sperm injection (ICSI) is a successful clinical procedure, which has helped to compensate for the failure of standard in vitro fertilization (IVF) techniques (Dell'Aquila *et al.* 1997, Hinrichs 2005, Carnevale *et al.* 2007, Galli *et al.* 2007). In part, because of the failure of IVF, limited numbers of equine zygotes have been available to study early embryo development. Some ICSI-produced equine zygotes have been evaluated with confocal microscopy (Tremoleda *et al.* 2003b). However, most of the research was conducted before reliable results were obtained using ICSI for the horse, and normal zygote development and fertilization failure have since received minimal attention.

In animal models, in vitro maturation (IVM) of oocytes has been successful with assisted breeding technologies (Binor & Wolf 1979, Hinrichs *et al.* 1993, Chian *et al.* 1994, Eppig 1996, Bing *et al.* 2002, Galli *et al.* 2007). In the horse, protocols for in vitro maturation of oocytes have improved in recent years, thus allowing the successful use of in vitro-matured oocytes in ART programs (Hinrichs *et al.* 1993, Galli *et al.* 2007). Further study is required to assess the developmental competence of oocytes matured in vitro. One potential risk of maturation in vitro is that nuclear and cytoplasmic maturation are not synchronized and can result in collateral effects on embryonic development (Smitz *et al.* 2011, Sanfins *et al.* 2015). Transcriptional profiling after in vitro maturation of oocytes from cattle, women and rhesus monkeys has confirmed changes in genes and pathways, which could affect post fertilization events (Rinaudo

& Schultz 2004, Mamo *et al.* 2011, El Hajj & Haaf 2013). An understanding of developmental differences for oocytes matured in vivo and in vitro would help further our knowledge of cytoskeletal and nuclear maturation prior to the first mitotic division. In our study, we used confocal microscopy to examine equine zygote development at timed intervals after ICSI of oocytes matured in vivo or in vitro.

Materials and Methods

Oocyte Collections

In vivo-matured oocytes (IVO) were collected from April to August in Fort Collins, CO (40° latitude) from light-horse mares between 4 and 16 years (yr) (mean $\pm$ s.e.m. of 10.82 ± 0.69 yr). Reproductive tracts were imaged using ultrasonography to evaluate follicular growth. Oocytes were collected from dominant follicle(s) during the follicular phase between 18 and 25 h (21 ± 0.3 h) after administration of hCG (human chorionic gonadotropin, 1500 IU, iv; Intervet Inc, Millsboro, DE, USA) and deslorelin acetate (SucroMate™, 0.75 mg, im; Bioniche Life Sciences Inc., Belleville, Ontario, CAN). Oocytes were retrieved by ultrasound-guided, transvaginal, follicle aspirations (Carnevale *et al.* 2000a) and cultured for 19.5 to 27 h (22 ± 0.3 h) in TCM-199 with Earle's salts (Gibco, Life Technologies, Grand Island, NY, USA) with additions of 10% fetal calf serum (FCS, Cell Generation LLC, Fort Collins, CO), 0.2 mM sodium pyruvate, and 25 µg/ml gentamicin sulfate (Sigma Aldrich, St. Louis, MO, USA)] at 38°C or 38.5°C in an atmosphere of 6% CO_2 and air.

Oocytes for in vitro maturation (IVM) were collected from excised ovaries in Cremona, Italy (45° latitude) during the natural breeding season (March 2014). Ovaries were obtained from mares of diverse breeds and unknown ages from a local abattoir. After removal, ovaries

were transported at 24°C and arrived at the laboratory within 4 h for collection of cumulus-oocyte complexes (COCs). Retrieved COCs were placed in culture medium [Dulbecco`s modified Eagle`s medium (DMEM)/F12 (D8900; Sigma Aldrich Milan, Italy) with 10% serum replacement (Life Technologies, Monza, Italy) and 0.1 IU/ml of human menopausal gonadotropin (HMG; Menopur 75, Ferring, Milan, Italy)] at 38.5°C in humidified atmosphere of 5% CO_2 and air (Galli *et al.* 2007).

ICSI and Zygote Culture

Oocytes matured in vivo were denuded of cumulus cells and injected with a frozen-thawed sperm from a single stallion as previously described (Carnevale *et al.* 2000a) at 49 to 49.5 h (43 ± 0.4 h) after administration of deslorelin/hCG to donor mares. Once oocytes collected had an extruded polar body, a motile sperm with normal morphology was selected for ICSI, which was performed using a piezo drill (Carnevale *et al.* 2000a). Potential zygotes were cultured in 30-μl drops of medium [DMEM/F12 (Sigma Aldrich, St. Louis, MO, USA) with 10% FCS] under mineral oil at 38.5 °C and in 5% CO_2, 5% O_2 and 90% N_2.

After culture for 28 h, oocytes were denuded of cumulus cells, and oocytes with an extruded first polar body were used for ICSI. Sperm injections were performed using a piezo drill and selecting motile sperm with normal morphology from frozen-thawed semen from one stallion of proven fertility (Galli *et al.* 2007). After sperm injection, oocytes were placed as a group in a 300-μl drop of mSOF medium with bovine serum albumin (BSA; Sigma-Aldrich, Milan Italy) and MEM amino acids (Sigma-Aldrich, Milan Italy) under mineral oil at 38.5 °C and in 5% CO_2, 5% O_2 until fixation (Tervit *et al.* 1972, Colleoni *et al.* 2011).

Samples Fixation and Immunostaining

Presumptive zygotes were fixed at room temperature in solution containing 2% formaldehyde and 0.1% Triton X-100 MTSB-XF [(Microtubule Stabilization Buffer Extraction Fix; (Messinger & Albertini 1991)] at 4 (n=5), 6 (n=6), 8 (n=5), 12 (n=5) and 16 (n=7) h (ICSI=0h) for in vivo-matured samples and at the same time points, 4 (n=8), 6 (n=8), 8 (n=8), 12 (n=10) and 16 (n=10) h for in vitro-matured samples. After fixation, oocytes were rinsed in a wash solution [phosphate-buffered saline (PBS) containing 1% BSA and 0.1% Triton X-100] and stored at 4°C until immunostaining.

Oocytes were incubated with diluted primary antibodies in 2% normal goat serum and positioned in four-well plates on rotating platform shaker for 4 h at 37°C at the following concentrations: α/β tubulin cocktail (1:100, mouse; Sigma Aldrich, St. Louis, MO, USA) and human-anti centromere antibody-CREST/ACA (1:100; Life Technologies, Grand Island, NY, USA). After primary incubation, oocytes were rinsed in 2% normal goat serum for a minimum of 12 h at 4°C, then incubated with secondary antibodies conjugated to either Alexa 488 or Alexa 647 (1:100; Jackson ImmunoResearch Laboratories, West Grove, PA, USA) diluted in 2% normal goat serum for 4 h. When secondary incubation was complete, the oocytes were washed in 2% normal goat serum for 5 h and then incubated with phalloidin (Alexa 561; Life Technologies) and Hoechst 33258-(1μg/ml; Life Technologies) for another 5 h at 37°C. For confocal imaging, samples were mounted onto coverslips (50% glycerol in PBS with 25 mg/ml sodium azide and 1μg/ml of Hoechst 33258) (Barrett & Albertini 2007).

Confocal images were acquired on an Olympus IX81 microscope (Waltham, MA, USA) fitted with a Yokogawa spinning disk (CSU22 head) using either a 60x/1.42 NA, DIC Planapochromatic or a 40x/1.35NA planapochromatic oil lens. The 40x objective was used to

image the entire oocyte using z-steps of 1-µm through the entire sample. The 60x objective was then used to image the same sample at 0.2-µm intervals throughout the oocyte. Samples were imaged with a Photometrics (Tucson, AZ, USA) Cascade II EM CCD camera and analyzed using SlideBook software (Intelligent Imaging Innovations, Denver, CO, USA).

Determination of Zygote Development Stages and Abnormalities after ICSI

Five different developmental events were observed in the presumptive equine zygotes: (1) condensed sperm chromatin (CSC), maternal chromosomes (MC) and extruded first polar body (PB1); (2) anaphase to telophase transition, including anaphase/telophase shift of MC, CSC, PB1, and second polar body (PB2) in process of extrusion or fully extruded; (3) formation of the male pronuclei and MC, PB1 and PB2; (4) male and female pronuclei, at distant positions; (5) male and female pronuclei in close apposition.

Male and female pronuclei were identified by characteristics of DNA and human-anti centromere antibody-CREST/ACA localization. Pericentric satellites were observed as ring structures found around the nucleolus-like structures of the two parental pronuclei.

Abnormalities of oocytes after ICSI were classified into five categories based on observations: (1) premature chromosome condensation (PCC), sperm head undergoing premature chromosome condensation with male chromosomes flanked by a bipolar spindle, caused by inactive/delayed activation of the oocyte; (2) multiple pronuclei (MPN), an abnormal phenotype caused by the possible failure of PB2 extrusion; (3) sperm chromatin induced ectopic-polar body (EPB), caused by PCC and leading to paternal chromatin loss; (4) multipolar spindles, with incorrect separation of chromosomes and presence of multiple centrosomes, a sign of chromosomal aberrations; (5) scattered maternal chromosomes and intact sperm head, due to

18

failure of oocyte activation and potentially causing abnormal chromosome separation or aneuploidy.

Statistical Analysis

Chi-Square analysis was used to determine overall effects across all time points for IVO versus IVM, and Fisher's exact test was used within each category for comparisons among time points if the overall difference was significant at P<0.05.

Results

Presumptive Zygote Developmental Events and Pronuclei Assessment

Similar events of zygote development were observed after ICSI of oocytes matured in vivo (IVO) and in vitro (IVM) (Fig 2.1, Table 2.1). The number of potential zygotes differed in developmental stage over time only for IVO when condensed sperm chromatin, maternal chromosomes and PB1 were observed (P=0.02, Fig 2.1A-C) and when distant pronuclei were present (P=0.06, Fig 2.2B), and IVM when pronuclei were apposed (P=0.008, Fig 2.2A) (Table 2.1). The number of potential zygotes with pronuclei (distant or apposed) was significantly elevated at 12 h for IVM (80%); although not different over time, the highest numerical percentages were observed at 6 h (67%) and 8 h (80%) for IVO.

Specific centromere-chromatin signatures were imaged in the pronuclei of equine zygotes as ring structures around nucleolus-like bodies in both maternal and paternal pronuclei (Fig 2.2). Pericentric heterochromatic organization around the nucleolar-like bodies were defined by CREST antibody localization; the number of ring structures in both parental pronuclei varied from three to seven. Pericentric heterochromatin patterns were imaged in all pronuclei when PB2 was not extruded and three pronuclei were present (Fig 2.3).
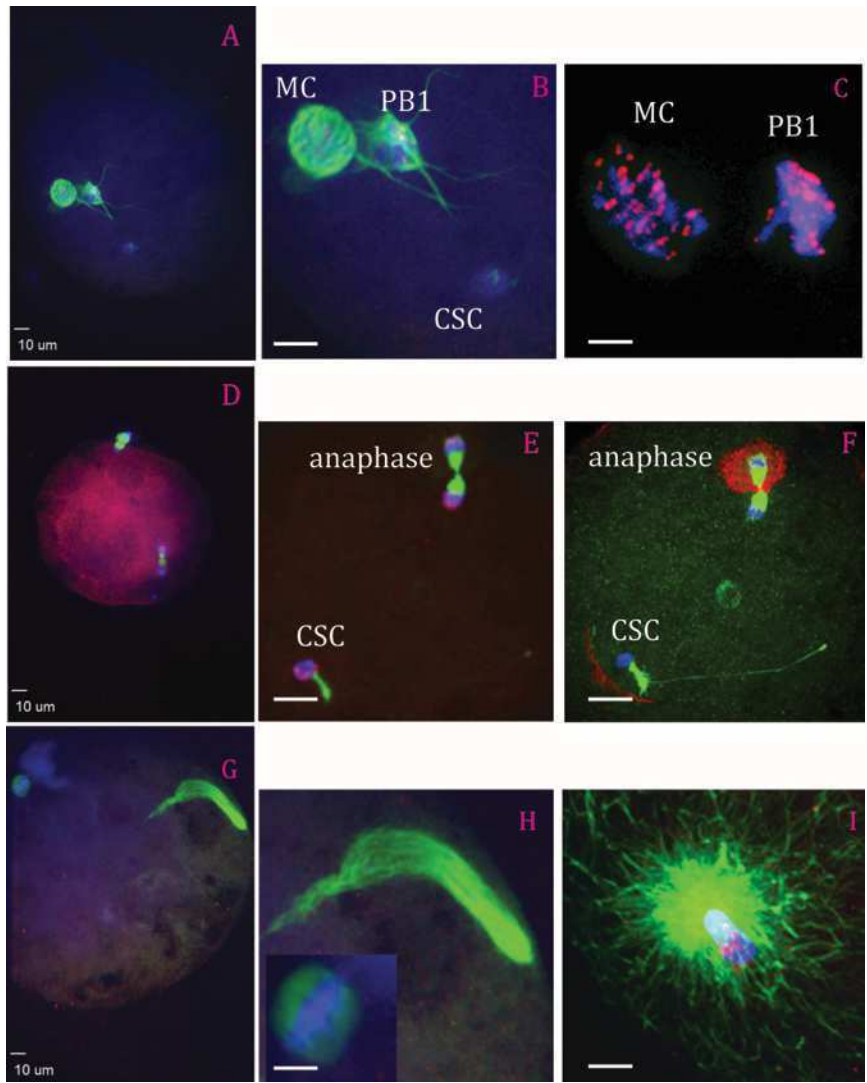
Fig 2.1
Events during zygote development observed between 4 and 16 h after ICSI. (A,B) condensed sperm chromatin (CSC, lower right), maternal chromosomes (MC, left) and first polar body (PB1, just to right of MC); (C) representation of the kinetochores localized on MC and PB1; (D,E) anaphase to telophase transition with CSC with acrosome portion of the sperm (lower left), anaphase/telophase of MC, extruding the second polar body; (F) actin cap surrounding the set of chromosomes being extruded in the second polar body, sperm tail visible next to CSC; (G,H) formation of the male pronucleus (indicated by elongated tubulin structure), MC (left insert); (I) tubulin aster formation around the sperm head at the time of sperm DNA decondensation (Blue, DNA; Red, centromeres and kinetochores, except panel F- actin; Green, tubulin).

Table 2.1. Numbers of potential equine zygotes at different points of development at 4, 6, 8, 12 and 16 h from all oocytes matured in vivo (IVO) or in vitro (IVM) and fertilized by ICSI. The total numbers of potential zygotes at the different points include those determined to have abnormal morphologies (see Table 2.2).

Overall P-values were not different for points of development over time for IVO and IVM. [AB] Values within rows with different superscripts differ at $P<0.05$.

Stages of development	4 h	6 h	8 h	12 h	16 h	P-Value
Condensed sperm chromatin, maternal chromosomes and first polar body						
IVO	4/5 (80)[a]	1/6 (17)[ab]	0/5 (0)[b]	0/5 (0)[b]	2/7 (29)[ab]	0.02
IVM	3/8 (38)	1/8 (13)	1/8 (13)	1/10 (10)	0/10 (0)	0.23
Anaphase to telophase transition, condensed sperm chromatin, first polar body						
IVO	1/5 (20)	1/6 (17)	1/5 (20)	1/5 (20)	0/7 (0)	0.81
IVM	2/8 (25)	2/8 (25)	1/8 (13)	0/10 (0)	0/10 (0)	0.24
Male pronuclei, maternal chromosomes, first and second polar bodies						
IVO	0/5 (0)	0/6 (0)	0/5 (0)	1/5 (20)	0/7 (0)	0.31
IVM	1/8 (13)	2/8 (25)	0/8 (0)	0/10 (0)	0/10 (0)	0.16
Distant male and female pronuclei						
IVO	0/5 (0)	3/6 (50)	1/5 (20)	0/5 (0)	0/7 (0)	0.06
IVM	0/8 (0)	0/8 (0)	0/8 (0)	2/10 (20)	1/10 (10)	0.32
Apposed male and female pronuclei						
IVO	0/5 (0)	1/6 (17)	3/5 (60)	2/5 (40)	3/7 (43)	0.26
IVM	0/8 (0)[a]	1/8 (13)[ab]	1/8 (13)[ab]	6/10 (60)[b]	6/10 (60)[b]	0.008
Pronuclei stages (combined distant and apposed)						
IVO	0/5 (0)	4/6 (67)	4/5 (80)	2/5 (40)	3/7 (43)	0.103
IVM	0/8 (0)[a]	1/8 (13)[a]	1/8 (13)[a]	8/10 (80)[b]	7/10 (70)[b]	0.001
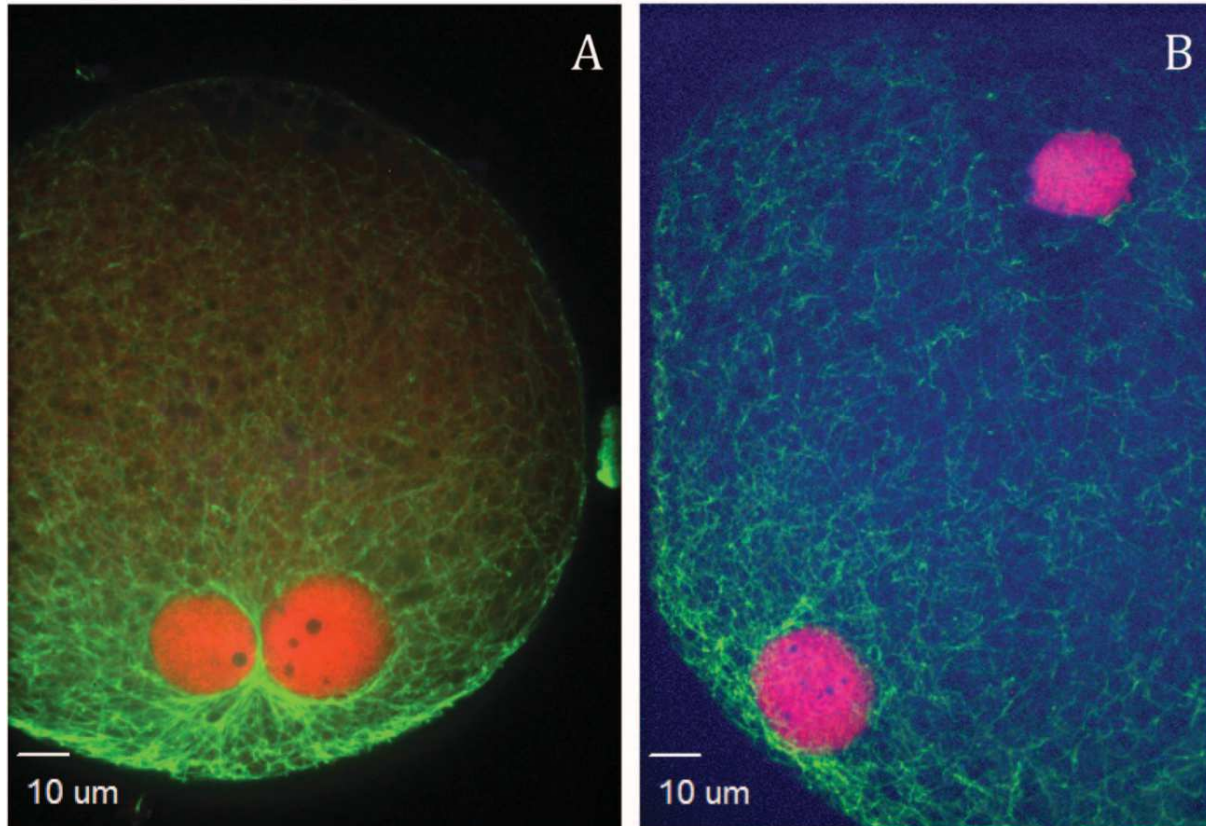
Fig 2.2

Centromeric chromatin signatures observed in equine zygotes at the pronuclei stage. Ring structures were apparent around nucleolus-like bodies within the ACA-CREST antibody localization for maternal and paternal pronuclei at apposed (A) or distant (B) locations, as a sign of pericentric heterochromatic organization. (Red, centromere; Green, tubulin).
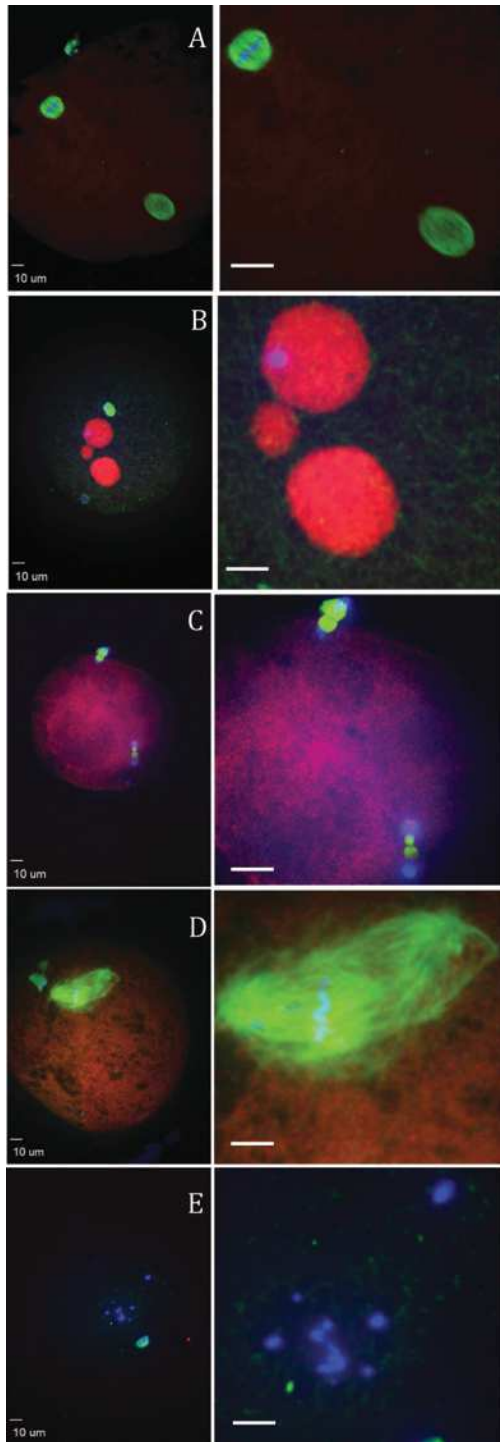
Fig 2.3

Abnormal morphologies of potential equine zygotes after ICSI. (A) premature chromosome condensation, female spindle top left, male chromosome flanked by a spindle structure lower right; (B) multiple pronuclei; (C) sperm chromatin induced ectopic polar body, represented by the two sets of chromosomes undergoing anaphase;

(D) multipolar spindle; (E) scattered maternal chromosomes (Blue, DNA; Red, centromeres and kinetochores; Green, tubulin).

Abnormalities Observed in Presumptive Zygotes after ICSI

Failure of zygote development was observed for IVO and IVM and was associated with abnormal cytoskeletal and chromatin configurations (Fig 2.3, 2.4). In vivo matured oocytes (IVO) had an incidence of abnormalities during zygote development of 3/28 (11%), with no significant differences for the various phenotypes across time (Table 2.2). Of the 44 potential zygotes from IVM, 13 (30%) had abnormal phenotypes, with PCC and EPB as the main, post-injection abnormalities. Overall, potential zygotes from IVM had a higher number of abnormal phenotypes per total injected oocytes than IVO (P=0.04, Table 2.2).
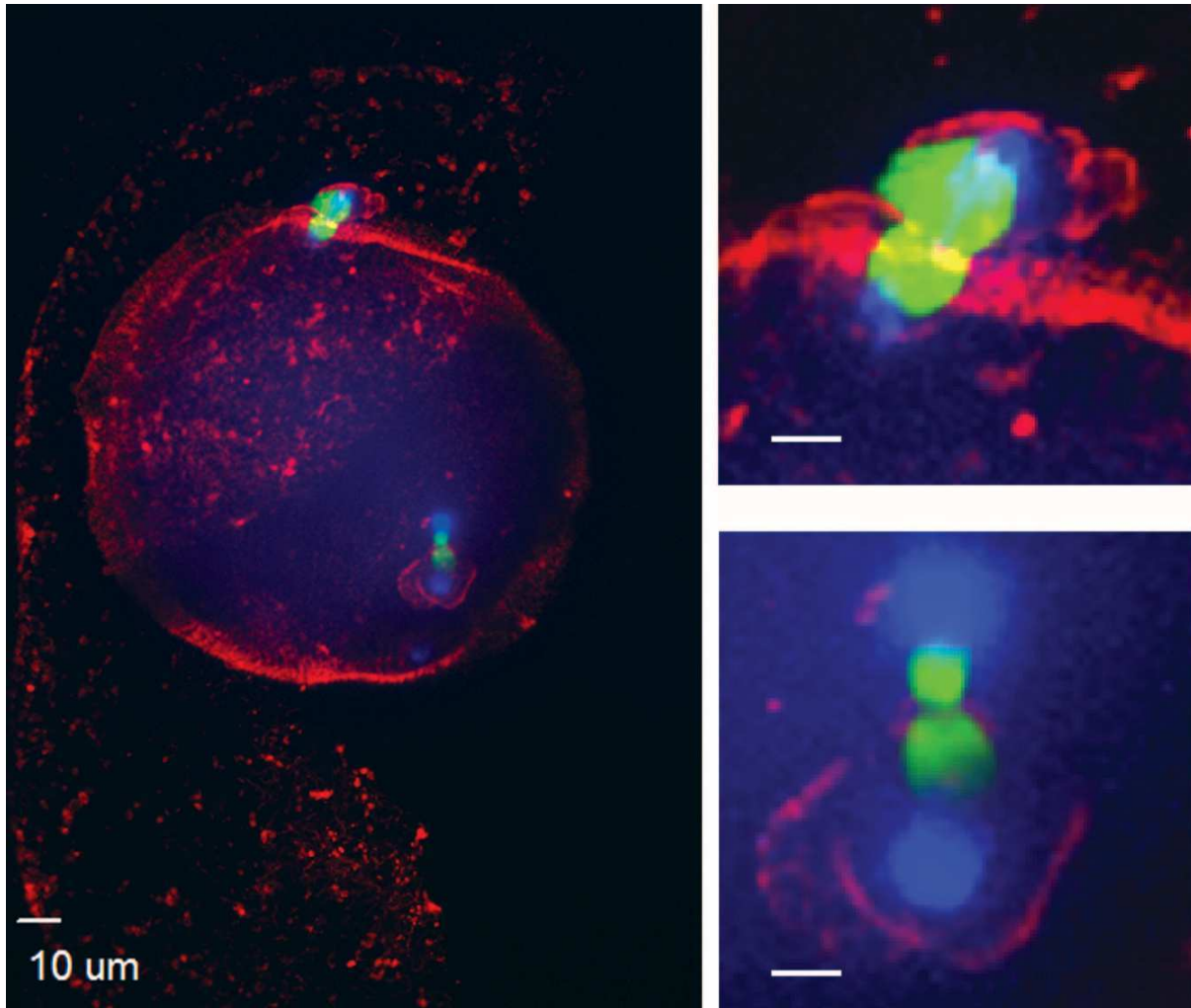
Fig 2.4
    Actin cytoskeleton localization during ectopic polar body extrusion. Left panel cortical actin concentrated around the two points of extrusion of DNA. Top right and bottom right panels are magnified images of the two points of extrusion. (Blue, DNA; Red, actin; Green, tubulin).

Table 2.2. Number of potential equine zygotes with abnormal morphologies at 4, 6, 8, 12 and 16 h after ICSI per total injected oocytes matured in vivo (IVO) or in vitro (IVM).
Overall P-values were not different for specific abnormalities over time for IVO and IVM; however, the total number of zygotes with morphologic abnormalities was higher (P=0.04) for IVM when compared to IVO (as denoted by bold numbers and different superscripts in the table).

Abnormality	4 h	6 h	8 h	12 h	16 h	Total Zygotes
Premature chromosome condensation						
IVO	0/5 (0)	0/6 (0)	0/5 (0)	0/5 (0)	0/7 (0)	0/28 (0)
IVM	1/8 (13)	1/8 (13)	2/8 (25)	0/10 (0)	1/10 (10)	5/44 (11)
Multiple (>2) pronuclei						
IVO	0/5 (0)	0/6 (0)	0/5 (0)	0/5 (0)	0/7 (0)	0/28 (0)
IVM	1/8 (13)	0/8 (0)	0/8 (0)	0/10 (0)	0/10 (0)	1/44 (3)
Sperm chromatin induced ectopic polar body						
IVO	0/5 (0)	0/6 (0)	0/5 (0)	0/5 (0)	0/7 (0)	0/28 (0)
IVM	0/8 (0)	1/8 (13)	3/8 (30)	0/10 (0)	0/10 (0)	4/44 (9)
Multipolar spindle						
IVO	0/5 (0)	0/6 (0)	0/5 (0)	1/5 (20)	0/7 (0)	1/28 (4)
IVM	0/8 (0)	0/8 (0)	0/8 (0)	0/10 (0)	1/10 (10)	1/44 (2)
Scattered chromosomes and sperm head intact						
IVO	0/5 (0)	0/6 (0)	0/5 (0)	0/5 (0)	2/7 (29)	2/28 (7)
IVM	0/8 (0)	0/8 (0)	0/8 (0)	1/10 (10)	1/10 (10)	2/44 (5)
Total abnormalities						
IVO	0/5 (0)	0/6 (0)	0/5 (0)	1/5 (20)	2/7 (29)	**3/28[a] (11)**
IVM	2/8 (25)	2/8 (25)	5/8 (63)	1/10 (10)	3/10 (30)	**13/44[b] (30)**

Discussion

The equine oocyte is a large cell, approximately 140 μm in diameter, with a high lipid content for metabolic energy (Ambruosi *et al.* 2009). These properties of the equine oocyte affect immunostaining and confocal imaging. Therefore, confocal microscopy can be challenging and tedious method to analyze the equine oocyte and zygote. However, because these samples are

difficult and expensive to obtain, confocal microscopy provides an efficient method to image limited samples. Although relatively few antibodies have been tested for use with the equine oocyte and zygote, we were able to use antibodies that were confirmed in other species.

The first detailed imaging of equine early embryo progression after ICSI of oocytes matured in vitro was published in 2003 (Tremoleda *et al.* 2003b). No studies have been conducted using zygotes developing from in vivo matured oocytes. Since the initial study, procedures for oocyte maturation, ICSI and embryo culture have progressed, and the procedures have been proven to be successful in producing embryos and offspring. In our study, we detailed development of the equine zygote and described abnormalities after ICSI of oocytes matured IVO or IVM using confocal microscopy. In this study, two systems (CSU and Italy) with consistent embryo production for oocytes matured IVO and IVM were utilized to evaluate early zygote development.

A time line of zygote development has not been established in the horse. Other studies have focused on cow and monkey zygotes, but these studies are very limited and are primarily centered around tubulin remodeling and oocytes that failed to fertilize after IVF or ICSI (Navara *et al.* 1994, Hewitson *et al.* 1996). In our study, five main events of early embryo development were observed in equine presumptive zygotes after ICSI of IVO and IVM oocytes. The first event observed during early embryo development was the female spindle arrested at metaphase II with aligned and compact chromosomes, first polar body and paternal DNA identified by the presence of the sperm head and, in some samples, the tail (Fig 2.1A, B). Kinetochores were associated with the maternal chromosomes at the metaphase plate and chromosomes of the extruded first polar body (Fig 2.1C). This early phase of development was predominantly observed at 4 h after ICSI, including 80% of IVO and 38% of IVM derived presumptive zygotes.

This stage was also observed in six presumptive zygotes (IVO, n=3, and IVM, n=3) at later time points, suggesting a delay or arrest in development.

The second phase of zygote development was defined as the anaphase to telophase transition in maternal chromatin (Fig 2.1D-F). Maternal chromosomes were approaching anaphase or extruding the second polar body during telophase, and a sperm head was observed. This stage was imaged after ICSI of IVO and IVM, with some presumptive zygotes appearing to be arrested at this point in later hours after ICSI.

The third event observed during zygote development was male chromatin decondensation, with a microtubule array around the sperm head nuclei, female chromosomes aligned at the metaphase plate, and the first polar body and, in some cases, the second polar body (Fig 2.1G-I). This stage was only observed in three oocytes, including oocytes (IVO) that appeared to be delayed in development at 12 h after ICSI.

The presence of male and female pronuclei in distant positions next observed (Fig 2.2B). Pronuclei were surrounded by a complex tubulin net, which was diffused throughout the developing zygote. The entire area of pronuclei was denoted by CREST-anticentromere staining, in which distinct areas were noted with no stain, representing the nucleolus-like bodies, which represent specific heterochromatin signatures at pericentric domains (Fig 2.2A). Pericentric heterochromatin domains are specific zygote transcriptional and epigenetic signatures involved in early zygote development prior to the first mitotic division and embryo genome activation (Probst & Almouzni 2011). When the two pronuclei were apposed (Fig 2.2A), the nucleolus-like bodies were still present within the pronuclei. The tubulin net was now concentrated and contracting at the site of apposition of the pronuclei. At 8 h for IVO and 12 h for IVM, 80% of zygotes had pronuclei.

Oocyte maturation in vivo requires resumption and completion of meiotic divisions and epigenetic reprogramming of the oocyte genome (Bromfield *et al.* 2007). Specific genes needed for correct oocyte maturation are altered subsequent to in vitro maturation and possibly affect early embryo development and genome reprogramming in many species, including humans, cows and mice (Gremeau *et al.* 2012, El Hajj & Haaf 2013, Salhab *et al.* 2013, Sanfins *et al.* 2015). The need to understand the impact of in vitro maturation on early fertilization events and embryonic progression is of utmost importance. Meiotic maturation prior to fertilization proceeds faster when mouse and bovine oocytes are matured in vitro than in vivo, compromising later oocyte developmental competence due to its unphysiological temporal progression (Hyttel *et al.* 1997, Gilchrist *et al.* 2001). Incorrect nuclear and cytoplasmic maturation are possible alterations of in vitro oocyte maturation (Smitz *et al.* 2011). Chromosome abnormalities and epigenetic changes, including histone incorporation and elevated transcriptional activity during the first hours after sperm entrance, can impact the organization of the zygote at specific developmental steps (Probst & Almouzni 2011, Smitz *et al.* 2011). In our study, in vivo matured oocytes seemed to develop to pronuclei sooner after ICSI than in vitro matured oocytes, although some of the oocytes appeared to be delayed or arrested at an early stage of development.

Abnormal morphologies were observed in some potential zygotes. Sperm-transmitted DNA damage leads to diverse abnormal reproductive outcomes and paternal genome loss, and it can be caused by different sperm chromatin defects, including premature sperm condensation and ectopic polar body extrusion after ICSI (Schmiday & Tandler-Schneider 1996, Marchetti & Wyrobek 2005, Deng & Li 2009, Marchetti *et al.* 2015). After aneuploidy, the most common cause of fertilization failure in human IVF and ICSI is premature sperm condensation (Edirisinghe *et al.* 1997, Moghbelinejad *et al.* 2013). Proper meiotic resumption is required in

the oocyte to help avoid sperm head premature condensation, which leads to DNA damage and aneuploidy in human oocytes (Manandhar & Toshimori 2003). In our study, premature sperm condensation was only found in oocytes matured in vitro; no oocytes matured in vivo had this abnormal phenotype. Another sperm related abnormality, specific to IVM in our study, was sperm chromatin-induced ectopic polar body extrusion, another possible cause of paternal genome loss in mammalian oocytes (Deng & Li 2009). This process causes the sperm chromatin to form a spindle in the oocyte, leading to failure of fertilization and zygote development. Premature sperm chromatin condensation and sperm chromatin induced ectopic polar bodies were only observed in oocytes matured in vitro, suggesting that progression to the pronuclei stage was interrupted due to activation delay in oocytes matured in vitro or due to alterations of sperm DNA specific packaging and protamine deficiency, both needed for successful fertilization. However, we cannot exclude the potential that intrinsic oocyte quality or the stallion affected these results, as these variables were also different in the two ICSI systems.

Additional zygote abnormalities included multiple pronuclei and multipolar spindle or presence of scattered maternal chromosomes and intact sperm head (chromosome fragmentation). Multiple pronuclei suggest the failure of extrusion of the second polar body, possibly due to low oocyte quality or sperm chromatin defects (Rosenbusch 2001). Multipolar spindles are a possible sign of failure in spindle assembly checkpoints, and they were observed in one oocyte matured in vivo and one oocyte matured in vitro (Sluder *et al.* 1997, Courtois *et al.* 2012). Scattered chromosomes and a sperm head were also observed in two potential zygotes from IVO and two from IVM. Overall, we observed more morphological abnormalities in zygotes from oocytes matured in vitro than in vivo.

Conclusions

In conclusion, we used confocal microscopy to observe equine zygote progression after ICSI of oocytes matured in vivo or in vitro. In this study there were differences in systems for oocytes injected in vivo and in vitro varied; therefore, our ability to make direct comparisons was limited. However, we observed a similar progression through the major events of maturation of potential zygotes regardless of type of oocyte maturation. Oocytes matured in vivo appeared to have a more rapid progression to pronuclei, although some of these potential zygotes appeared to be delayed or arrested in development. Abnormal zygote morphologies were observed more frequently in oocytes matured in vitro than in vivo. Confocal microscopy provided a feasible method to assess zygote development after in vivo or in vitro oocyte maturation using a limited number of samples available.

CHAPTER III: EFFECT OF MATERNAL AGING ON EQUINE ZYGOTE DEVELOPMENT AFTER ICSI[2]

Summary

The effect of the oocyte donor age on equine zygote development has not been studied. The aim of our study was to compare early zygote development after intracytoplasmic sperm injection (ICSI) of oocytes from young and old mares, using confocal microscopy to analyze cytoskeletal and chromatin configurations. We evaluated zygote development at 4, 8, 16 and 20 h after ICSI of oocytes collected from young mares (4-16 yr) and old mares (20-29 yr). After fixation, zygotes were incubated with α/β tubulin antibodies and human anticentromere antibody (CREST/ACA) and washed in Alexa 488, 647, 561-Phalloidin, and Hoechst 33258. An Olympus IX81 spinning disk confocal microscope was used to collect images. Chi-Square analysis, Fisher's exact test, and student's t-test were used to analyze data. Similar stages of zygote development were observed in young and old mares, although actin vesicles were observed more often (P=0.001) in zygotes of old than young mares. The number of zygotes that reached the pronuclear stage was similar between groups; however, marked differences were observed in the pronuclei from young and old zygotes. Although present in all pronuclei from young mares' zygotes, no nucleolus like bodies were observed in the pronuclei of old mares' zygotes, and CREST and DNA localization also differed with age group. Our study is the first to describe the effect of maternal aging on equine zygote development after ICSI.

---

[2] Authors include: Elena Ruggeri and Elaine M. Carnevale
Equine Reproduction Laboratory, College of Veterinary Medicine & Biomedical Sciences, Colorado State University, 1693 Campus Delivery, Fort Collins, Colorado, USA.

Introduction

Fertility declines with maternal aging in the mare, and the decline in fertility is associated with an increase in early embryo loss (Ginther 1979, Carnevale & Ginther 1995, Carnevale 2008). Early embryo loss in old mares is potentially accentuated by decreased oocyte developmental quality in old mares (Carnevale & Ginther 1995, Carnevale 2008). Problems associated with oocytes from old mares include chromosomal misalignment at metaphase II and alterations of the actin cytoskeleton in sperm-injected oocytes that failed to cleave (Carnevale *et al.* 2012, Carnevale & Sessions 2012, Ruggeri *et al.* 2015). Therefore, maternal aging in the mare affects oocyte competence acquisition and early embryo development. As with horses, fertility in women also declines with increasing age and is associated with a loss in oocyte quality and a consequent increase in chromosomal abnormalities, including aneuploidy (Battaglia *et al.* 1996, Kuliev *et al.* 2003).

Intracytoplasmic sperm injection (ICSI) is the primary method used for assisted fertilization of equine oocytes (Choi *et al.* 2002, Galli *et al.* 2002). Donor age does not impact the cleavage rates after ICSI (Altermatt *et al.* 2007). However, not all presumptive zygotes undergo the first mitotic division after ICSI. Limited information is available regarding equine zygote development before the first cleavage and cytoskeletal and nuclear remodeling after ICSI (Goudet *et al.* 1997, Tremoleda *et al.* 2003b). Zygote development has not been compared between young and old mares using confocal microscopy.

We hypothesized that cytoskeletal and chromosomal configurations will be altered in ICSI-produced zygotes with maternal aging. Objectives of the present research were to compare potential zygotes from sperm-injected oocytes of young or old mares at 4, 8, 16 and 20 h after

ICSI for: 1) stage of development, 2) nuclear remodeling, 3) cytoskeletal structure, 4) morphology of pronuclei, and 5) abnormal zygote morphology.

Materials and Methods

Oocyte Collection

Mares were housed at Colorado State University's Equine Reproduction Laboratory (Fort Collins, CO, USA), Nonlactating mares of light-horse breeds and between 400 and 550 kg were classified as young, 4 to16 yr (11.00 ± 0.80 yr, mean ± SEM, n=23) or old, 20-29 yr (23.53 ± 0.48 yr, n=30). Reproductive tracts were monitored by ultrasonography to determine stage of the estrous cycle and follicle development. Oocytes were retrieved by ultrasound-guided, transvaginal follicular aspirations (Carnevale *et al.* 2000a). Oocytes were collected from follicular-phase, dominant follicles. When follicles were approximately 35 mm in diameter, human chorionic gonadotropin (hCG; 1500 IU, i.v.; Intervet, Millsboro, DE, USA) and deslorelin acetate (Sucromate; 0.72 mg, i.m.; Bioniche Life Sciences, Belleville, Canada) were administered to donors, and oocytes were collected 18 to 24 h later. After collection, oocytes were cultured for 19 to 24 h in TCM-199 with Earle's salts (Gibco, Life Technologies, Grand Island, NY, USA) with additions of 10% fetal calf serum (FCS, Cell Generation LLC, Fort Collins, CO), 0.2 mM sodium pyruvate, and 25 µg/ml gentamicin sulfate (Sigma Aldrich, St. Louis, MO, USA)] at 38°C to 38.5°C in an atmosphere of 6% CO_2 and air. Oocytes were injected with a sperm 40 to 45 h after administration of deslorelin/hCG.

Sperm Injection and Culture after ICSI

Oocytes were injected with frozen-thawed sperm from a single ejaculate of one stallion. All oocytes had a polar body prior to injection. A motile sperm with normal morphology was

selected and injected using a piezo drill (Carnevale *et al.* 2000a). Potential equine zygotes were cultured individually in drops of 30-μl of medium [DMEM/F12 (Sigma Aldrich, St. Louis, MO, USA) with 10% FCS] under mineral oil at 38.5 °C and in 5% CO_2, 5% O_2 and 90% N_2.

Fixation and Immunostaining of Presumptive Zygotes

Presumptive zygote fixation was performed at room temperature in a solution containing 2% formaldehyde and 0.1% Triton X-100 MTSB-XF [(Microtubule Stabilization Buffer Extraction Fix (Messinger & Albertini 1991)]. Potential zygotes from sperm-injected oocytes from young mares (Young) and old mares (Old), respectively, were fixed at 4 h (n=5 and 7), 8 h (n=5 and 9), 16 h (n=7 and 6) and 20 h (n=6 and 8) after ICSI. After fixation, oocytes were rinsed in a wash solution [phosphate-buffered saline (PBS) containing 1% BSA and 0.1% Triton X-100)] and stored at 4°C.

Oocytes were incubated in primary antibodies [(α/β tubulin cocktail, 1:100, mouse; Sigma Aldrich, St. Louis, MO, USA) and human-anti centromere antibody-CREST/ACA, 1:100; Life Technologies, Grand Island, NY, USA)] diluted in 2% normal goat serum and distributed in four-well plates on a rotating platform shaker for 4 h at 37°C. After incubation with the primary antibodies, oocytes were rinsed in 2% normal goat serum for a minimum of 12 h at 4°C and then incubated with secondary antibodies conjugated to either Alexa 488 or Alexa 647 (1:100; Jackson ImmunoResearch Laboratories, West Grove, PA, USA) diluted in 2% normal goat serum for 4 h. Oocytes were washed for 5 h in 2% normal goat serum and incubated for another 5 h with phalloidin (Alexa 561; Life Technologies) and Hoechst 33258-(1μg/ml; Life Technologies) at 37°C. Samples were mounted onto coverslips (50% glycerol in PBS with 25

mg/ml sodium azide and 1µg/ml of Hoechst-33258) for confocal imaging (Barrett & Albertini 2007).

Confocal Imaging and Morphometric Analysis

Confocal images were acquired on an Olympus IX81 microscope (Waltham, MA, USA) fitted with a Yokogawa spinning disk (CSU22 head) using either a 60x/1.42 NA, DIC planapochromatic or a 40x/1.35NA planapochromatic oil lens. The 40x objective was used to image the entire oocyte using z-steps of 1 µm through the sample. The 60x objective was then used to image the same sample at 0.1-µm intervals. Images were acquired with a Photometrics (Tucson, AZ, USA) Cascade II CCD camera and analyzed using SlideBook software (Intelligent Imaging Innovations, Denver, CO, USA).

Presumptive zygotes were classified in different developmental stages based on male and female chromatin contribution and remodeling at the different time points of fixation. Zygote development was classified into five progressive stages. Zygotes in Stage 1 had a condensed sperm head, a female metaphase II spindle, and the first polar body. In Stage 2, a condensed sperm head and first polar body were again imaged; but the female chromosomes had progressed to anaphase. In Stage 3, female and male complements of DNA were image with diffusion of associated tubulin. In Stage 4, pronuclei were formed and positioned either distant or apposed. Stage 5 included the early anaphase to telophase transition prior to the first mitotic cleavage. In the final stage, Stage 6, cleavage had occurred with complete cell separation and actin borders between the two cells.

Pronuclei localization was determined by DNA staining with Hoechst 33258 and constitutive heterochromatin staining using CREST-anticentromere antibody. When male and female pronuclei were observed, measurements for the areas of each of the pronuclei were at

their largest diameter from compressed stacks collected at 60x magnification at 0.1-μm intervals of the top to the bottom using the "mask-draw function" on Slidebook software. The male and female pronuclei were presumptively differentiated based upon relative size, as the literature in other species states that the male pronucleus is larger than the female pronucleus (Scott 2012). The location of the male and female pronuclei could not be definitively confirmed by the location of the polar body and/or sperm tail using methods in this experiment.

Chromosome alignment at the female meiotic spindle was determined at stage 1 of zygote development, as well as the presence of a symmetrical, barrel-shaped microtubule-based spindle containing the chromosomes. Presence or absence of tubulin multiasters within the zygote cytoplasm and tubulin net at the pronuclei stage was determined.

When actin vesicles were observed in the presumptive zygotes, the total integrated fluorescence intensity of actin was determined from compressed images selecting the stacks occupied by the vesicles at 40x magnification at 1-µm intervals, using the "mask-draw function" on SlideBook software. The area and perimeter of the actin vesicles was determined from compressed stacks collected at 40x.

Statistical Analysis

Chi-Square analyses were used to determine differences across the time points for developmental stages of Young and Old. If there was a significant ($P<0.05$) overall difference, Fisher's exact test was used within each stage of development and abnormality for comparisons among time points. Student's t-test was used to compare Young and Old for area per pronucleus, difference in pronuclei area, area of presumptive male and female pronuclei, and the number of nucleolus like bodies (NLBs) per pronucleus.

Results

Images from some oocytes and some time points for Young were used in a previous study comparing zygote development of oocytes matured in vivo and in vitro. For age groups, intervals were similar for time from administration of deslorelin/hCG to follicular aspiration (Young, 20.8 ± 0.4 h and Old, 21.7 ± 0.3 h, P=0.08) and time from administration of deslorelin/hCG to ICSI (Young, 43.3 ± 0.5 h and Old, 43.5 ± 0.2 h, P=0.58).

Zygote Development in Young and Old Mares

Zygotes from young and old mares' oocytes went through similar developmental stages. The number of presumptive zygotes differed (P=0.01) over time for the first stages of development for Young and the second stage of development for Old, with the highest numerical percentages of potential zygotes at 4 h for Young in Stage 1 (condensed sperm head and female spindle, 80%) and for Old in Stage 2 (condensed sperm head and female anaphase, 57%) (Table 3.1). The presence of pronuclei differed (P=0.04) with time for Young, with the numerically highest percentage of pronuclei (80%) observed at 8 h; in Old, the numerically highest percentage of pronuclei (50%) was observed at 16 h. Later stages did not differ over time, and two zygotes in each group were cleaved by 20 h (Figure 3.1).

Chromosomes at the metaphase plate of the female spindle at Stage 1 were consistently aligned on the plate and the spindle was always bipolar and barrel shaped. Tubulin multiasters were not observed on any of the zygotes analyzed. A distinct tubulin net around the pronuclei was observed in all samples.

Actin vesicles were more frequently (P=0.001) observed in Old than Young (Old, 13/30, 43% and Young, 1/23, 4%, Table 3.1). For Old, one to six actin vesicles were imaged per presumptive zygote (Figure 3.2) with an average area of 6.08×10^2 μm^2, perimeter of 1.16×10^2

38

μm, sum intensity of all vesicles of 147.6 x10^6 ADU, and sum intensity per vesicle of 59.1 x10^5 ADU. Only one Young had actin vesicles (14 total vesicles), which were observed at the first stage of development, with an average area of 308.8 μm^2, perimeter of 250.5 μm, sum intensity of all vesicles of 75.0 x10^6 ADU, and a sum intensity per actin vesicle of 5.4 x10^5 ADU.

Two forms of abnormal development were observed. The abnormalities included multiple pronuclei (n=1) and premature sperm chromosome condensation (n=2). Abnormal morphologies were all observed in Old (Table 3.1).

Table 3.1. Numbers of potential equine zygotes in normal stages of development and with abnormal developmental characteristics after injection of sperm into oocytes from young mares (Y) and old mares (O) at 4, 8, 16 and 20 h after ICSI, total number per all zygotes, and overall P-values among times.

[AB] Values within a row for 4, 8, 16 or 20 h with different subscripts differ (P<0.05).
[ab] Values with different superscripts within a column for a specific endpoint differ (P<0.05) between Young and Old.

	4 h	8 h	16 h	20 h	Total	P-value
Stages of development:						
Condensed sperm head, female spindle and first polar body						
Y	4/5 (80)^A	0/5 (0)^B	2/7 (29)^{AB}	0/6 (0)^B	6/23 (26)	0.01
O	3/7 (43)	3/9 (33)	1/6 (17)	0/8 (0)	7/30 (23)	0.21
Condensed sperm head and female anaphase and first polar body						
Y	1/5 (20)	1/5 (20)	0/7 (0)	0/6 (0)	2/23 (9)	0.42
O	4/7 (57)^A	1/9 (11)^{AB}	0/6 (0)^{AB}	0/8 (0)^B	5/30 (17)	0.01
Spindle tubulin structure with male and female chromosomes						
Y	0/5 (0)	0/5 (0)	2/7 (29)	1/6 (17)	3/23 (13)	0.38
O	0/7 (0)	2/9 (22)	0/6 (0)	3/8 (38)	5/30 (17)	0.15
Two pronuclei (distant or apposed)						
Y	0/5 (0)^A	4/5 (80)^B	3/7 (43)^{AB}	1/6 (17)^{AB}	8/23 (35)	0.04
O	0/7 (0)	3/9 (33)	3/6 (50)	1/8 (13)	7/30 (23)	0.14
Early anaphase to telophase prior to cytokinesis						
Y	0/5 (0)	0/5 (0)	0/7 (0)	2/6 (33)	2/23 (9)	0.10
O	0/7 (0)	0/9 (0)	1/6 (17)	0/8 (0)	1/30 (3)	0.25
Cleaved						
Y	0/5 (0)	0/5 (0)	0/7 (0)	2/6 (33)	2/23 (9)	0.10
O	0/7 (0)	0/9 (0)	1/6 (17)	1/8 (13)	2/30 (7)	0.47
Abnormal developmental characteristics:						
Presence of actin vesicles						
Y	1/5 (20)	0/5 (0)	0/7 (0)^a	0/6 (0)^a	1/23 (4)^a	0.29
O	1/7 (14)^A	2/9 (22)^{AB}	4/6 (67)^{AB,b}	6/8 (75)^{B,b}	13/30 (43)^b	0.12
Multiple pronuclei						
Y	0/5 (0)	0/5 (0)	0/7 (0)	0/6 (0)	0/23 (0)	N/A
O	0/7 (0)	0/9 (0)	0/6 (0)	1/8 (13)	1/30 (3)	0.42
Premature sperm chromosome condensation						
Y	0/5 (0)	0/5 (0)	0/7 (0)	0/6 (0)	0/23 (0)	N/A
O	0/7 (0)	0/9 (0)	0/6 (0)	2/8 (25)	2/30 (7)	0.12
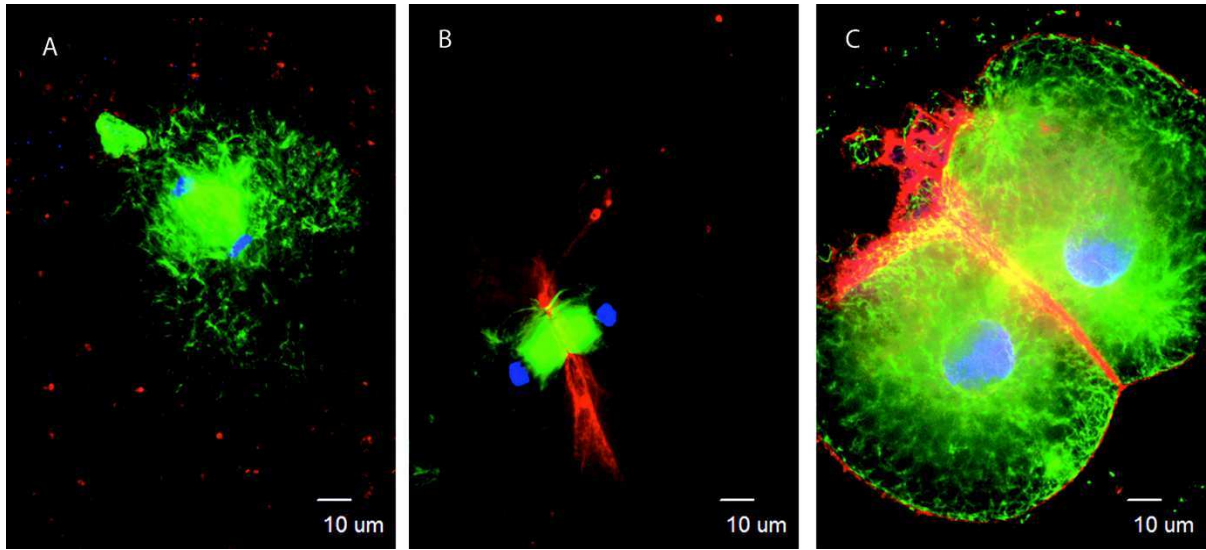
Fig 3.1
Early anaphase to telophase transition (A and B) and first mitotic cleavage (C) of the equine zygote, with the actin ridge imaged at the cleavage furrow (B and C). (Blue, DNA; Red, actin; Green, tubulin).
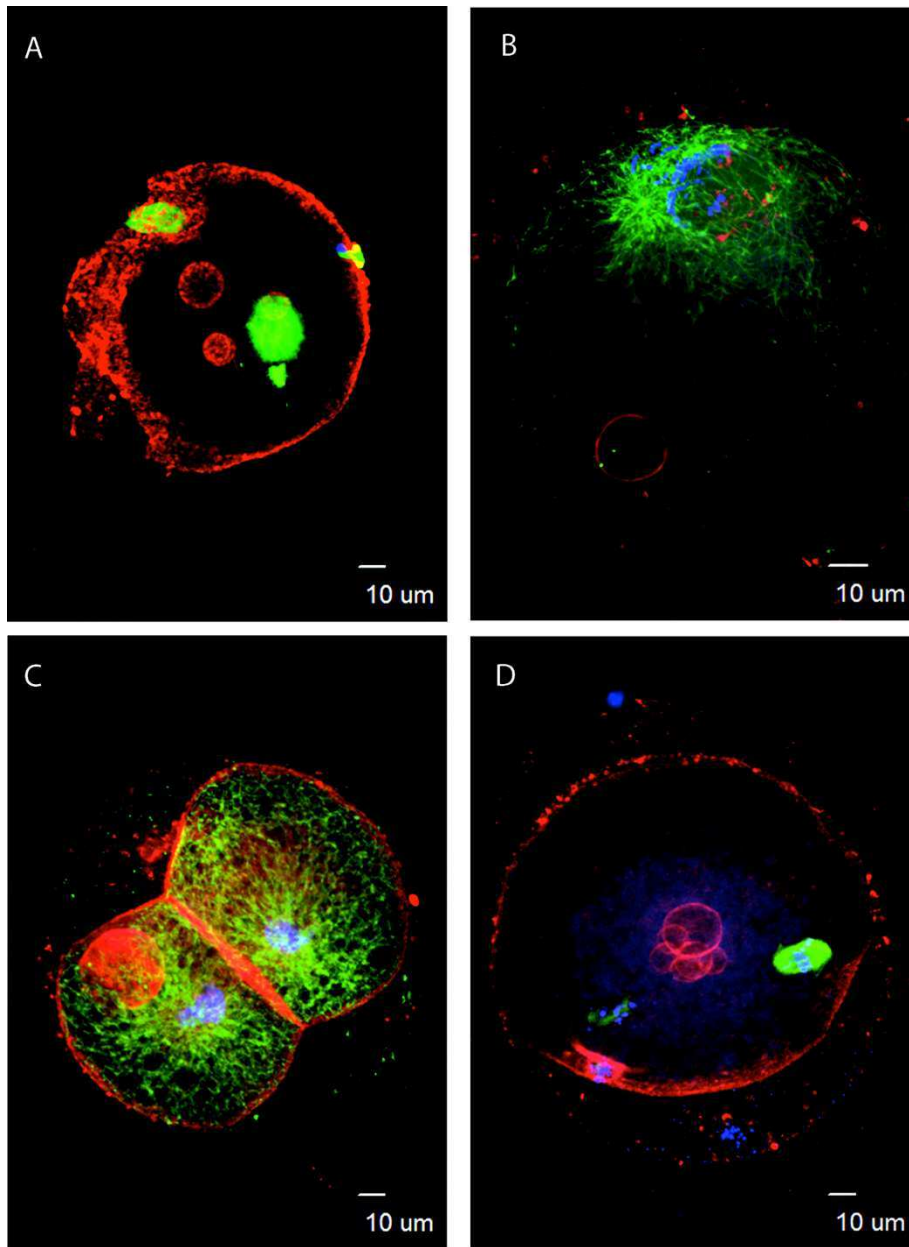
Fig 3.2

Images of different stages of zygote development after sperm injection of oocytes from old mares, which demonstrate the distribution of actin vesicles. A) Polar body on the top left, female spindle (middle) and male midpiece with diffusion of associated tubulin; B) Pronucleus chromosomes and surrounding tubulin net; C) Cleaved embryo; D) Premature sperm chromosome condensation. (Blue, DNA; Red, actin; Green, tubulin).

Pronuclear Area and Constitutive Heterochromatin Localization in the Equine Zygote

Between Young and Old, the number of zygotes with two pronuclei, the average area per pronuclei, and the difference in the area between presumptive male and female pronuclei did not differ (Table 3.2). The mean area of the presumptive male pronuclei was significantly larger than the female pronuclei (Table 3.2).

Nucleolus like bodies (NLBs) were not observed in the pronuclei of zygotes from Old, while all pronuclei in Young had NLBs (Table 3.2). Numbers of NLBs in Young ranged from 2 to 10 per pronuclei, with unequal numbers and no predominance in presumptive female or male pronuclei (P=0.79).

In pronuclei of Young, CREST and DNA localization was diffuse to the entire pronuclear area and concentrated pericentrically around NLBs. In Old, constitutive heterochromatin, represented by CREST and DNA staining, was only at the periphery of the pronuclear area and distinctively localized as knob foci at the DNA filaments, which were polarized at each of the pronuclei (Figures 3.3 and 3.4).

Table 3.2. Parameters observed and quantified (mean ± SEM) for pronuclei from zygotes of young and old mares.
[a,b] Values between the average area of the male and female pronuclei with different subscripts differ (P<0.05).

	Total or Mean ±SEM		P-value
	Young	Old	
Number of zygotes with pronuclei per total injected oocytes	8/23 (35%)	6/30 (20%)	0.35
Average area of pronucleus (μm^2)	622.58 ± 79.63	483.08 ± 80.58	0.28
Difference in pronuclei areas within a zygote (μm^2)	266.02 ±77.46	118.17 ± 38.08	0.23
Number of pronuclear stage zygotes with pronuclei containing nucleolar like bodies	8/8 (100%)	0/6 (0%)	0.0001
Average number of nucleolar like bodies per pronucleus	5.06 ± 0.68	0	0.0000065
Average area of presumptive male pronuclei (μm^2)	755.59 ± 122.82[a]	542.16 ±122.73[a]	0.30
Average area of presumptive female pronuclei (μm^2)	489.56 ± 83.88[b]	423.99 ± 113.63[b]	0.66
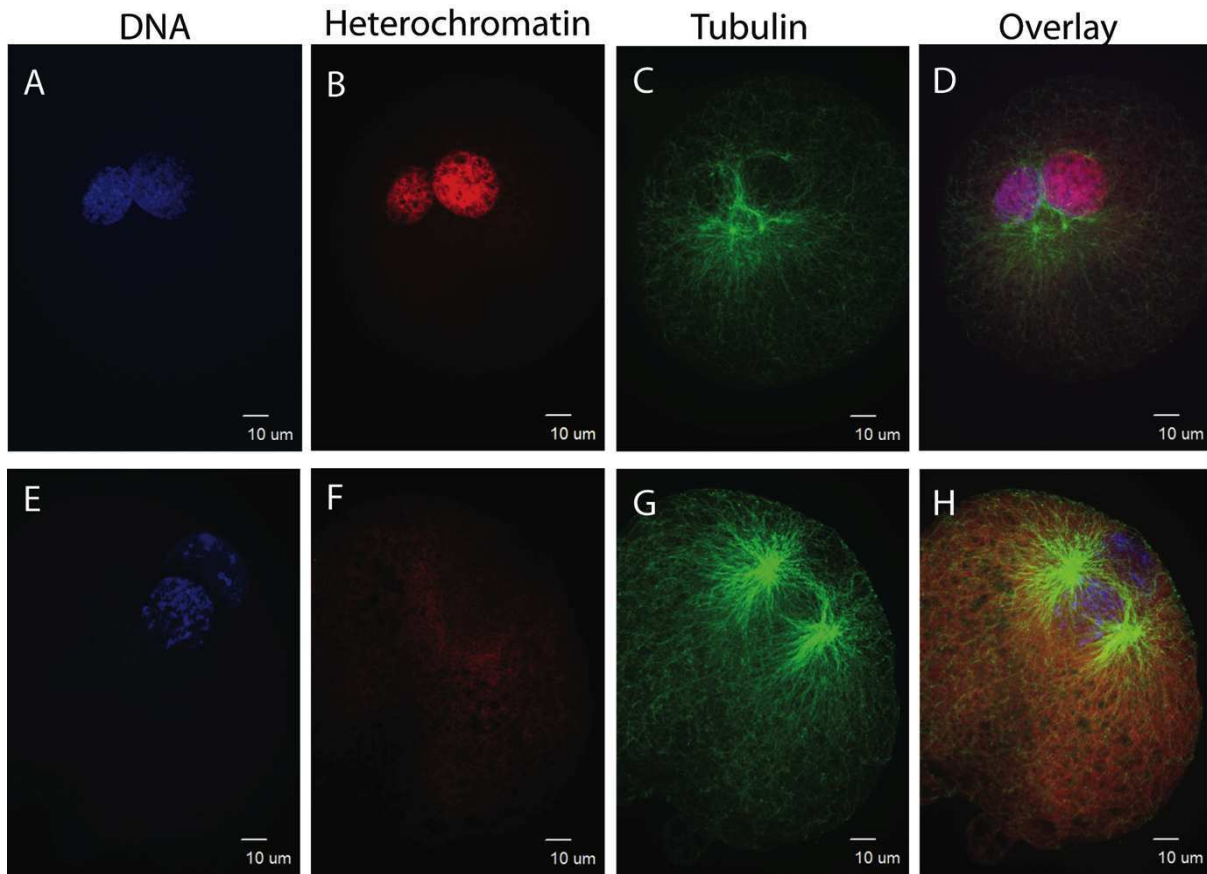
Fig 3.3

Representative zygotes from Young (A-D) and Old (E-H) at pronuclear stage of development. Images A and E demonstrate differences in DNA distribution between Young (diffuse) and Old (condensed and scattered). Images B and F show the diffuse CREST antibody in Young pronuclei; while in Old, heterochromatin localization is limited. A network of tubulin was observed for Young and Old (Images C and G). Images D and H represent an overlay of all stains (Blue, DNA; Red, heterochromatin; Green, tubulin).
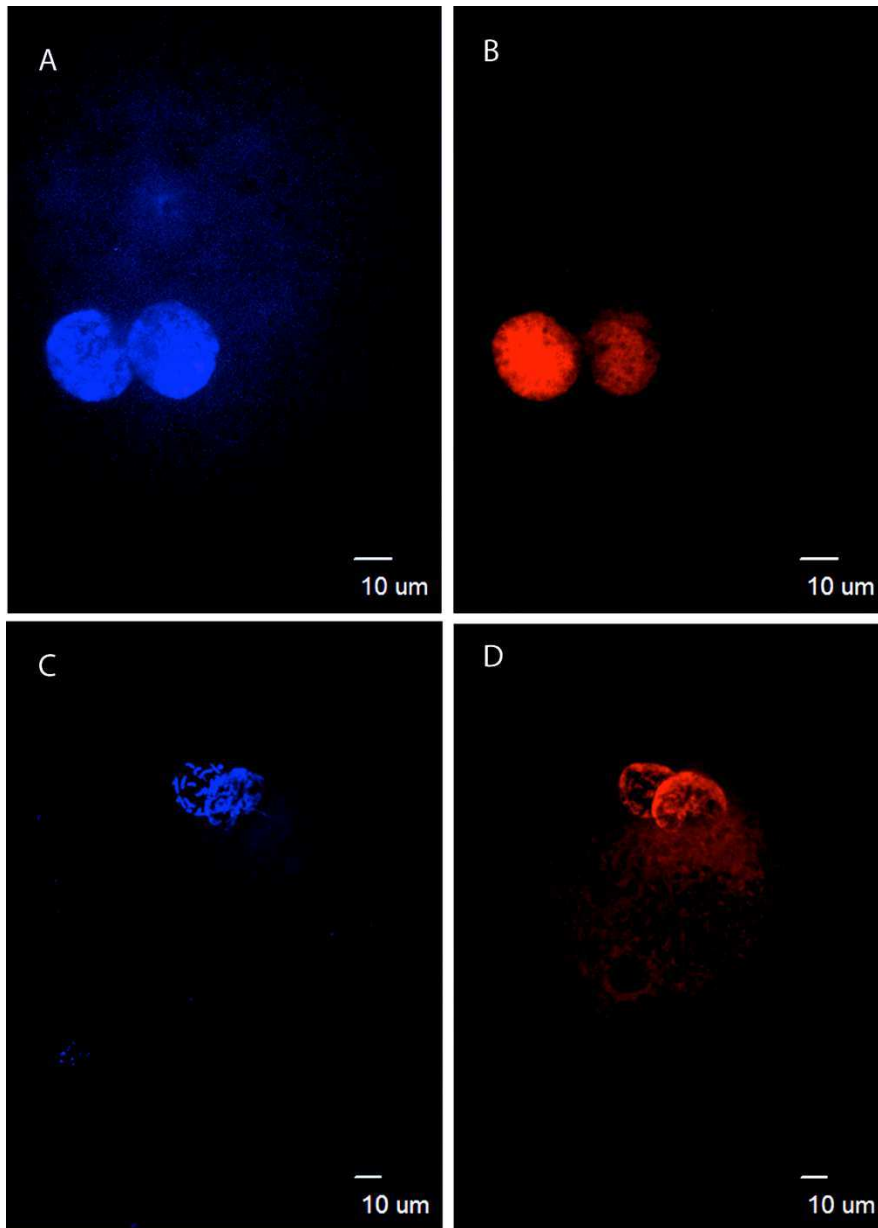
Fig 3.4

Differences in DNA and constitutive heterochromatin in equine zygotes at the pronucleus stage. Zygote developing from a young mare's oocyte with DNA and heterochromatin diffused to the entire pronuclear area and nucleolus like bodies (A and B). Zygote developing from the oocyte of an old mare in which DNA is organized in filaments and polarized in the pronuclei; heterochromatin is localized to the periphery of the pronuclear area (C and D). (Blue, DNA; Red, heterochromatin).

Discussion

To evaluate the impact of maternal age on early embryo development, we compared presumptive zygotes after sperm injection of oocytes from young mares (Young) and old mares (Old) through the use of confocal microscopy. Although sample numbers were limited, the zygotes appeared to progress through similar stages of development after sperm injection. At 4 h, the female spindle and sperm head were still intact in most Young zygotes; in contrast, Old zygotes had an intact female spindle or were undergoing anaphase. At 8 h after ICSI, most zygotes from Young were at the pronuclear stage, while Old were scattered across the different stages of development. We cannot determine whether old mares' zygotes were arrested or simply slower in approaching the pronuclear stage. Two common causes of zygote progression failure were observed, in three Old zygotes, and included premature chromosome condensation of the sperm and multiple pronuclei. No abnormal zygote morphology was observed in the young mares' zygotes.

The most prevalent difference in cytoskeletal remodeling between Young and Old was associated with actin configurations and was represented by the formation of spherical actin vesicles within the cytoplasm. Actin vesicles were present in significantly more zygotes from Old than Young (43% and 4%, respectively) zygotes. While one Young zygote contained 14 actin vesicles at 4 h, one to six vesicles were observed in Old zygotes, with vesicles in Old occurring at all time points. In a previous study, presumptive zygotes that failed to cleave in our clinical program were fixed for confocal microscopy at 24 to 51 h after ICSI (Ruggeri et al., 2015). Although the incidence of actin vesicles did not statistically differ with oocyte donor age, sperm-injected oocytes from old mares (20 to 25 yr) when compared to young mares (9 to 13 yr) had significantly more actin vesicles per presumptive zygote, and they occupied a larger area

(Ruggeri *et al.* 2015). In the study, actin vesicles were observed in a high percentage (71%) of sperm-injected oocytes, although they were observed less frequently (approximately 15%) in oocytes collected from an abattoir and allowed to age for 24 or 48 h after polar body extrusion without the injection of sperm. The actin vesicles appeared to be moving toward the periphery from earlier to later hours after ICSI (Ruggeri *et al.* 2015).

The cause and function of the actin vesicles within equine presumptive zygotes is not well known. Actin vesicles and filaments are important across species in the cytoskeleton of the oocyte and zygote. Spindle positioning and anchoring to the cortex is an actin dependent mechanism and actin polymerization and depolymerization is a dynamic process subject to disruption and remodeling during oocyte maturation (Tremoleda *et al.* 2003a, Yi & Li 2012, Coticchio *et al.* 2014). In human oocytes, it has been recently suggested that maternal aging may be associated with a reduction in the solidity of the actin cytoskeleton infrastructure causing compromised oocyte competence throughout maturation (Coticchio *et al.* 2014).

Actin microfilaments are also involved in cell cleavage during embryo development (Maro *et al.* 1986). In the sea urchin zygote, focal adhesion kinase (FAK) has been found to play a key role in the disassembly of actin filaments in the cytoskeleton and stabilization and regulation of vesicle trafficking (Schumpert *et al.* 2013). In the mouse, symmetric cell division of the zygote requires an actin network and actin-dependent spindle position checkpoints ensuring the developing mouse embryo (Chew *et al.* 2012, Metchat *et al.* 2015). We speculate that normal actin distribution can be perturbed during early embryo development and cell cleavage in zygotes from old mares and potentially is a factor in poor morphology noted for their early embryos (Carnevale *et al.* 1993b). Possible break down of the cortical actin cytoskeleton during ICSI in old mares might cause the appearance of actin vesicle structures; however, we

need to determine the role of actin vesicles in cell remodeling and potential roles in developmental failure.

The formation of pronuclei is a critical step in zygote development. At 8 h after ICSI, 80% of presumptive zygotes from Young reached the pronuclei stage, while only 33% of total presumptive zygotes (43% of normally developing zygotes) from Old were at the same stage of development. Therefore, although zygotes seemed slightly advanced for Old at the initial stage of development, progression appeared to have slowed prior to pronucleus formation.

The morphology of pronuclei was markedly different between zygotes from the two age groups. Nucleolus-like bodies were imaged in all pronuclei in Young zygotes, but none were observed in Old zygotes. In pronuclei of zygotes from Young, NLBs were unequally distributed within each pronucleus, and they were not aligned. The number of NLBs ranged from 2 to 10 for both the male and female pronuclei, with no significant difference. Nucleolus-like bodies, also called nucleolus precursor bodies (NPBs), are spherical structures visible in the pronuclei of the fertilized oocyte (Scott 2012). Nucleolus-like bodies are part of the nucleoli of each dividing cell and are sites of ribosomal RNA (rRNA). Nucleoli are positioned on the DNA of the pronuclei at the sites where genes for rRNA are located and form nucleolar-organizing regions (NORs) where heterochromatin is concentrated (Schwarzacher & Wachtler 1993). In humans, there are only five NORs with heterochromatic chromosomes situated at the nucleoli of the pronuclei, and they are the chromosomes most likely to be abnormal and cause aneuploidy (Finn *et al.* 2010, Scott 2012). In addition, NLB formation plays a key role in embryonic genome activation and the first mitotic division (Svarcova *et al.* 2009). This is the first description of NLBs in equine zygotes.

In our study, morphology of NLBs in pronuclei differed between Young and Old zygotes. In Young, NLBs were observed as expected in the form of ring-heterochromatin rich regions in

pronuclei. However, in Old, knobs of CREST antibody were localized mostly peripheral to the pronuclear area and concentrated in a polarized fashion on one side of the pronuclei, attached to the DNA filaments. In humans, synchrony of the nucleoli is necessary to avoid aberrant chromosome function and abnormal meiotic/mitotic events (Tesarik & Greco 1999). Many small, scattered nucleoli can localize at condensed DNA regions on the pronuclei and represent a very early stage of nucleoli development. This morphological status of the pronuclei with pinpoint nucleoli is a sign of slow nucleolar and cytoplasmic maturation and leads to implantation and pregnancy failure (Tesarik & Greco 1999, Scott *et al.* 2000). This observation was similar to the pattern of the nucleoli we observed in presumptive zygotes from old mares. Specifically, we observed scattered, small, pinpoint concentrations of the CREST antibody, co-localized on DNA dense filaments polarized at the two pronuclei. The difference in the pronuclei status between Young and Old could imply a nuclear and cytoplasmic asynchrony between the female and male pronuclei and a consequent failure of the zygote to proceed to successfully implant. Different pronuclear DNA content and unpaired synchronization of the cytoplasmic and nuclear maturation has been studied looking at the volume of the pronuclei as parameter of pronuclear quality. In studies conducted in mice, parthenogenetic eggs had mean nucleolar volumes less then the male and female pronuclear volume in fertilized eggs, concluding that there was less formative "material" in the cytoplasm of the egg to fulfill the correct pronuclear formation and embryo development (Kaufman 1983). We suggest that the different scattered status of the DNA and the heterochromatin signatures at the NLBs in zygotes from old mares is a sign of oocyte ooplasm incompetence to undergo chromatin decondensation.

Young and Old pronuclei were similar in size (area). Pronuclei were assumed to be male or female based on size, as reported across other species in the literature (Scott 2012). In Young

and Old zygotes, presumptive male pronuclei were significantly larger than presumptive female pronuclei. However, the mean pronucleus area was approximately 140 μm^2 larger in Young, which corresponded with a mean difference of over 200 μm^2 between presumptive male pronuclei. Potentially, more samples are needed to determine if there is a reduction in size of the male pronuclei in Old zygotes, which could suggest the Old zygotes are less competent at processing sperm chromatin.

A grading system of the human zygote has been developed to increase the incidence of implantation, and specific morphological parameters have been successfully used to predict embryo development (Scott & Smith 1998, Tesarik & Greco 1999, Scott 2012). Pronucleus formation and morphology has been largely studied in the human field to determine the developmental potential of presumptive zygotes (Tesarik & Greco 1999, Scott *et al.* 2000, Kattera & Chen 2004). Because of the importance of the role of the NLBs, pronuclear scoring has been determined based on their number, distribution and size in both male and female pronuclei and it successfully predicts implantation of the embryo (Scott 2012). For successful implantation, based of the pronuclear scoring system, the zygote pronuclei should have aligned, equally distributed and the same number of NLBs in both male and female pronuclei (Scott 2012). Therefore, the difference we observed in the pronuclei from zygotes from young and old mares may indicate differences in zygote quality and potential to develop into a viable embryo.

In conclusion, our study is the first to describe equine zygote development after ICSI of oocytes from young and old mares. In general, similar stages of zygote development were observed after ICSI of oocytes from young and old mares, with the presence of actin vesicles imaged more frequently in Old than Young zygotes. Differences in pronuclei for zygotes from Young and Old included the presence of NLBs only in Young and a defined pericentric

heterochromatin pattern in Old zygote pronuclei. Our study represents the first attempt to characterize zygote development after ICSI of oocytes from young and old mares, with the use of confocal microscopy.

CHAPTER IV: CYTOSKELETAL ALTERATIONS ASSOCIATED WITH DONOR AGE AND CULTURE INTERVAL FOR EQUINE OOCYTES AND POTENTIAL ZYGOTES THAT FAILED TO CLEAVE AFTER ICSI[3]

Summary

Intracytoplasmic sperm injection (ICSI) is an established method to fertilize equine oocytes, but not all oocytes cleave after ICSI. The aims of the present study were to examine cytoskeleton patterns in oocytes after aging in vitro for 0, 24 or 48 h (Experiment 1) and in potential zygotes that failed to cleave after ICSI of oocytes from donors of different ages (Experiment 2). Cytoplasmic multiasters were observed after oocyte aging for 48 h ($P < 0.01$). A similar increase in multiasters was observed with an increased interval after ICSI for young mares (9-13 years) but not old (20-25 years) mares. Actin vesicles were observed more frequently in sperm-injected oocytes from old than young mares. In the present study, multiasters appeared to be associated with cell aging, whereas actin vesicles were associated with aging of the oocyte donor.

Introduction

Intracytoplasmic sperm injection (ICSI) is an established assisted reproductive technology in human fertility clinics, and in the past decade, ICSI has been modified for equine clinical use, to produce offspring from stallions with limited or poor quality sperm and older, subfertile mares (Grondahl *et al.* 1997, Choi *et al.* 2002, Galli *et al.* 2002, Hinrichs *et al.* 2002,

---

[3] A preliminary report of the research in this chapter was published by Ruggeri, E. et al. (2015) Reproduction, Fertility, and Development *27(6)* 944-956. Published figures include 4.1, 4.2, 4.3, 4.4, and 4.5

Tremoleda *et al.* 2003b, Altermatt *et al.* 2009, Palermo *et al.* 2014). However, not all sperm-injected oocytes undergo the first cleavage division. The cause of this developmental failure is probably multifactorial and has not been adequately studied in either species.

Maternal aging is associated with a decline in fertility in both the mare and woman. Fertility is reduced in mares as they enter their teen years, but the decline in fertility is marked in old (≥20 years) mares and associated with a high incidence of early embryo loss (Ginther 1979, Carnevale & Ginther 1992, Carnevale 2008). The primary factor associated with reduced fertility in the old mare is oocyte developmental quality (Carnevale & Ginther 1995). Recent findings suggest chromosomal misalignment frequently occurs in MII oocytes of old mares (Carnevale *et al.* 2012). A similar decline in fertility is noted in women and is associated with reduced oocyte quality and, specifically, increased aneuploidy (Battaglia *et al.* 1996, Kuliev *et al.* 2003). Although the age-associated decline in oocyte quality is generally accepted in both species, relatively little is known regarding the inherent capabilities of oocytes from donors of different ages for fertilization and zygote development.

Nuclear and cytoskeletal rearrangements are involved in oocyte maturation and competence acquisition (Combelles *et al.* 2002, Sun & Schatten 2006, Barrett & Albertini 2010, Yi & Li 2012). Actin and microtubules are important contributors to spindle organization and the oocyte's ability to activate after fertilization (Schatten 1994, Dell'Aquila *et al.* 2001, Tremoleda *et al.* 2001, Yi *et al.* 2013, Yu *et al.* 2014). The close apposition of paternal and maternal genomes in equine zygotes is characterized by a series of cytoskeleton-mediated events, mostly involving microtubule and chromatin remodeling (Tremoleda *et al.* 2003b). The effects of aging of the oocyte donor and cell senescence on changes in actin and tubulin patterns have not been studied in the equine oocyte before or after fertilization, and understanding modifications of the

54

actin and microtubule cytoskeleton that are associated with donor aging in relationship to oocyte maturation and fertilization has been untouched (Coticchio *et al.* 2014).

The aim of the present studies was to elucidate changes in the oocyte associated with failure of zygote development after equine ICSI, with a focus on cytoskeletal changes associated with donor aging and cellular senescence. We hypothesized that cytoskeletal alterations are associated with oocyte aging *in vitro* and affected by age of the oocyte donor. The specific objectives of the present study were to: (1) determine cellular alterations, especially with regard to actin and microtubules, that occur with oocyte aging *in vitro*; (2) examine oocytes that failed to cleave after sperm injection to determine potential causes of failure of zygote development; (3) identify characteristics of oocytes that fail to cleave after ICSI that are associated with cellular aging or aging of the oocyte donor; and (4) determine whether cytoskeleton remodeling and chromosome organization are different in oocytes that failed to cleave after sperm injection that were obtained from young (9-13 years) versus old (20-25 years) mares.

Materials and Methods

Samples used to examine cytoskeleton patterns in oocytes after aging *in vitro* for 0, 24 or 48 h (Experiment 1) were collected at Avantea (Cremona, Italy), whereas those used to examine potential zygotes that failed to cleave after ICSI of oocytes from donors of different ages (Experiment 2) were collected at Colorado State University, Equine Reproduction Laboratory (Fort Collins, CO, USA).

Oocyte Collection and Manipulation

Experiment 1

For Experiment 1, samples were collected in Cremona (Italy; 45° latitude) during the natural breeding season (March and April 2014). Ovaries from mares of different breeds were collected from a local abattoir and transported within approximately 2 h at 24°C to the laboratory, where all cumulus oocyte complexes (COCs) were collected within an approximate 2-h interval. After retrieval, the COCs were placed in culture media (Dulbecco's modified Eagle's medium (DMEM)/F12 (D8900; Sigma Aldrich, Milan, Italy) containing 10% serum replacement (Life Technologies, Monza, Italy) and 0.1 IU ml^{-1} human menopausal gonadotropin (HMG) (Menopur 75; Ferring, Milan, Italy) at 38.5°C in 5% CO_2 and air. After culture for 28 h, oocytes were denuded of cumulus cells. Only oocytes with a well-defined polar body were used for the study, with some oocytes fixed at 28 h and others returned to culture for an additional 24 or 48 h prior to fixation. Oocytes were fixed as described previously in a solution containing 2% formaldehyde and 0.1% Triton X-100 (Microtubule Stabilization Buffer Extraction Fix (MTSB-XF); Messinger and Albertini 1991) at room temperature at three different time points: (1) Time 0, equivalent to the expected time of MII (28 h in culture; $n = 11$); (2) Time 24, after an additional 24 h of culture, equivalent to 52 h in culture ($n = 14$); and (3) Time 48, after an additional 48 h culture after Time 0, equivalent to 76 h in culture ($n = 13$). After fixation in MTSB-XF, oocytes were rinsed and stored at 4°C in wash solution (phosphate-buffered saline (PBS) containing 1% bovine serum albumin (BSA) and 0.1% Triton X-100).

Experiment 2

The mares used in Experiment 2 were between 9 and 25 years of age, housed in Fort Collins (CO, USA; 40° latitude), and were part of a clinical ICSI program. Reproductive cycles were monitored by ultrasonography to determine follicular growth and stage oocyte collections. Oocytes were collected during the follicular phase from the dominant follicle(s) approximately 35 mm in diameter. Oocytes were collected by ultrasound-guided transvaginal follicular aspirations (Carnevale *et al.* 2000a) approximately 24 h after administration of human chorionic gonadotropin (hCG; 1500 IU, i.v.; Intervet, Millsboro, DE, USA) and deslorelin acetate (SucroMate; 0.75 mg, i.m.; Bioniche Life Sciences, Belleville, Canada). Collected oocytes were cultured in medium (TCM-199 with Earle's salts; Gibco BRL Life Technologies, Grand Island, NY, USA) containing 10% fetal calf serum (FCS; Cell Generation, Fort Collins, CO, USA), 0.2 mM sodium pyruvate, and 25 μg mL^{-1} gentamicin sulfate (Sigma Aldrich, St. Louis, MO, USA) at 38°C or 38.5°C in an atmosphere of 6% CO_2 and air.

Approximately 44 h after the time of deslorelin and hCG administration to donor mares, oocytes were denuded of cumulus cells and injected with frozen spermatozoa from various stallions. Potential zygotes were cultured in medium DMEM/F12 (Sigma-Aldrich) with 10% FCS under paraffin oil at 38.5 C° and in 5% CO_2, 5% O_2 and 90% N_2. Injected oocytes were assessed after approximately 24 h for initial cleavage. Between 24 and 51 h after ICSI, injected oocytes that had not cleaved and did not show signs of cleavage (fragmentation or indentation of oolemma) were fixed in MTSB-XF at room temperature before being washed with a solution containing 1% bovine serum albumin (BSA) and 0.1% Triton X-100 and stored at 4°C until being moved into wash solution before immunostaining.

Primary antibodies were diluted in 2% normal goat serum and incubated with the oocyte on a rotating platform shaker for 4 h at 37°C. Oocytes were stained with the following primary antibodies: α/β-tubulin cocktail (1:100, mouse; Sigma-Aldrich) and human-anti centromere antibody CREST/ACA (1:100; Life Technologies). Following incubation with the primary antibody, oocytes were washed in 2% normal goat serum for at least 12 h at 4°C, and then incubated for 4 h with secondary antibodies conjugated to either Alexa 488 or Alexa 647 (1:100; Jackson ImmunoResearch Laboratories, West Grove, PA, USA) diluted in 2% normal goat serum. Oocytes were rinsed for 5 h in 2% normal goat serum and incubated for another 5 h with phalloidin (Alexa 561; Life Technologies) and Hoechst 33258-(1μg mL^{-1}; Life Technologies) at 37°C. Oocytes were then mounted onto coverslips (50% glycerol in PBS with 25 mg mL^{-1} sodium azide and 1 μg mL^{-1} Hoechst 33258) for imaging (Barrett & Albertini 2007).

Images were acquired on an Olympus (Waltham, MA, USA) IX81 spinning disk confocal (CSU22 head) microscope using either a 60x/1.42 Numerical Apperature (NA) Differential Interference Contrast (DIC) planapochromatic or a 40x/1.35NA planapochromatic oil lens. Z-stacks were acquired at a magnification of 60x and at 0.2-μm intervals. Magnification at 40x was used to image the entire oocyte at 1-μm intervals. Images were acquired with a Photometrics (Tucson, AZ, USA) Cascade II CCD camera and analyzed using SlideBook software (Intelligent Imaging Innovations, Denver, CO, USA).

Actin and α/β-Tubulin Morphometric Analysis of Oocyte Measurements

Oocytes were imaged for: the presence or absence of sperm head or tail; tubulin multiasters and their respective shapes (gamma, twisted elliptical or star); actin vesicles and their position within the oocyte (cortex, cortex and internal, or internal); the presence of the meiotic

spindle and the orientation for the first and, if present, the second spindle observed in the oocyte with polarity (bipolar or multipolar); and transzonal projections (TZPs; dense or thin filaments of actin at the projections).

The total integrated fluorescence intensity of actin was determined from compressed images collected at 1-μm intervals at 40x, where actin vesicles were selected using the "draw function" in Slidebook. For spindle perimeter and area measurements, the entire oocyte was imaged at x40 magnification at 1-μm intervals. SlideBook software was use to determine the perimeter and area measurements.

Widths of the zona pellucida (ZP) and perivitelline space (PVS) were determined by taking the average of two measurements at the widest and the narrowest widths of the oocyte. The inner zona pellucida (IZP) was determined by subtracting the measurement of the ZP from the full oocyte diameter, which was the average of four separate measurements.

Statistical Analysis

For Experiment 1, data were analyzed using Chi-square analysis. In Experiment 2, continuous data (using mares of all ages and potential zygotes fixed at all hours after ICSI) were compared using Student's *t*-test, and correlations were analyzed using Spearman correlation. Additional analyses were performed for Experiment 2 using subsets of the data for mare age (Young (9-13 years) and Old (20-25 years) mares) and time from ICSI to fixation (24-28 h and 44-51 h); analyses were performed using Fisher's exact test (proportions) or Student's t-test (continual data). For analyses of oocytes having multiple spindles, analyses were performed on each spindle.

Results

Experiment 1

No significant differences were observed in the number of oocytes at Time 0 ($n = 11$),

Time 24 ($n = 14$) or Time 48 ($n = 13$) in terms of the presence of actin vesicles or kinetochores,

position and polarity of spindles, or configuration of DNA. However, more ($P < 0.05$) oocytes

had microtubule multiasters at Time 48 than at Times 0 and 24 (Table 4.1; Fig. 4.1).

Table 4.1: Number of oocytes with specific morphologies after maturation and culture *in vitro* to Time 0 (expected time of MII), Time 24 (culture for 24 h after MII) and Time 48 (culture for 48 h after MII)
With rows, values with different superscript letter differ ($P < 0.05$)

Morphological end-point	0 h	24 h	48 h	Overall *P*-value
Actin vesicles	1/11 (9)	2/14 (14)	2/13 (15)	0.89
Chromatin				
Condensed	11/11 (100)	12/14 (86)	10/13 (77)	0.25
Diffuse	0/11 (0)	2/14 (14)	3/13 (23)	0.25
Kinetochores	11/11 (100)	13/14 (93)	11/13 (85)	0.38
Spindle				
Bipolar	11/11 (100)	13/14 (93)	10/13 (77)	0.16
Multipolar	0/11 (0)	1/14 (7)	3/13 (23)	0.16
Spindle position				
Centered	1/11 (9)	4/14 (29)	5/13 (39)	0.26
Cortical	10/11 (91)	10/14 (71)	8/13 (62)	0.26
Tubulin multiasters	1/11 (9)[a]	2/14 (14)[a]	11/13 (85)[b]	<0.001
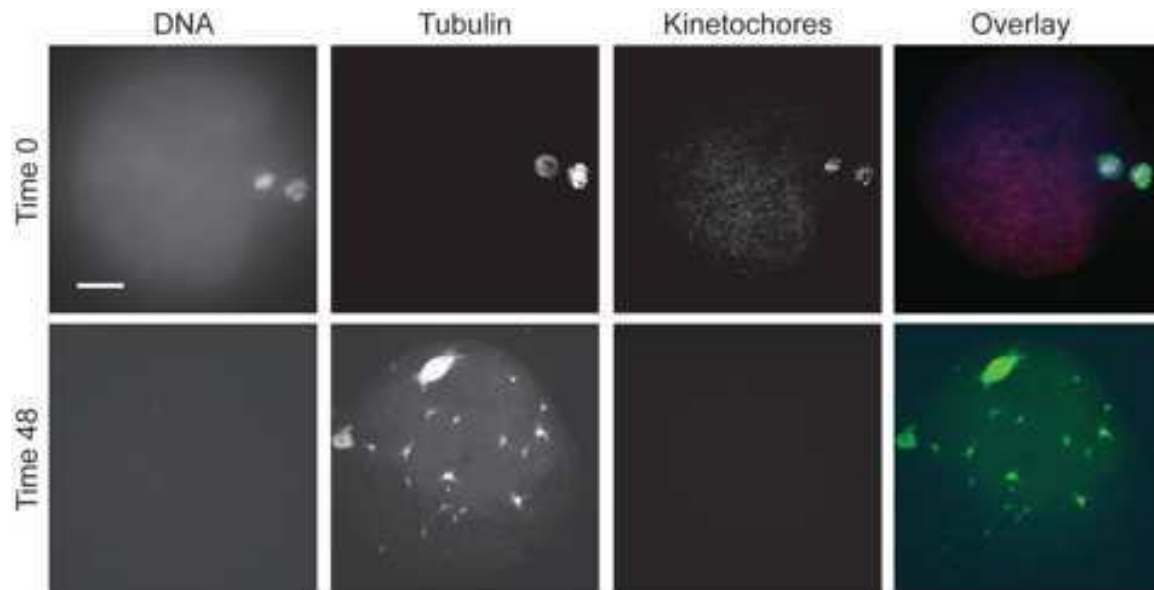
Fig. 4.1
    Equine oocytes cultured *in vitro* for 28 h (Time 0; predicted time of MII) with no tubulin multiasters and for a further 48 h (Time 48) with diffuse foci of tubulin asters. Blue, chromatin; Green, tubulin; Red, kinetochores. Scale bar = 20 μm.

Experiment II

All potential zygotes ($n = 52$) were used to compare mares of all ages (9-25 years) and number of hours from ICSI (ICSI = 0 h) to fixation (24-51 h) for various morphologic parameters. Similar morphologic parameters were also compared for subgroups of mares classified as Young (9-13 years; $n = 11$) and Old (20-25 years; $n = 32$) and potential zygotes fixed at 24-28 h ($n = 29$) or 44-51 h ($n = 17$) after ICSI. The time to fixation was not different for mares classified as Young or Old (mean ($\pm$ SEM) of 38.1 $\pm$ 3.7 and 33.6 $\pm$ 1.8 h, respectively; $P = 0.24$).

Sperm Head or Tail

An intact sperm head or tail was observed in 9 of 52 (17%) presumptive zygotes after ICSI. Donor age did not affect the number of observations; however, the mean hour of fixation was lower for oocytes with than without an intact sperm head or tail (Table 4.2), and the frequency of an observed sperm was higher ($P = 0.04$) for oocytes fixed at 24-28 h than 44-51 h (Table 4.3).

Table 4.2: Comparison of mean donor age (years) and hours from intracytoplasmic sperm injection to fixation for presence or absence of observed morphological end-points ($n = 52$)
Data show the mean ± s.e.m. with number of observations in parentheses. Spindle 1, first spindle; spindle 2, second spindle; TZPs, transzonal projections

Morphological end-point	Donor age			Hours after ICSI		
	Yes	No	P-value	Yes	No	P-value
Actin vesicles	18.7 ± 0.9 (37)	19.7 ± 1.3 (15)	0.56	35.2 ± 1.8 (37)	32.2 ± 2.4 (15)	0.37
Actin vesicle position						
Cortex	16.2 ± 3.6 (5)	19.3 ± 0.8 (33)	0.22	47.2 ± 1.2 (5)	33.1 ± 1.9 (33)	0.01
Cortex and inside	19.0 ± 1.9 (8)	18.7 ± 0.9 (31)	0.89	39.5 ± 4.7 (8)	33.6 ± 1.8 (31)	0.18
Inside	19.2 ± 0.9 (24)	18.1 ± 1.6 (15)	0.55	31.3 ± 1.9 (24)	40.5 ± 3.0 (15)	0.01
Aster shape						
Gamma	17.8 ± 1.0 (25)	18.1 ± 2.2 (7)	0.88	35.2 ± 2.2 (25)	39.6 ± 3.7 (7)	0.35
Twisted elliptical	18.2 ± 1.2 (17)	17.5 ± 1.4 (15)	0.73	35.3 ± 2.6 (17)	37.1 ± 2.8 (15)	0.65
Star	18.9 ± 1.1 (23)	15.3 ± 1.6 (9)	0.08	36.3 ± 2.3 (23)	35.7 ± 3.6 (9)	0.88
Multiasters	17.9 ± 0.9 (32)	20.8 ± 1.1 (20)	0.05	36.1 ± 1.9 (32)	31.5 ± 2.2 (20)	0.13
No. of spindles						
One	19.2 ± 0.8 (40)	-	0.45	34.1 ± 1.6 (40)	-	0.80
Two	17.8 ± 2.0 (9)	-		35.1 ± 4.2 (9)	-	
Sperm head or tail	19.8 ± 1.8 (9)	18.8 ± 0.8 (43)	0.62	26.3 ± 0.4 (9)	36.0 ± 1.7 (43)	0.01
Spindle orientation						
Bipolar spindle 1	18.5 ± 1.1 (22)	19.3 ± 1.0 (27)	0.57	32.6 ± 2.3 (22)	35.7 ± 2.0 (27)	0.31
Bipolar spindle 2	19.5 ± 1.9 (6)	14.3 ± 4.4 (3)	0.23	30.8 ± 4.3 (6)	43.7 ± 7.8 (3)	0.16
Multipolar spindle 1	19.3 ± 1.0 (27)	18.8 ± 1.1 (23)	0.70	35.7 ± 2.0 (27)	32.4 ± 2.2 (23)	0.26
Multipolar spindle 2	14.3 ± 4.4 (3)	17.0 ± 3.0 (2)	0.69	43.7 ± 7.8 (3)	26.0 ± 2.0 (2)	0.18
TZPs						
Dense	18.2 ± 0.8 (37)	-	0.10	32.7 ± 1.6 (37)	-	0.07
Thin	20.9 ± 1.5 (15)	-		38.5 ± 3.1 (15)	-	

Table 4.3: Number of injected oocytes in which different morphological end-points were observed according to donor age group and time of fixation after intracytoplasmic sperm injection

Young, mares 9-13 years of age; Old, mares 20-25 years of age; ICSI, intracytoplasmic sperm injection; Spindle 1, first spindle; spindle 2, second spindle; TZPs, transzonal projections

Morphological end-point	Donor age (years)			Hours (h)		
	Young ($n = 11$)	Old ($n = 32$)	P-value	24-28 h ($n = 29$)	44-51 h ($n = 13$)	P-value
Actin vesicles	9/11 (82%)	22/32 (69%)	0.70	19/29 (66%)	10/13 (77%)	0.72
Actin vesicle position						
Cortex	3/9 (33%)	2/23 (9%)	0.12	0/20 (0%)	5/10 (50%)	0.002
Cortex and inside	1/9 (11%)	5/23 (22%)	0.65	3/21 (14%)	1/10 (10%)	1.00
Inside	5/9 (56%)	15/23 (65%)	0.70	16/21 (76%)	4/10 (40%)	0.10
Aster shape						
Gamma	6/8 (75%)	11/15 (73%)	1.00	12/14 (86%)	7/11 (64%)	0.35
Twisted elliptical	3/8 (38%)	8/15 (53%)	0.67	10/14 (71%)	5/11 (45%)	0.24
Star	5/8 (63%)	13/15 (87%)	0.30	9/14 (64%)	8/11 (73%)	1.00
Multiasters	8/11 (73%)	15/32 (47%)	0.18	14/29 (48%)	11/13 (85%)	0.04
Sperm head or tail	2/11 (18%)	7/32 (22%)	1.00	9/29 (31%)	0/13 (0%)	0.04
Spindle orientation						
Bipolar spindle 1	5/10 (50%)	13/30 (43%)	0.73	15/27 (56%)	4/13 (31%)	0.18
Bipolar spindle 2	0/2 (0%)	4/5 (80%)	0.14	5/6 (83%)	0/1 (0%)	0.28
Multipolar spindle 1	5/10 (50%)	17/31 (55%)	1.00	12/28 (43%)	9/13 (69%)	0.18
Multipolar spindle 2	2/2 (100%)	1/2 (50%)	1.00	1/3 (33%)	1/1 (100%)	1.00
TZPs						
Dense	8/11 (73%)	20/32 (63%)	0.72	22/29 (76%)	8/13 (62%)	0.46
Thin	3/11 (27%)	12/32 (38%)		7/29 (24%)	5/13 (38%)	

Spindle measurements, number and polarity

Of the 52 presumptive zygotes, 44 (85%) had one spindle, nine (17%) had two spindles, and three (6%) had no observed spindle (Fig. 4.2). The total number of spindles observed was

58; of these, 28 spindles (48%) were bipolar and 30 (52%) were multipolar (Fig. 4.3). The

number of spindles, spindle orientation, and size were not affected by donor age (Tables 4.2-4.4),

but the mean area of the spindle was greater ($P = 0.01$) and the mean length of the perimeter was

longer ($P = 0.03$) if fixation occurred at 44-51 versus 24-28 h after ICSI (Table 4.4).
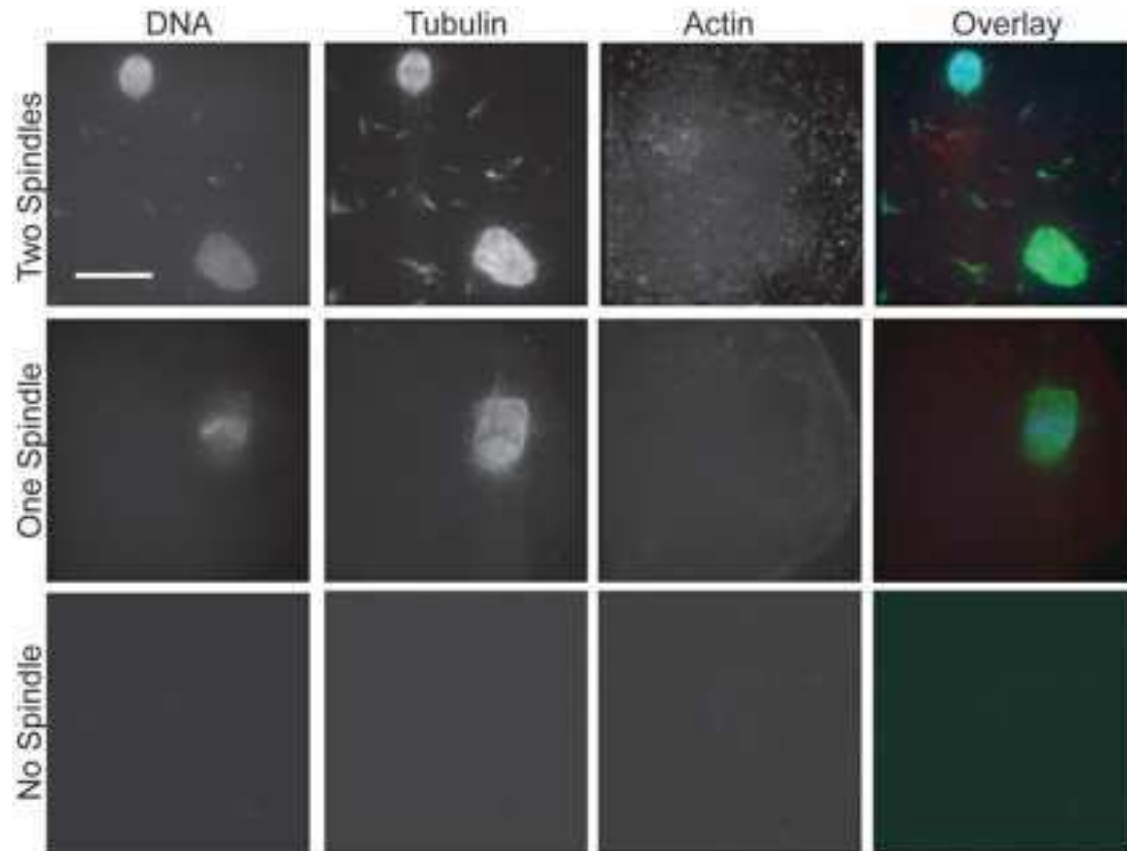
Fig. 4.2
Sperm-injected oocytes had different numbers of spindles after failing to cleave. Two
spindles represent the female and male sets of chromosomes; one spindle represents the
female set of chromosomes; no spindles were present after degeneration and
decondensation of the spindle structures. Blue, chromatin; green, tubulin; red, actin. Scale
bar= 20 μm.
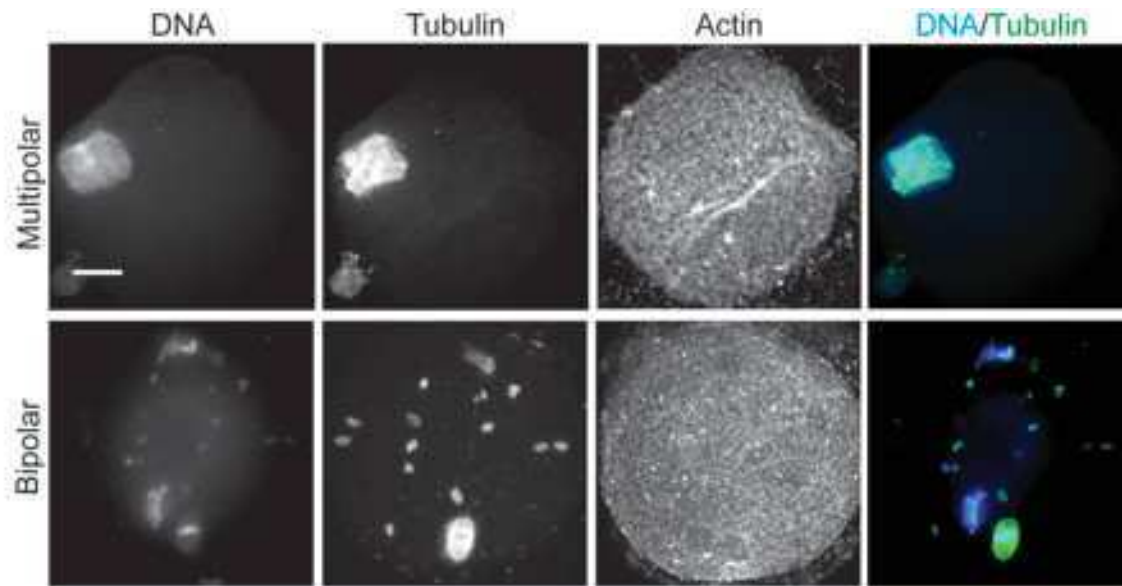
Fig. 4.3

Multipolar and bipolar spindles in equine failed zygotes, with four poles imaged in the multipolar spindle. Blue, chromatin; green, tubulin. Scale bar= 20 μm.

Table 4.4: Spindle and actin vesicle parameters according to donor age group and time of fixation after intracytoplasmic sperm injection

Data show the mean ± s.e.m. Young, mares 9-13 years of age; Old, mares 20-25 years of age; ICSI, intracytoplasmic sperm injection; Spindle 1, first spindle; spindle 2, second spindle; ADU, Analog-Digital-Unit

| Morphological end-point	Donor age			Time after ICSI (h)		
	Young ($n = 11$)	Old ($n = 32$)	P-value	24-28 ($n = 29$)	44-51 ($n = 13$)	P-value
Actin vesicles						
Area (μm^2)	573±226	1570±377	0.05	744±200	1720±491	0.04
Perimeter (μm)	109±20	215±35	0.05	145±30	225±42	0.06
No. of actin vesicles	2.0±0.2	8.1±1.8	0.05	3.71±1.03	8.5±2.5	0.05
Sum intensity of actin vesicles ($x10^7$ ADU)	4.6±1.4	29.8±15.0	0.12	6.4±2.0	81.6±40.8	0.01
Sum intensity per actin vesicle ($x10^7$ ADU)	2.6±0.7	6.2±2.3	0.91	4.5±2.0	7.5±2.5	0.10
Time after ICSI (h)	34.7±4.0	32.1±2.7	0.78	-	-	-
Spindle						
Area (μm^2)	124±16	123±14	0.46	119±14	270±96	0.01
Perimeter (μm)	285±37	258±22	0.42	227±14	318±38	0.03
Time after ICSI (h)	35.7±4.5	32.5±4.5	0.90	-	-	-

Chromosome configurations and presence of kinetochore proteins

Chromosome configuration was determined and categorized based on the state and localization of the chromatin within the spindle (Table 4.5). Of the 58 spindles observed, 19 (33%) had chromosomes not aligned on the spindle plate, with chromatin dispersed on the spindle microtubules. Another 19 spindles (33%) had dispersed chromatin on the spindle microtubules, but no chromosomes. Although most of the chromosome configurations were in these two categories, no significant differences were found among all categories. Misaligned chromosomes were observed in 43% of the sperm-injected oocytes, but chromosome

misalignment did not differ with donor age or hours after ICSI. Kinetochore proteins were

observed in only 8 of 58 (14%) spindles.

Table 4.5: Number of injected oocytes in each category of chromatin localization according to donor age group and time of fixation after intracytoplasmic sperm injection
 Chromatin localization was categorized as follows: 1, chromosomes aligned compact at the metaphase plate; 2, chromosomes aligned and compact at the metaphase plate and chromatin dispersed throughout the spindle; 3, compact chromosomes scattered and not aligned at the metaphase plate; 4, compact chromosomes scattered, not aligned at the metaphase plate and chromatin dispersed throughout the spindle; 5, chromatin only dispersed throughout the spindle; 6, compact chromosomes aligned at the metaphase plate and elongated chromosomes positioned out of the plate. Young, mares 9-13 years of age; Old, mares 20-25 years of age; ICSI, intracytoplasmic sperm injection; Spindle 1, first spindle; spindle 2, second spindle

Endpoints	Donor age			Time ICSI to Fixation		
	Young (%)	Old (%)	P-value	24-28 h (%)	44-51 h (%)	P-value
Spindle 1						
1	1/10 (10)	2/30 (7)		2/27 (7)	1/13 (8)	
2	1/10 (10)	5/30 (17)		5/27 (19)	0/13 (0)	
3	1/10 (10)	5/30 (17)	0.76	1/27 (4)	4/13 (31)	0.15
4	2/10 (20)	8/30 (27)		7/27 (26)	4/13 (31)	
5	5/10 (50)	7/30 (23)		10/27 (37)	3/13 (23)	
6	0/10 (0)	3/30 (10)		2/27 (7)	1/13 (8)	
Spindle 2						
1	0/2 (0)	0/5 (0)		0/6 (0)	0/1 (0)	
2	0/2 (0)	0/5 (0)		1/6 (17)	0/1 (0)	
3	0/2 (0)	0/5 (0)	1.00	0/6 (0)	0/1 (0)	1.00
4	2/2 (100)	3/5 (60)		3/6 (50)	1/1 (100)	
5	0/2 (0)	2/5 (40)		2/6 (33)	0/1 (0)	
6	0/2 (0)	0/5 (0)		0/6 (0)	0/1 (0)	

Multiasters

Within the 52 oocytes analyzed, 32 (62%) contained microtubule asters with differing

shapes, including gamma, twisted elliptical, and star shapes. Of the 32 oocytes with multiasters,

25 (78%) had gamma-shaped asters, 17 (53%) had twisted elliptical shaped asters, and 23 (72%)

had star-shaped asters. There were no significant differences between the different categories

observed. The mean number of multiasters per potential zygote was higher ($P = 0.03$) in Young

versus Old mares (Table 4.6), and the mean age of the oocyte donor was younger ($P = 0.05$)

when multiasters were observed compared with when they were not observed (Table 4.2; Fig.

4.4). A negative correlation between mare age and number of multiasters was observed: as mare

age increased, the number of multiasters decreased ($P = 0.04$, $r = -0.28$). Multiasters were more

prevalent at 44-51 h than 24-28 h after ICSI ($P = 0.04$; Table 4.3). The presence of multiasters

was not correlated to the number of spindles, the presence of multipolar spindles or the presence

of actin vesicles.

Table 4.6: Number of actin vesicles and tubulin multiasters and fixed oocyte measurements according to donor age group and time of fixation after intracytoplasmic sperm injection
Data show the mean ± s.e.m. Young, mares 9-13 years of age; Old, mares 20-25 years of age; ICSI, intracytoplasmic sperm injection; IZP, inner zona pellucida diameter; PVS, perivitelline space width; ZP, zona pellucida thickness.

	Donor age		P-value	Time after ICSI (h)		P-value
	Young ($n = 11$)	Old ($n = 32$)		24-28 ($n = 29$)	44-51 ($n = 13$)	
No. of actin vesicles	1.73 ± 0.30	6.37 ± 1.60	0.01	3.45 ± 1.35	6.54 ± 2.15	0.22
No. of multiasters	9.45 ± 2.47	4.47 ± 1.01	0.03	5.14 ± 1.24	8.85 ± 1.77	0.10
Width ($\times 10^3$ μm)						
IZP	87.0 ± 1.4	88.8 ± 1.5	0.37	90.2 ± 1.4	86.2 ± 2.9	0.17
PVS	8.03 ± 1.62	8.37 ± 0.52	0.85	8.43 ± 0.66	9.53 ± 1.43	0.43
ZP	19.9 ± 0.7	19.3 ± 0.6	0.52	18.9 ± 0.5	19.9 ± 1.0	0.15
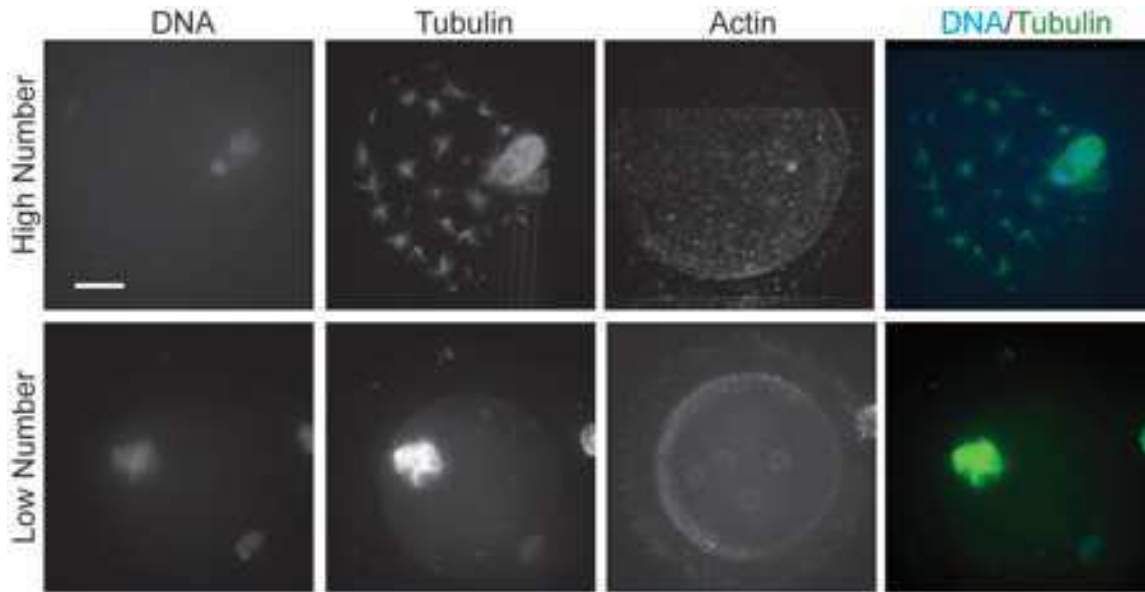
Fig. 4.4

Tubulin multiasters in failed equine oocytes that failed to cleave after intracytoplasmic sperm injection, with representative high and low numbers of tubulin multiaster foci. Blue, chromatin; green, tubulin. Scale bar= 20µm.

Actin vesicles: presence, position, dimensions, number and intensity

Actin vesicles were present in 37 of 52 oocytes (71%; Fig. 4.5). The position of actin vesicles within the ooplasm was affected by time after ICSI, because the mean hour of fixation was significantly sooner when actin vesicles were observed within the ooplasm and later when vesicles were observed at the cortex (Table 4.2). Within the presumptive zygotes from Old versus Young mares, actin vesicles occupied a larger ($P = 0.05$) area, and more ($P = 0.05$) actin vesicles were observed (Table 4.4). The mean perimeter around the actin vesicles was greater ($P = 0.05$) in presumptive zygotes from Old than Young mares (Table 4.4). The sum intensity of actin vesicles was greater in oocytes fixed at 44-51 than 24-28 h ($P = 0.01$; Table 4.4). The mean number of actin vesicles and the area occupied by actin vesicles were greater when fixation occurred at 44-51 than 24-28 h after ICSI ($P = 0.05$ and $P = 0.04$, respectively; Table 4.4).
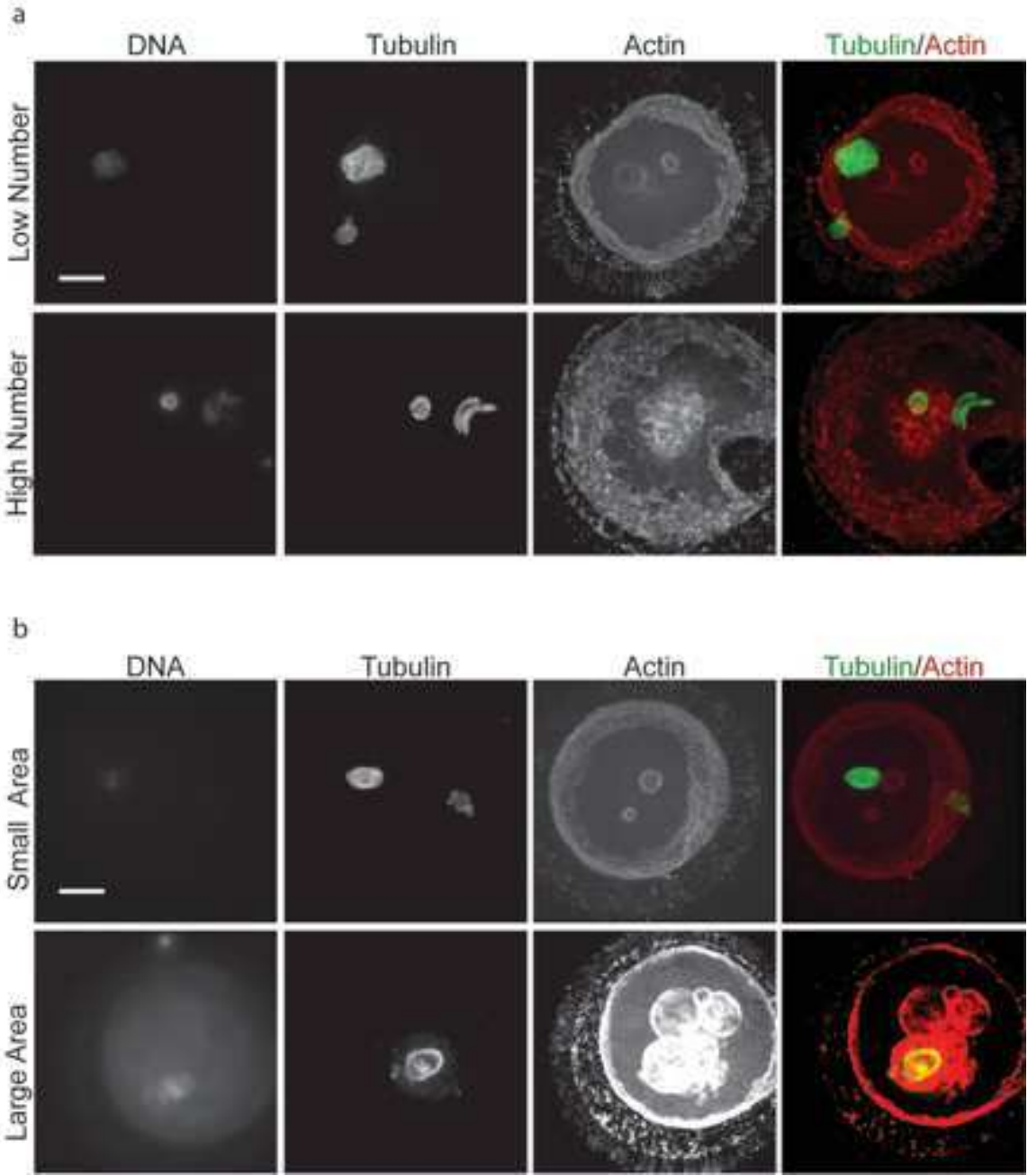
70

Fig. 4.5
Equine oocytes that failed to cleave after intracytoplasmic sperm injection, with (*a*) low and high numbers of actin vesicles and (*b*) small and large areas of actin vesicles. Green, tubulin; red, actin. Scale bar= 20 μm

Discussion

ICSI has been successfully applied to equine and human oocytes when fertilization needs to be improved and for cases of infertility (Squires *et al.* 2003b, Butts *et al.* 2014). At Colorado State University's Equine Reproduction Laboratory, cleavage rates after experimental equine ICSI have ranged from 61% to 85%, but a percentage of sperm-injected equine oocytes will fail to complete fertilization and cleave (Altermatt *et al.* 2009, Sessions-Bresnahan *et al.* 2014). Zygote arrest and failure of embryo development was previously reported after equine ICSI, and the researchers determined that in the 24% of sperm-injected oocytes that did not complete fertilization; most defects were associated with failures of sperm integration or completion of meiosis, and oocyte activation did not occur (Tremoleda *et al.* 2003b). In the present study, we examined equine potential zygotes from our clinical program that failed to complete the first cleavage division or show signs of cleavage (fragmentation or indentation of the oolemma) starting at approximately 24 h after ICSI. Samples were collected during one breeding season in which an overall cleavage rate of 60.5% was obtained. In our experience, after the first check, sperm-injected oocytes displaying no signs of cleavage will fail to cleave if they are kept in culture, and if delayed cleavage does occur, the embryos will arrest at an early stage. However, we did maintain some potential zygotes in culture for up to 51 h to confirm the failure of cleavage. In our clinical program, mares were used as oocyte donors because of: (1) mare subfertility, which is often associated with aging; (2) availability of limited or poor quality spermatozoa; or (3) a combination of the two. Sperm factors, which we were not able to analyze, would have had an effect on fertilization failure, as many sperm injections were done with spermatozoa with unknown or poor viability. Consequently, we focused on two aspects of aging

related to the oocyte (i.e. cellular senescence associated with time in culture and maternal aging of the oocyte donor) and their influence on chromosome integrity and cytoskeletal structure.

The cytoskeleton has an essential role in fertilization and zygote development, and cytoskeletal remodeling should be in synchrony with nuclear events, which include crossover of the female and male genomes (Tremoleda *et al.* 2001). In the present study, we evaluated two major cytoskeletal components, microtubules and actin. Microtubules are present in the oocyte during fertilization, and assemble in the cytoplasm soon after sperm incorporation (Schatten *et al.* 1985, Tremoleda *et al.* 2003b). The role of the microtubules at fertilization and during zygote development has been studied in mammalian murine, porcine, bovine, equine and primate oocytes (Schatten *et al.* 1985, Schatten 1994, Kim *et al.* 1996, Tremoleda *et al.* 2003b, Delimitreva *et al.* 2011, Hara *et al.* 2012). In the oocyte, microtubule multiasters are required for zygote and embryo development, and they are involved in multiple rearrangements and configuration changes in the cytoskeleton microtubule matrix (Schatten *et al.* 1985, Schatten *et al.* 1986, Schatten 1994). Depending on species, centrosomes are located at the center of microtubule multiasters and are of both maternal and paternal origin, as in the mouse and cow, or are of paternal origin, as in humans (Schatten 1994). During fertilization of equine oocytes, microtubule organization is predominantly triggered by the sperm forming the sperm aster; therefore, the zygote's centrosome, as in most other mammalian species, is predominantly paternally inherited (Tremoleda *et al.* 2003b). However, both sham-injected equine oocytes and parthenogenetic zygotes assemble a microtubule network in the form of multiasters, leading to the conclusion that the equine oocyte itself has the ability to form functional centrosomes, supporting the origin of the horse zygote centrosomes from both parents (Tremoleda *et al.*

2003b). This finding was also supported in the present study, because we observed multiasters

in aged oocytes, which could be interpreted as a sign of parthenogenetic activation of the oocyte.

In the horse, as in the mouse, microtubules can be generated independently by the oocyte,

and they play a role in proper congression of maternal chromosomes, activation and positioning

of the male and female pronuclei (Schatten *et al.* 1985, Tremoleda *et al.* 2003b). The presence

of multiple microtubule foci, as we also observed, can originate from fragmentation of defective

meiotic spindles, resulting in meiotic arrest of oocytes (Tremoleda *et al.* 2003b). Observations

from the studies on equine zygotes that fail to cleave after ICSI demonstrate defective

organization of microtubules into multiple asters and incorrect reconstruction of centrosomes,

with zygotic arrest and failure of further development.

Actin is a key component in the migration of the meiotic spindle and asymmetrical

positioning in murine and porcine oocytes (Yi *et al.* 2013, Yu *et al.* 2014). In particular, the roles

of actin vesicles as pushing forces and actomyosin contractile machinery have been suggested as

regulators of the oocyte maturation process (Yi & Li 2012, Holubcova *et al.* 2013, Coticchio *et*

al. 2014). Cytoplasmic actin morphodynamics have been studied and linked to quality of the

oocyte and ability to progress through maturation. Although the role of actin is poorly defined

during and after fertilization in mammalian species, it has been evaluated in sea urchins. A few

minutes after fertilization in the sea urchin, actin bundles move centrally with the incorporation

of the spermatozoa (Vasilev *et al.* 2012, Santella *et al.* 2014). Once the spermatozoon enters the

egg, the fertilization cone forms and contains actin filaments. If the actin cytoskeleton is

perturbed at this point, multiple fertilization cones form, and they fail to incorporate the

spermatozoa (Santella *et al.* 2014). Actin cytoskeleton remodeling and localization is involved in

human oocyte maturation, and IVM affects the actin network and amount of actin present before

fertilization (Coticchio *et al.* 2014). The role of actin in equine oocyte maturation and fertilization has not been studied.

After attainment of MII, the oocyte has a limited lifespan. Because injected oocytes were cultured for various intervals in the present study, we anticipated alterations associated with cellular aging. In Experiment 1, equine oocytes were cultured up to 48 h after MII to determine the features associated with aging *in vitro*. With the limited number of samples, the only significant change was an increase in microtubule multiasters by 48 h of culture. However, other cellular changes were beginning to occur in association with cell aging, with non-significant increases in the percentages of multipolar spindles, failure to observe kinetochores, movement of the spindle from a cortical to central position, and more diffuse chromatin.

In Experiment 2, microtubule multiasters were also observed more frequently as the time from ICSI to fixation increased. The time groups in Experiment 2 (fixation at 24-48 and 44-51h after ICSI) approximately correspond to the two time groups of aged oocytes in Experiment 1 (24 h and 48 h after polar body extrusion). Tubulin multiasters appeared to be associated with oocyte activation after sperm injection or parthenogenetic activation if the oocyte was aged *in vitro*. Polymerization and depolymerization of the microtubule filaments is essential for stable chromosome-tubulin connections, and energy from GTP hydrolysis is needed to correctly organize the microtubule stability and instability (Delimitreva *et al.* 2012). The stabilization of microtubule filaments is mediated by various factors such as kinesins, dyneins and pericentrin that determine polarity of the spindle and correct stabilization or destabilization of microtubule filaments attached to the chromosomes during different maturation stages of the oocyte (Brunet & Maro 2005, Sun & Schatten 2006, Delimitreva *et al.* 2012). Perturbation of these components

causes altered microtubule organization and a disorganized microtubule network, leading to oocyte spindle abnormality and incapability to succeed in fertilization (Delimitreva *et al.* 2012).

In the present study, microtubule multiasters were more often present in oocytes retrieved from young donors compared to old donors. The multiasters observed primarily in oocytes from young donors at 48-51 h after ICSI in Experiment 2 were similar to what was observed for oocytes aged *in vitro* for 48 h in Experiment 1, suggesting this was a consistent indicator of cellular aging and potentially an attempt of activation by the oocyte. Energy (GTP and ATP) storage supply and active presence of microtubule stabilizing factors and motor proteins, as kinesins and dyneins, could be sufficient in oocytes from a young healthy donor to trigger microtubule aster formation, and therefore, activation of the equine oocyte. It has been proposed that mitochondrial functionality and quantity are perturbed and decreased with maternal aging of the mare, which results in reduced fertility (Tilly 2001, Heffner 2004, Rambags *et al.* 2014). Perturbations of any of the components involved in microtubules organization and stabilization could lead to fragmentation of existent spindle structure and incorrect reconstruction of the zygote centrosome, as reported in both human IVF oocytes and equine ICSI zygotes (Asch *et al.* 1995, Tremoleda *et al.* 2003b).

Because of the predominance of older, subfertile mares in our ICSI program, maternal age of oocyte donors could have a substantial impact on results. The association of maternal aging with reduced fertility has been well documented in mares and women (Carnevale *et al.* 1993a, Carnevale 2008, Butts *et al.* 2014, Stoop *et al.* 2014). Aging-related changes in chromosome and cytoskeletal organization in the oocyte can contribute to failure of fertilization and combination of the two gametes in the woman (Mau-Holzmann 2005). The effect of mare aging on cytoskeletal aspects of the oocyte has not been studied; however, the incidence of

chromosomal misalignment is significantly increased for old mares (≥20 years) versus young

mares (4 to 11 years) (Carnevale *et al.* 2012). In the present study, various chromosome patterns

were observed with no significant effect of donor age or hours from ICSI to fixation. However,

the 'normal' chromosome arrangement, with chromosomes compact and aligned at the

metaphase plate, was observed in <10% of potential zygotes. In addition, the chromosomes

differed in their condensation and/or decondensation status, possibly due to nuclear remodeling

after sperm injection and failure to develop into the two parental pronuclei. We acknowledge

that some of the oocytes that failed to cleave after ICSI were injected with a sperm of poor or

compromised quality, which could have led to sperm-specific defective decondensation patterns

and delayed formation of the male pronuclei. Kinetochores were observed in only 14% of the

spindles, probably due to the failure of zygote development and resulting degradation of these

proteins, which are attached on the sister chromatids. In contrast, the kinetochores were observed

in all oocytes fixed at MII (Time 0) in Experiment 1, and even after 48 h of aging *in vitro*, 85%

of the oocytes had discernible kinetochores. Our findings suggest that cellular changes were

occurring after ICSI, which were not exclusively consistent with cell or donor aging. Our

findings support the hypothesis that microtubule cytoskeletal organization does play a role in

oocyte quality and ability to succeed in fertilization.

We observed actin vesicles, spherical filamentous actin structures, in 37 of 52 samples

(71%) analyzed. In eukaryotic cells, actin filaments determine the movement of vesicles at

specific cell locations and contribute to transport of intracellular proteins and the secretory

pathway (Khaitlina 2014). Actin is a mediator and sensor of apoptosis (membrane blebbing and

cell rounding) and it regulates apoptosis signaling (Desouza *et al.* 2012). In the mouse oocyte,

actin filaments modulate asymmetric spindle positioning. In the starfish egg, actin filaments help

chromosome collection, creating an actin network at the germinal vesicle breakdown stage (Lamash & Eliseikina 2006, Yi & Li 2012); networks of different density can be generated by adjusting vesicle volume, modulation that is essential for spindle positioning (Holubcova *et al.* 2013). In the present study, the presence of actin vesicles was associated with advanced donor age and did not appear to be as relevant during the senescence process of the oocyte. The results suggest that actin vesicle structures are a cytoskeletal component in zygote development, but their function at this stage of development is not well known. The increased presence of actin structures in oocytes collected from older mares could be interpreted as a marked remodeling of the oocyte cytoskeleton to compensate for the inability of the oocyte to organize chromosomes and cytoskeleton before and after the introduction of spermatozoa.

The actin filament structures in Experiment 2 were observed centrally within the ooplasm, although the location of the actin vesicles was more peripheral with increased time after ICSI. The trafficking of actin vesicles from the inner cytoplasm to the cortical area could be an attempt from the cytoskeleton to organize the actin filaments and facilitate the oocyte's degenerative progression. Directionality of this process seems to follow the asymmetrical cortical polarization and positioning of the spindle by actin filaments, as presented in the literature, which leads us to believe that there is a possible one-directional movement and build-up of these vesicles as the aging process continues (Yi & Li 2012, Coticchio *et al.* 2013, Holubcova *et al.* 2013).

Maternal aging causes a decline in reproductive success in various species and age-associated alterations, including mitochondrial changes and oxidative stress (Tilly 2001, Heffner 2004, Rambags *et al.* 2014). In yeast, a decrease in actin turnover, and consequent production of aggregates of F-actin, causes an increase in reactive oxygen species in the cytosol, which leads to

both senescence of the cell and apoptosis (Gourlay & Ayscough 2005). We observed components of cell aging and programmed cell death, because actin vesicle number, area and sum intensity were significantly higher in injected oocytes from older mares and at a later time after ICSI. The increase in actin filaments in oocytes from older mares could indicate a suboptimal environment, causing a cascade of events to develop and trigger failure of zygote and embryo development. Quantity and diffusion of actin spherical filaments within the oocyte could be altered and incorrectly timed during zygote early development in oocytes from older donors due to altered energy generation and lack of correct maturation progression and, therefore, cytoskeleton remodeling. The present study is the first to investigate the role of actin spherical filaments in oocyte senescence and alterations due to maternal aging. Although aspects of oocyte aging *in vivo* (donor aging) and *in vitro* (culture) have been postulated to be similar, our findings demonstrate that different mechanisms are occurring, at least in some aspects of the cytoskeleton. Understanding the modifications of both microtubules and actin due to natural cell aging or failure of the oocyte to be fertilized will allow us to determine what role the cytoskeleton plays in fertilization and early zygote development and the effects of maternal aging on zygote cytoskeletal modifications.

In conclusion, we found that microtubule multiasters were associated with oocyte aging *in vitro* and oocyte maternal centrosome activation. Multiasters were more prevalent in sperm-injected oocytes collected from younger versus older donors, and the tubulin multiasters appeared to be involved in cell aging and oocyte activation in oocytes from younger mares. Actin vesicles were associated with sperm-injected oocytes from older donor mares; these structures could be indicative of a deleterious process within the fertilized oocytes of older donors. Further determination of the normal diffusion and quantity of microtubule and actin structures during the

first 24 h of normal equine zygote development is necessary to establish how these cytoskeleton alterations differ from normal embryo development and potentially why cytoskeletal remodeling appears to be different in oocytes from old and young donors.

CHAPTER V: CONCLUDING REMARKS

The research projects reported in this dissertation were designed to address the relevance and novelty of cytoskeletal and nuclear analyses using confocal microscopy of the equine zygote after intracytoplasmic sperm injection (ICSI) of oocytes from young and old mares. This primary focus was on the modifications of the actin and tubulin cytoskeleton and chromatin conformation in the oocyte after the two parental sets of DNA meet due to fertilization. We focused on detecting possible alterations due to (1) failure of fertilization and/or (2) maternal aging of the oocyte donor.

The aims of the studies included (1) describing early zygote development after ICSI of oocytes matured in vivo or in vitro in the young mare, (2) determining changes in zygote development after ICSI in oocytes collected from young and old mares, and (3) elucidating changes in the oocyte after ICSI associated with failure of zygote development due to maternal aging or cell senescence.

Confocal microscopy is a unique method for analyzing early zygote progression, allowing us to image the cytoskeleton and chromosome configurations during zygote development. The ability to evaluate the different layers of the cell gives detailed information of the entire oocyte during oogenesis or zygote at different hours after sperm injection. This technique lets us determine specific cytoskeletal or nuclear modifications within the oocyte, and temporal progression after ICSI.

Limits to the use of confocal microscopy for analyzing early zygote development in the mare are: (1) interpreting highly variable developmental stages and abnormal stages observed in the first 24 h after sperm injection in a weakly studied animal model, (2) lack of sufficient

literature that describes in detail the cytoskeletal and nuclear changes across the stages of zygote progression before first mitotic cleavage in the young and old mare, and (3) targeting a large cell such as the mare zygote that is rich in lipids to perform specific immunostaining and develop high quality confocal imaging with a limited number of excitation lasers for specific parameters of interest.

Based upon the first chapter, equine zygote progression in the young mare after ICSI of oocytes matured in vivo or in vitro can be summarized as follows: first, the female spindle is observed with aligned metaphase II chromosomes and the sperm head and/or tail are still condensed and intact after sperm injection. Afterwards, the female set of chromosomes undergoes anaphase and approaches extrusion of the second polar body followed by the decondensation of the male chromatin and remodeling of the microtubules around the sperm DNA. These events occur at variable hours after ICSI, depending on the sample, and generally by 12 h after injection of the sperm, presumptive zygotes were expected to approach pronuclei formation with no differences between in vivo or in vitro matured oocytes. At 8 h for in vivo matured and 12 h for in vitro matured oocytes, 80% of the zygotes had the two parental pronuclei formed. From our first study, in vivo matured equine oocytes seemed to achieve the pronucleus stage sooner after sperm injection than in vitro matured oocytes; a higher incidence of zygote developmental arrest or delay was observed for in vitro matured oocytes. This study focused on the first 16 h of equine zygote development and determined the time line of equine zygote progression after ICSI for both in vivo and in vitro matured oocytes.

Our next study (chapter 3) focused on the effect of maternal aging on zygote development in the mare. This study concentrated on the first 20 h of zygote development in oocytes collected from young or old mares. We described common stages of zygote development

in oocytes from both young and old mares, coinciding with the ones described in our first study. In addition, at 20 h after ICSI, early anaphase to telophase transition and first mitotic cleavage was observed. Morphological characteristics of pronuclei differed between young and old mares. DNA and heterochromatin localized at the centromeres was diffused homogenously in zygotes from young mares, compared to the old mares, which had DNA filaments polarized at the periphery of the pronuclei and heterochromatin concentrated as dense, knob-like structures. Presence of actin vesicles after ICSI was also observed in zygotes from old mares, as a possible sign of remodeling or degeneration of the oocyte. The main characteristics associated with maternal aging were the presence of actin vesicles, the diverse heterochromatin and DNA localization at the pronucleus stage, and a few abnormal zygote morphologies due to fertilization failure or delay.

After ICSI, not all equine oocytes cleave and develop into viable embryos. There are multiple potential reasons why the fertilized oocytes may not cleave and develop into an embryo. The problem can be due to either the sperm or the egg. The sperm could undergo premature chromosome condensation or failure of the sperm head to decondense (Flaherty *et al.* 1995). A primary cause of ICSI failure is the lack of the oocyte to be activated (Flaherty *et al.* 1998).

The goal of the third study was to determine changes in the oocyte after sperm injection due to failure of fertilization and understand reasons for zygote developmental arrest. We studied both cytoskeletal and chromosomal changes associated with donor aging and cellular senescence in equine oocytes that failed to fertilize. We found that oocyte aging in vitro is associated with tubulin multiasters and maternal centrosome activation, which were also more prevalent in sperm-injected oocytes collected from younger mares that failed to fertilize. Actin vesicles were a predominant structure associated with sperm-injected oocytes from older donors that failed to

fertilize after ICSI. Interestingly, actin vesicles did not appear to be as relevant in oocytes that were aged in vitro. The presence of actin vesicles in oocytes that failed to fertilize from old mares revealed the importance of actin remodeling after ICSI in oocytes collected from mares of advanced maternal age.

The results compiled in the dissertation provide a comprehensive description of equine zygote development after ICSI using confocal microscopy, focused on the effects of oocyte maturation method and donor age on cytoskeletal and chromosomal remodeling after sperm injection. From these three studies we found that the equine zygote, as in other mammalian species, follows the main developmental steps towards first mitotic cleavage with a variety of normal and abnormal reorganization events within the oocyte. In vitro maturation and donor maternal aging were both associated with higher incidence of zygote abnormal morphology leading to fertilization delay or arrest. Actin vesicles were present predominantly in oocytes from donors of advanced age that were both successfully or unsuccessfully fertilized. The presence of actin vesicles in zygotes from older mares revealed a novel role of actin as a main cytoskeletal remodeling factor after fertilization using ICSI associated with maternal aging. Due to the limitation that in vitro fertilization cannot be performed in the equine oocyte, we could not determine whether actin vesicle presence predominantly in oocytes from older donors is due to the technique of ICSI affecting more the cytoskeletal structure of the oocyte, or purely due to a different actin reorganization in oocytes retrieved from older donors. For future studies, investigation of actin motor proteins, such as myosin, and actin disassembling proteins, such as cofilin, should be pursued in regards on their activity in zygote development in the mare, especially looking at the mare aging effect on the function of these proteins.

Our secondary most relevant finding concerned the chromatin status at the pronucleus stage in the equine zygote and the chromosomal configurations observed across time after ICSI. This finding was entirely attributed to the first successful utilization of the CREST antibody, targeting centromeres in the equine zygote. Development of CREST immunostaining in both equine oocytes and zygotes allowed us to have a detailed perception of the chromatin status across time after sperm injection and allowed characterization of pronuclei DNA and heterochromatin patterns between young and old mares. DNA and constitutive heterochromatin labeled by the CREST antibody showed localization and status differences between zygotes from young or old mares. The dense DNA filaments and knob-like heterochromatin observed in old mare's pronuclei suggested an alteration in chromatin status and possible breakage in the DNA due to the poor quality of the two parental pronuclei. For the young mare's zygote, the pronuclei showed crisp diffused staining of DNA, and the CREST antibody allowed us to appreciate and visualize nucleolus-like bodies within the pronuclei that are involved in epigenetic zygote reprogramming; these were not present in the old mare's zygotes. For future studies, attention on epigenetic markers for zygote quality and development should be considered. Zygote pronuclei formation is a key step in developmental progression that allows the embryo to result in a pregnancy; therefore, a molecular approach to epigenetic analysis could give a better insight into the quality of the future embryo. In conclusion, this dissertation revealed novel aspects and approaches to study equine zygote development after ICSI and the effects of oocyte maturation and maternal aging in the mare.

REFERENCES

Altermatt J, Suh T, Stokes J, Campos-Chillon L & Carnevale E 2007 Effect of mare age on oocyte morphology and developmental competence after intracytoplasmic sperm injection. *Reprod Fertil Dev* **20** 215-216.

Altermatt JL, Suh TK, Stokes JE & Carnevale EM 2009 Effects of age and equine follicle-stimulating hormone (eFSH) on collection and viability of equine oocytes assessed by morphology and developmental competency after intracytoplasmic sperm injection (ICSI). *Reprod Fertil Dev* **21** 615-623.

Ambruosi B, Lacalandra GM, Iorga AI, De Santis T, Mugnier S, Matarrese R, Goudet G & Dell'aquila ME 2009 Cytoplasmic lipid droplets and mitochondrial distribution in equine oocytes: Implications on oocyte maturation, fertilization and developmental competence after ICSI. *Theriogenology* **71** 1093-1104.

Armstrong D 2001 Effects of maternal age on oocyte developmental competence. *Theriogenology* **55** 1303-1322.

Asch R, Simerly C, Ord T, Ord VA & Schatten G 1995 The stages at which human fertilization arrests: microtubule and chromosome configurations in inseminated oocytes which failed to complete fertilization and development in humans. *Hum Reprod* **10** 1897-1906.

Barrett SL & Albertini DF 2007 Allocation of gamma-tubulin between oocyte cortex and meiotic spindle influences asymmetric cytokinesis in the mouse oocyte. *Biol Reprod* **76** 949-957.

Barrett SL & Albertini DF 2010 Cumulus cell contact during oocyte maturation in mice

   regulates meiotic spindle positioning and enhances developmental competence. *J*

   Assist Reprod Genet **27** 29-39.

Battaglia DE, Goodwin P, Klein NA & Soules MR 1996 Influence of maternal age on

   meiotic spindle assembly in oocytes from naturally cycling women. *Hum Reprod* **11**

   2217-2222.

Ben-Meir A, Burstein E, Borrego-Alvarez A, Chong J, Wong E, Yavorska T, Naranian T,

   Chi M, Wang Y, Bentov Y, Alexis J, Meriano J, Sung HK, Gasser DL, Moley KH,

   Hekimi S, Casper RF & Jurisicova A 2015 Coenzyme Q10 restores oocyte

   mitochondrial function and fertility during reproductive aging. *Aging Cell* **14** 887-

   895.

Bézard J, Magistrini M, Duchamp G & Palmer E 1989 Chronology of equine fertilisation

   and embryonic development in vivo and in vitro. *Equine Veterinary Journal* **21** 105-

   110.

Bezard J, Mekarska A, Goudet G, Duchamp G & Palmer E 1997 Meiotic stage of the

   preovulatory equine oocyte at collection and competence of immature oocytes for in

   vitro maturation: effect of interval from induction of ovulation to follicle puncture.

   Theriogenology **1** 386.

Bing YZ, Hirao Y, Iga K, Che LM, Takenouchi N, Kuwayama M, Fuchimoto D,

   Rodriguez-Martinez H & Nagai T 2002 In vitro maturation and glutathione

   synthesis of porcine oocytes in the presence or absence of cysteamine under

   different oxygen tensions: role of cumulus cells. *Reprod Fertil Dev* **14** 125-131.

Binor Z & Wolf DP 1979 In-vitro maturation and penetration of mouse primary oocytes

    after removal of the zona pellucida. *J Reprod Fertil* **56** 309-314.

Boudoures AL & Moley KH 2015. Insights into Mechanisms Causing the Maternal Age-

    Induced Decrease in Oocyte Quality. In *Biennial Review of Infertility*, pp. 43-55.

Bromfield J, Messamore W & Albertini DF 2007 Epigenetic regulation during

    mammalian oogenesis. *Reprod Fertil Dev* **20** 74-80.

Brunet S & Maro B 2005 Cytoskeleton and cell cycle control during meiotic maturation of

    the mouse oocyte: integrating time and space. *Reproduction* **130** 801-811.

Butts SF, Owen C, Mainigi M, Senapati S, Seifer DB & Dokras A 2014 Assisted hatching

    and intracytoplasmic sperm injection are not associated with improved outcomes in

    assisted reproduction cycles for diminished ovarian reserve: an analysis of cycles in

    the United States from 2004 to 2011. *Fertil Steril* **102** 1041-1047 e1041.

Carnevale E, Bergfelt D & Ginther O 1993a Aging effects on follicular activity and

    concentrations of FSH, LH, and progesterone in mares. *Anim Reprod Sci* **31** 287-299.

Carnevale E, da Silva MC, Preis K, Stokes J & Squires E. 2004. Establishment of

    pregnancies from oocytes collected from the ovaries of euthanized mares. In

    Proceedings of the 50th Annual Convention of the American Association of Equine

    Practitioners, Denver, Colorado, USA, 4-8 December, 2004., pp. 531-533.

Carnevale E & Ginther O 1993 Use of a linear ultrasonic transducer for the transvaginal

    aspiration and transfer of oocytes in the mare. *J Equine Vet Sci* **13** 331-333.

Carnevale E & Ginther O 1995 Defective oocytes as a cause of subfertility in old mares.

    Biol Reprod **Mono 1**

 209-214.

Carnevale E, Griffin P & Ginther O 1993b Age‐associated subfertility before entry of

embryos into the uterus in mares. *Equine Vet J* **25** 31-35.

Carnevale E, Maclellan L, Ruggeri E & Albertini D 2012 Meiotic spindle configurations in

metaphase II oocytes from young and old mares. *J Equine Vet Sci* **32** 410-411.

Carnevale EM 2008 The mare model for follicular maturation and reproductive aging in

the woman. *Theriogenology* **69** 23-30.

Carnevale EM & Ginther OJ 1992 Relationships of age to uterine function and

reproductive efficiency in mares. *Theriogenology* **37** 1101-1115.

Carnevale EM & Maclellan LJ 2006 Collection, evaluation, and use of oocytes in equine

assisted reproduction. *Vet Clin North Am Equine Pract* **22** 843-856.

Carnevale EM, Maclellan LJ, Coutinho da Silva MA, Scott TJ & Squires EL 2000a

Comparison of culture and insemination techniques for equine oocyte transfer.

Theriogenology **54** 981-987.

Carnevale EM, Ramirez RJ, Squires EL, Alvarenga MA, Vanderwall DK & McCue PM

2000b Factors affecting pregnancy rates and early embryonic death after equine

embryo transfer. *Theriogenology* **54** 965-979.

Carnevale EM & Sessions DR 2012 In vitro production of equine embryos. *J Equine Vet Sci*

32 367-371.

Carnevale EM, Stokes J, Squires EL, Campos-Chillon LF, Altermatt J & Suh TK. 2007.

Clinical use of intracytoplasmic sperm injection in horses. In *Proc Am Assoc Equine

Pract*, pp. 560.

Chen ZQ, Ming TX & Nielsen HI 2010 Maturation arrest of human oocytes at germinal

vesicle stage. *J Hum Reprod Sci* **3** 153-157.

Chew TG, Lorthongpanich C, Ang WX, Knowles BB & Solter D 2012 Symmetric cell division of the mouse zygote requires an actin network. *Cytoskeleton* **69** 1040-1046.

Chian RC, Niwa K & Sirard MA 1994 Effects of cumulus cells on male pronuclear formation and subsequent early development of bovine oocytes in vitro. *Theriogenology* **41** 1499-1508.

Chiang T, Schultz RM & Lampson MA 2012 Meiotic origins of maternal age-related aneuploidy. *Biol Reprod* **86** 1-7.

Choi Y, Okada Y, Hochi S, Braun J, Sato K & Oguri N 1994 In vitro fertilization rate of horse oocytes with partially removed zonae. *Theriogenology* **42** 795-802.

Choi YH, Love CC, Love LB, Varner DD, Brinsko S & Hinrichs K 2002 Developmental competence in vivo and in vitro of in vitro-matured equine oocytes fertilized by intracytoplasmic sperm injection with fresh or frozen-thawed spermatozoa. *Reproduction* **123** 455-465.

Choi YH, Roasa LM, Love CC, Varner DD, Brinsko SP & Hinrichs K 2004 Blastocyst formation rates in vivo and in vitro of in vitro-matured equine oocytes fertilized by intracytoplasmic sperm injection. *Biol Reprod* **70** 1231-1238.

Colleoni S, Lagutina I, Lazzari G, Rodriguez-Martinez H, Galli C & Morrell JM 2011 New methods for selecting stallion spermatozoa for assisted reproduction. *J Equine Vet Sci* **31** 536-541.

Combelles CM, Cekleniak NA, Racowsky C & Albertini DF 2002 Assessment of nuclear and cytoplasmic maturation in in-vitro matured human oocytes. *Hum Reprod* **17** 1006-1016.

Cook N, Squires E, Ray B & Jasko D 1993 Transvaginal ultrasound‐guided follicular aspiration of equine oocytes. *Equine Veterinary Journal* **25** 71-74.

Coticchio G, Dal Canto M, Mignini Renzini M, Guglielmo MC, Brambillasca F, Turchi D, Novara PV & Fadini R 2015 Oocyte maturation: gamete-somatic cells interactions, meiotic resumption, cytoskeletal dynamics and cytoplasmic reorganization. *Hum Reprod Update* **21** 427-454.

Coticchio G, Guglielmo MC, Albertini DF, Dal Canto M, Mignini Renzini M, De Ponti E & Fadini R 2014 Contributions of the actin cytoskeleton to the emergence of polarity during maturation in human oocytes. *Mol Hum Reprod* **20** 200-207.

Coticchio G, Guglielmo MC, Dal Canto M, Fadini R, Mignini Renzini M, De Ponti E, Brambillasca F & Albertini DF 2013 Mechanistic foundations of the metaphase II spindle of human oocytes matured in vivo and in vitro. *Hum Reprod* **28** 3271-3282.

Courtois A, Schuh M, Ellenberg J & Hiiragi T 2012 The transition from meiotic to mitotic spindle assembly is gradual during early mammalian development. *J Cell Biol* **198** 357-370.

De La Fuente R, Viveiros MM, Burns KH, Adashi EY, Matzuk MM & Eppig JJ 2004 Major chromatin remodeling in the germinal vesicle (GV) of mammalian oocytes is dispensable for global transcriptional silencing but required for centromeric heterochromatin function. *Dev Biol* **275** 447-458.

Delimitreva S, Tkachenko OY, Berenson A & Nayudu PL 2011 Variations of chromatin, tubulin and actin structures in primate oocytes arrested during in vitro maturation and fertilization—what is this telling us about the relationships between cytoskeletal and chromatin meiotic defects? *Theriogenology* **77** 1297-1311.

Delimitreva S, Tkachenko OY, Berenson A & Nayudu PL 2012 Variations of chromatin, tubulin and actin structures in primate oocytes arrested during in vitro maturation and fertilization--what is this telling us about the relationships between cytoskeletal and chromatin meiotic defects? *Theriogenology* **77** 1297-1311.

Dell'Aquila M, Fusco S, Lacalandra G & Maritato F 1996 In vitro maturation and fertilization of equine oocytes recovered during the breeding season. *Theriogenology* **45** 547-560.

Dell'Aquila ME, Albrizio M, Maritato F, Minoia P & Hinrichs K 2003 Meiotic competence of equine oocytes and pronucleus formation after intracytoplasmic sperm injection (ICSI) as related to granulosa cell apoptosis. *Biol Reprod* **68** 2065-2072.

Dell'Aquila ME, Cho YS, Minoia P, Traina V, Fusco S, Lacalandra GM & Maritato F 1997 Intracytoplasmic sperm injection (ICSI) versus conventional IVF on abattoir-derived and in vitro-matured equine oocytes. *Theriogenology* **47** 1139-1156.

Dell'Aquila ME, Masterson M, Maritato F & Hinrichs K 2001 Influence of oocyte collection technique on initial chromatin configuration, meiotic competence, and male pronucleus formation after intracytoplasmic sperm injection (ICSI) of equine oocytes. *Mol Reprod Dev* **60** 79-88.

Deng M & Li R 2009 Sperm chromatin-induced ectopic polar body extrusion in mouse eggs after ICSI and delayed egg activation. *PLoS One* **4** e7171.

Desouza M, Gunning PW & Stehn JR 2012 The actin cytoskeleton as a sensor and mediator of apoptosis. *Bioarchitecture* **2** 75-87.

Edirisinghe WR, Murch A, Junk S & Yovich JL 1997 Cytogenetic abnormalities of unfertilized oocytes generated from in-vitro fertilization and intracytoplasmic sperm injection: a double-blind study. *Hum Reprod* **12** 2784-2791.

El Hajj N & Haaf T 2013 Epigenetic disturbances in in vitro cultured gametes and embryos: implications for human assisted reproduction. *Fertil Steril* **99** 632-641.

Eppig JJ 1996 Coordination of nuclear and cytoplasmic oocyte maturation in eutherian mammals. *Reprod Fertil Dev* **8** 485-489.

Evans MJ & Irvine CH 1975 Serum concentrations of FSH, LH and progesterone during the oestrous cycle and early pregnancy in the mare. *J Reprod Fertil Suppl*193-200.

Finn A, Scott L, O'Leary T, Davies D & Hill J 2010 Sequential embryo scoring as a predictor of aneuploidy in poor-prognosis patients. *Reprod Biomed Online* **21** 381-390.

Flaherty SP, Payne D & Matthews CD 1998 Fertilization failures and abnormal fertilization after intracytoplasmic sperm injection. *Hum Reprod* **13 Suppl 1** 155-164.

Flaherty SP, Payne D, Swann NJ & Mattews CD 1995 Aetiology of failed and abnormal fertilization after intracytoplasmic sperm injection. *Hum Reprod* **10** 2623-2629.

Franciosi F, Lodde V, Goudet G, Duchamp G, Deleuze S, Douet C, Tessaro I & Luciano AM 2012 Changes in histone H4 acetylation during in vivo versus in vitro maturation of equine oocytes. *Mol Hum Reprod* **18** 243-252.

Fulka J, Jr. & Okolski A 1981 Culture of horse oocytes in vitro. *J Reprod Fertil* **61** 213-215.

Galli C, Colleoni S, Duchi R, Lagutina I & Lazzari G 2007 Developmental competence of equine oocytes and embryos obtained by in vitro procedures ranging from in vitro

maturation and ICSI to embryo culture, cryopreservation and somatic cell nuclear transfer. *Anim Reprod Sci* **98** 39-55.

Galli C, Colleoni S, Duchi R, Lagutina I & Lazzari G 2013 Equine assisted reproduction and embryo technologies. *Anim Reprod* **10** 334-343.

Galli C, Crotti G, Turini P, Duchi R, Mari G, Zavaglia G, Duchamp G, Daels P & Lazzari G 2002 Frozen–thawed embryos produced by Ovum Pick Up of immature oocytes and ICSI are capable to establish pregnancies in the horse. *Theriogenology* **58** 705-708.

Gilchrist RB, Ritter LJ & Armstrong DT 2001 Mouse oocyte mitogenic activity is developmentally coordinated throughout folliculogenesis and meiotic maturation. *Dev Biol* **240** 289-298.

Ginther O 1979 *Reproductive biology of the mare. Basic and applied aspects*. Cross Plains, WI: Equiservices.

Goudet G, Bezard J, Duchamp G, Gerard N & Palmer E 1997 Equine oocyte competence for nuclear and cytoplasmic in vitro maturation: effect of follicle size and hormonal environment. *Biol Reprod* **57** 232-245.

Gourlay CW & Ayscough KR 2005 Identification of an upstream regulatory pathway controlling actin-mediated apoptosis in yeast. *J Cell Sci* **118** 2119-2132.

Gremeau AS, Andreadis N, Fatum M, Craig J, Turner K, McVeigh E & Child T 2012 In vitro maturation or in vitro fertilization for women with polycystic ovaries? A case-control study of 194 treatment cycles. *Fertil Steril* **98** 355-360.

Grondahl C, Hansen TH, Hossaini A, Heinze I, Greve T & Hyttel P 1997 Intracytoplasmic sperm injection of in vitro-matured equine oocytes. *Biol Reprod* **57** 1495-1501.

Hara H, Hwang IS, Kagawa N, Kuwayama M, Hirabayashi M & Hochi S 2012 High
incidence of multiple aster formation in vitrified-warmed bovine oocytes after in
vitro fertilization. *Theriogenology* **77** 908-915.

Hawley L, Enders A & Hinrichs K. 1995. Comparisons of equine and bovine oocytes-
cumulus morphology within the ovarian follicle.

Heffner LJ 2004 Advanced maternal age--how old is too old? *N Engl J Med* **351** 1927-1929.

Hendriks WK, Colleoni S, Galli C, Paris DB, Colenbrander B, Roelen BA & Stout TA
2015 Maternal age and in vitro culture affect mitochondrial number and function in
equine oocytes and embryos. *Reprod Fertil Dev*.

**Hewitson LC, Simerly CR, Tengowski MW, Sutovsky P, Navara CS, Haavisto AJ &
Schatten G** 1996 Microtubule and chromatin configurations during rhesus
intracytoplasmic sperm injection: successes and failures. *Biol Reprod* **55** 271-280.

Hinrichs K 2005 Update on equine ICSI and cloning. *Theriogenology* **64** 535-541.

Hinrichs K, Kenney D & Kenney R 1990 Aspiration of oocytes from mature and immature
preovulatory follicles in the mare. *Theriogenology* **34** 107-112.

Hinrichs K, Love CC, Brinsko SP, Choi YH & Varner DD 2002 In vitro fertilization of in
vitro-matured equine oocytes: effect of maturation medium, duration of maturation,
and sperm calcium ionophore treatment, and comparison with rates of fertilization
in vivo after oviductal transfer. *Biol Reprod* **67** 256-262.

Hinrichs K, Schmidt AL, Friedman PP, Selgrath JP & Martin MG 1993 In vitro
maturation of horse oocytes: characterization of chromatin configuration using
fluorescence microscopy. *Biol Reprod* **48** 363-370.

Holubcova Z, Howard G & Schuh M 2013 Vesicles modulate an actin network for asymmetric spindle positioning. *Nat Cell Biol* **15** 937-947.

Hyttel P, Fair T, Callesen H & Greve T 1997 Oocyte growth, capacitation and final maturation in cattle. *Theriogenology* **47** 23-32.

Kageyama S-i, Liu H, Kaneko N, Ooga M, Nagata M & Aoki F 2007 Alterations in epigenetic modifications during oocyte growth in mice. *Reproduction* **133** 85-94.

Kattera S & Chen C 2004 Developmental potential of human pronuclear zygotes in relation to their pronuclear orientation. *Hum Reprod* **19** 294-299.

Kaufman MH 1983 *Early mammalian development: parthenogenetic studies*. Trumpington Street, Cambridge: University of Cambridge.

Khaitlina SY 2014 Intracellular transport based on actin polymerization. *Biochemistry (Mosc)* **79** 917-927.

Kim NH, Simerly C, Funahashi H, Schatten G & Day BN 1996 Microtubule organization in porcine oocytes during fertilization and parthenogenesis. *Biol Reprod* **54** 1397-1404.

Kuliev A, Cieslak J, Ilkevitch Y & Verlinsky Y 2003 Chromosomal abnormalities in a series of 6,733 human oocytes in preimplantation diagnosis for age-related aneuploidies. *Reprod Biomed Online* **6** 54-59.

Lamash N & Eliseikina M 2006 Rearrangement of the actin-spectrin cytoskeleton during oocyte maturation of the starfish Asterias amurensis. *J Mar Biol* **32** 115-119.

Li L, Meintjes M, Graff K, Paul J, Denniston R & Godke R. 1995. In vitro fertilization and development of in vitro-matured oocytes aspirated from pregnant mares.

Lundin K, Bergh C & Hardarson T 2001 Early embryo cleavage is a strong indicator of embryo quality in human IVF. *Hum Reprod* **16** 2652-2657.

Mamo S, Carter F, Lonergan P, Leal CL, Al Naib A, McGettigan P, Mehta JP, Evans AC & Fair T 2011 Sequential analysis of global gene expression profiles in immature and in vitro matured bovine oocytes: potential molecular markers of oocyte maturation. *BMC Genomics* **12** 151.

Manandhar G & Toshimori K 2003 Fate of postacrosomal perinuclear theca recognized by monoclonal antibody MN13 after sperm head microinjection and its role in oocyte activation in mice. *Biol Reprod* **68** 655-663.

Marchetti F, Bishop J, Gingerich J & Wyrobek AJ 2015 Meiotic interstrand DNA damage escapes paternal repair and causes chromosomal aberrations in the zygote by maternal misrepair. *Sci Rep* **5** 7689.

Marchetti F & Wyrobek AJ 2005 Mechanisms and consequences of paternally-transmitted chromosomal abnormalities. *Birth Defects Res C Embryo Today* **75** 112-129.

Maro B, Howlett SK & Houliston E 1986 Cytoskeletal dynamics in the mouse egg. *J Cell Sci Suppl* **5** 343-359.

Mau-Holzmann UA 2005 Somatic chromosomal abnormalities in infertile men and women. *Cytogenet Genome Res* **111** 317-336.

Messinger SM & Albertini DF 1991 Centrosome and microtubule dynamics during meiotic progression in the mouse oocyte. *J Cell Sci* **100 (Pt 2)** 289-298.

Metchat A, Eguren M, Hossain JM, Politi AZ, Huet S & Ellenberg J 2015 An actin-dependent spindle position checkpoint ensures the asymmetric division in mouse oocytes. *Nat Commun* **6** 7784.

Moghbelinejad S, Mozdarani H & Rezaeian Z 2013 The rates of premature chromosome condensation and embryo development after injection of irradiated sperms into hamster oocytes. *Iran J Reprod Med* **11** 391-398.

Mrazek M & Fulka Jr J, Jr. 2003 Failure of oocyte maturation: possible mechanisms for oocyte maturation arrest. *Hum Reprod* **18** 2249-2252.

Murakoshi Y, Sueoka K, Takahashi K, Sato S, Sakurai T, Tajima H & Yoshimura Y 2013 Embryo developmental capability and pregnancy outcome are related to the mitochondrial DNA copy number and ooplasmic volume. *J Assist Reprod Genet* **30** 1367-1375.

Navara CS, First NL & Schatten G 1994 Microtubule organization in the cow during fertilization, polyspermy, parthenogenesis, and nuclear transfer: the role of the sperm aster. *Dev Biol* **162** 29-40.

Navot D, Bergh PA, Williams MA, Garrisi GJ, Guzman I, Sandler B & Grunfeld L 1991 Poor oocyte quality rather than implantation failure as a cause of age-related decline in female fertility. *Lancet* **337** 1375-1377.

Palermo GD, Kocent J, Monahan D, Neri QV & Rosenwaks Z 2014 Treatment of male infertility. *Methods Mol Biol* **1154** 385-405.

Palmer E, Bezard J, Magistrini M & Duchamp G 1990 In vitro fertilization in the horse. A retrospective study. *J Reprod Fertil Suppl* **44** 375-384.

Pomar FR, Teerds K, Kidson A, Colenbrander B, Tharasanit T, Aguilar B & Roelen B 2005 Differences in the incidence of apoptosis between in vivo and in vitro produced blastocysts of farm animal species: a comparative study. *Theriogenology* **63** 2254-2268.

Probst AV & Almouzni G 2011 Heterochromatin establishment in the context of genome-wide epigenetic reprogramming. *Trends Genet* **27** 177-185.

Rambags BP, van Boxtel DC, Tharasanit T, Lenstra JA, Colenbrander B & Stout TA 2014 Advancing maternal age predisposes to mitochondrial damage and loss during maturation of equine oocytes in vitro. *Theriogenology* **81** 959-965.

Rinaudo P & Schultz RM 2004 Effects of embryo culture on global pattern of gene expression in preimplantation mouse embryos. *Reproduction* **128** 301-311.

Rosenbusch B 2001 Digynic triploidy: possible mechanisms. *Prenat Diagn* **21** 234.

Ruggeri E, DeLuca KF, Galli C, Lazzari G, DeLuca JG & Carnevale EM 2015 Cytoskeletal alterations associated with donor age and culture interval for equine oocytes and potential zygotes that failed to cleave after intracytoplasmic sperm injection. *Reprod Fertil Dev*.

Salhab M, Dhorne-Pollet S, Auclair S, Guyader-Joly C, Brisard D, Dalbies-Tran R, Dupont J, Ponsart C, Mermillod P & Uzbekova S 2013 In vitro maturation of oocytes alters gene expression and signaling pathways in bovine cumulus cells. *Mol Reprod Dev* **80** 166-182.

Sanfins A, Plancha CE & Albertini DF 2015 Pre-implantation developmental potential from in vivo and in vitro matured mouse oocytes: a cytoskeletal perspective on oocyte quality. *J Assist Reprod Genet* **32** 127-136.

Santella L, Limatola N & Chun JT 2014. Actin Cytoskeleton and Fertilization in Starfish Eggs. In *Sexual Reproduction in Animals and Plants*, pp. 141-155.

Schatten G 1994 The centrosome and its mode of inheritance: the reduction of the centrosome during gametogenesis and its restoration during fertilization. *Dev Biol* **165** 299-335.

Schatten G, Simerly C & Schatten H 1985 Microtubule configurations during fertilization, mitosis, and early development in the mouse and the requirement for egg microtubule-mediated motility during mammalian fertilization. *Proc Natl Acad Sci U S A* **82** 4152-4156.

Schatten G, Simerly C & Schatten H 1986 Microtubules in mouse oocytes, zygotes, and embryos during fertilization and early development: unusual configurations and arrest of mammalian fertilization with microtubule inhibitors. *Ann N Y Acad Sci* **466** 945-948.

Schmiday H & Tandler-Schneider A 1996 Premature chromosome condensation of sperm nucleus after ICSI. *Hum Reprod* **4** 989-995.

Schumpert B, Garcia MG, Wessel GM, Wordeman L & Hille MB 2013 Roles for focal adhesion kinase (FAK) in blastomere abscission and vesicle trafficking during cleavage in the sea urchin embryo. *Mech Dev* **130** 290-303.

Schwarzacher HG & Wachtler F 1993 The nucleolus. *Anat Embryol (Berl)* **188** 515-536.

Scott L 2012. Pronuclear Scoring in Human In Vitro Fertilization. In *Practical Manual of In Vitro Fertilization*, pp. 379-384.

Scott L, Alvero R, Leondires M & Miller B 2000 The morphology of human pronuclear embryos is positively related to blastocyst development and implantation. *Hum Reprod* **15** 2394-2403.

Scott LA & Smith S 1998 The successful use of pronuclear embryo transfers the day
following oocyte retrieval. *Hum Reprod* **13** 1003-1013.

Sessions-Bresnahan D, Graham J & Carnevale E 2014 Validation of a heterologous
fertilization assay and comparison of fertilization rates of equine oocytes using< i>
in vitro</i> fertilization, perivitelline, and intracytoplasmic sperm injections.
Theriogenology.

Shabpareh V, Squires E, Seidel G & Jasko D 1993 Methods for collecting and maturing
equine oocytes in vitro. *Theriogenology* **40** 1161-1175.

Siddiqui MA, Gastal EL, Ju JC, Gastal MO, Beg MA & Ginther OJ 2009 Nuclear
configuration, spindle morphology and cytoskeletal organization of in vivo maturing
horse oocytes. *Reprod Domest Anim* **44** 435-440.

Sluder G, Thompson EA, Miller FJ, Hayes J & Rieder CL 1997 The checkpoint control for
anaphase onset does not monitor excess numbers of spindle poles or bipolar spindle
symmetry. *J Cell Sci* **110 (Pt 4)** 421-429.

Smitz JE, Thompson JG & Gilchrist RB 2011 The promise of in vitro maturation in
assisted reproduction and fertility preservation. *Semin Reprod Med* **29** 24-37.

Squires E, Carnevale E, McCue P & Bruemmer J 2003a Embryo technologies in the horse.
Theriogenology **59** 151-170.

Squires E, Wilson J, Kato H & Blaszczyk A 1996 A pregnancy after intracytoplasmic
sperm injection into equine oocytes matured in vitro. *Theriogenology* **1** 306.

Squires EL, Carnevale EM, McCue PM & Bruemmer JE 2003b Embryo technologies in the
horse. *Theriogenology* **59** 151-170.

Stoop D, Cobo A & Silber S 2014 Fertility preservation for age-related fertility decline. *Lancet* **384** 1311-1319.

Sun QY & Schatten H 2006 Regulation of dynamic events by microfilaments during oocyte maturation and fertilization. *Reproduction* **131** 193-205.

Svarcova O, Dinnyes A, Polgar Z, Bodo S, Adorjan M, Meng Q & Maddox-Hyttel P 2009 Nucleolar re-activation is delayed in mouse embryos cloned from two different cell lines. *Molecular Reproduction and Development* **76** 132-141.

Tervit HR, Whittingham DG & Rowson LE 1972 Successful culture in vitro of sheep and cattle ova. *J Reprod Fertil* **30** 493-497.

Tesarik J & Greco E 1999 The probability of abnormal preimplantation development can be predicted by a single static observation on pronuclear stage morphology. *Hum Reprod* **14** 1318-1323.

Tilly JL 2001 Commuting the death sentence: how oocytes strive to survive. *Nat Rev Mol Cell Biol* **2** 838-848.

Tremoleda JL, Schoevers EJ, Stout TA, Colenbrander B & Bevers MM 2001 Organisation of the cytoskeleton during in vitro maturation of horse oocytes. *Mol Reprod Dev* **60** 260-269.

Tremoleda JL, Stout TA, Lagutina I, Lazzari G, Bevers MM, Colenbrander B & Galli C 2003a Effects of in vitro production on horse embryo morphology, cytoskeletal characteristics, and blastocyst capsule formation. *Biol Reprod* **69** 1895-1906.

Tremoleda JL, Van Haeften T, Stout TA, Colenbrander B & Bevers MM 2003b Cytoskeleton and chromatin reorganization in horse oocytes following

intracytoplasmic sperm injection: patterns associated with normal and defective fertilization. *Biol Reprod* **69** 186-194.

Trounson A, Anderiesz C & Jones G 2001 Maturation of human oocytes in vitro and their developmental competence. *Reproduction* **121** 51-75.

van den Berg IM, Eleveld C, van der Hoeven M, Birnie E, Steegers EA, Galjaard RJ, Laven JS & van Doorninck JH 2011 Defective deacetylation of histone 4 K12 in human oocytes is associated with advanced maternal age and chromosome misalignment. *Hum Reprod* **26** 1181-1190.

Vasilev F, Chun JT, Gragnaniello G, Garante E & Santella L 2012 Effects of ionomycin on egg activation and early development in starfish. *PLoS One* **7** e39231.

Yi K & Li R 2012 Actin cytoskeleton in cell polarity and asymmetric division during mouse oocyte maturation. *Cytoskeleton (Hoboken)* **69** 727-737.

Yi K, Rubinstein B, Unruh JR, Guo F, Slaughter BD & Li R 2013 Sequential actin-based pushing forces drive meiosis I chromosome migration and symmetry breaking in oocytes. *J Cell Biol* **200** 567-576.

Young LE, Fernandes K, McEvoy TG, Butterwith SC, Gutierrez CG, Carolan C, Broadbent PJ, Robinson JJ, Wilmut I & Sinclair KD 2001 Epigenetic change in IGF2R is associated with fetal overgrowth after sheep embryo culture. *Nat Genet* **27** 153-154.

Young LE, Sinclair KD & Wilmut I 1998 Large offspring syndrome in cattle and sheep. *Rev Reprod* **3** 155-163.

Yu XJ, Yi Z, Gao Z, Qin D, Zhai Y, Chen X, Ou-Yang Y, Wang ZB, Zheng P, Zhu MS, Wang H, Sun QY, Dean J & Li L 2014 The subcortical maternal complex controls

symmetric division of mouse zygotes by regulating F-actin dynamics. *Nat Commun* **5** 4887.

Zhang J, Boyle M, Allen W & Galli C 1989 Recent studies on in vivo fertilisation of in vitro matured horse oocytes. *Equine Vet J* **21** 101-104.

Zhang JJ, Muzs LZ & Boyle MS 1990 In vitro fertilization of horse follicular oocytes matured in vitro. *Molecular Reproduction and Development* **26** 361-365.

APPENDICES

APPENDIX 1: PROTOCOL TO FIX AND EXTRACT EQUINE OOCYTES AND ZYGOTES

- Fixative MTSB-XF (Messinger & Albertini 1991) is stored at 4°C in a stock solution of 10 mL in a 15 mL conical tube.

- Aliquot some of the stock solution in small volumes of 200-300 μl in eppendorf tubes for the storage of the single oocytes.

- At specific oocyte`s fixation time remove an eppendorf tube with fixative from 4°C and leave at room temperature on the bench top while getting the oocyte out of the incubator.

- Prepare two drops of 20-50 μl of fixative on a petri dish to rinse the oocyte when you remove it from the culture dish.

- Oocytes cleaned and denuded from cumulus cells prior to or after sperm injection are removed from the culture media at the time of fixation and washed in the two drops of fixative prepared previously to remove any oil from the culture drops.

- With a 20 μl pipette pick up the oocyte from the second rinsing drop of fixative and gently move and pipette down to the bottom of the Eppendorf tube ready to store the oocyte at 4°C.

- Fixation of the oocyte needs to occur for at least 24 h for both extraction and fixation of the oocyte/zygote prior to immunostaining. Extraction and fixation using the microtubule stabilizing buffer fixative solution happens at the same time; therefore, the oocyte can be used for immunostaining after 24 h in fixative solution.

- The oocyte can be left in the eppendorf of fixative for 24 h to 2 to 3 weeks and need to be transferred to a wash solution after that for long-term conservation and preservation.

- Remember to make fixative MTSB-XF fresh every 3 to 4 weeks.

APPENDIX 2: PROTOCOL TO PERFORM IMMUNOSTAINING OF EQUINE OOCYTES

AND ZYGOTES

- Wash solution (Messinger & Albertini 1991) is the base solution for all the steps needed to perform immunostaining of equine oocytes and zygotes.

- Prepare 200 mL of fresh solution every 7-10 days for the experiments and store at 4°C.

- On Day 0, prepare four-well plates with 300 µl of wash solution in each well. Each oocyte should be put into a single well of the plate, unless the experiment pools oocytes together with no discrimination of an individual mare`s sample.

- Take the oocytes from the stored Eppendorf tube and put each oocyte into wash solution wells for at least 4 h to rinse and deterge at 38°C. If needed, the oocytes can be left overnight in wash solution at 4°C to start the immunostaining the morning after. Positioning of the four well plates on a constantly rotating platform shaker is necessary to permeabilize the large cell, both in incubations at 38 or 4°C.

- After the first wash, on Day 1, the oocytes are ready to incubate with the primary antibodies.

- The confocal microscope utilized by our laboratory has access to four lasers to see four distinct specific staining of parameters of interest. Two antibodies can be used to stain the equine oocytes, if Hoechst staining for DNA and Phalloidin for actin staining will be used as well, summing up at 4 different observable variables.

- Primaries' incubation uses antibodies at different concentrations depending on the specific ones of interest.

- For oocytes or zygotes removed from the cumulus cells, the oocyte needs to incubate in primary for at least 4 h at 38°C on the rotating platform. Usually, you want to incubate the oocyte with primary antibodies for 6 to 8 h at 38°C to allow binding to the specific antigens in the oocyte.

- If needed, oocytes can be left for longer hours, including overnight, of incubation but moved to a 4°C fridge on rotating platform.

- After primary incubation, on Day 2, the oocytes or zygotes go through a second long wash, frequently overnight at 4°C on rotating platform. If not performed overnight, the second wash after primaries' incubation should be done for at least 6-8 h at 38°C on rotating platform.

- On Day 3, the oocytes or zygotes are ready to be incubated with secondary antibodies; depending on the antibodies of interest, the concentrations will change.

- The secondary antibodies incubation is of at least 4 h at 38°C on the rotating platform. Preferably incubate the oocytes or zygotes with secondary antibodies for 6 to 8 h at 38°C on rotating platform. Cover the plates with aluminum foil because of the light sensitivity of the secondary antibodies.

- After secondary antibody incubation, the oocytes or zygotes need another wash, frequently done overnight at 4°C on rotating platform. If not performed overnight, incubation should be done for at least 6-8 h at 38°C on rotating platform.

- After secondary antibodies incubation, the oocytes or zygotes are usually stained for both DNA and actin, using Hoechst and Phalloidin staining respectively. The incubation should be done for at least 5 hours at 38°C on a rotating platform, keeping the plates covered with aluminum foil.

- Wash the oocytes or zygote in wash solution for 1 h at 38°C to remove any possible debris before mounting the samples on slides.

- While the oocytes or zygotes rinse one more time, prepare clean slides and coverslips with 70% ethanol and be sure to not have any debris or scratch signs on the surfaces.

- The final step is to mount the oocytes on polarized microscope slides using the glycerol based mounting media (Messinger & Albertini 1991). Take a single oocyte from the wash solution and with minimum volume of wash carried with the oocyte/zygote, place in the center of the slide. Add multiple (4-6) small drops of mounting media around the oocyte/zygote. Take the coverslip and add small columns of glue (1:1:1 of vaseline: lanolin: paraffin wax) at the corners of the coverslips and gently place on top of the oocyte. Put even pressure on the four corners of the coverslips, using a pencil or pen tip, to compress the oocyte. Be sure the cell is not moving, is flat and not broken.

- Seal the coverslip to the slide using nail polish, preferably clear.

- Let dry and store in slide boxes at 4°C.